



National Library
of Canada

Bibliothèque nationale
du Canada

Canadian Theses Service

Services des thèses canadiennes

Ottawa, Canada
K1A 0N4

CANADIAN THESES

THÈSES CANADIENNES

NOTICE

The quality of this microfiche is heavily dependent upon the quality of the original thesis submitted for microfilming. Every effort has been made to ensure the highest quality of reproduction possible.

If pages are missing, contact the university which granted the degree.

Some pages may have indistinct print especially if the original pages were typed with a poor typewriter ribbon or if the university sent us an inferior photocopy.

Previously copyrighted materials (journal articles, published tests, etc.) are not filmed.

Reproduction in full or in part of this film is governed by the Canadian Copyright Act, R.S.C. 1970, c. C-30. Please read the authorization forms which accompany this thesis.

**THIS DISSERTATION
HAS BEEN MICROFILMED
EXACTLY AS RECEIVED**

AVIS

La qualité de cette microfiche dépend grandement de la qualité de la thèse soumise au microfilmage. Nous avons tout fait pour assurer une qualité supérieure de reproduction.

S'il manque des pages, veuillez communiquer avec l'université qui a conféré le grade.

La qualité d'impression de certaines pages peut laisser à désirer, surtout si les pages originales ont été dactylographiées à l'aide d'un ruban usé ou si l'université nous a fait parvenir une photocopie de qualité inférieure.

Les documents qui font déjà l'objet d'un droit d'auteur (articles de revue, examens publiés, etc.) ne sont pas microfilmés.

La reproduction, même partielle, de ce microfilm est soumise à la Loi canadienne sur le droit d'auteur, SRC 1970, c. C-30. Veuillez prendre connaissance des formules d'autorisation qui accompagnent cette thèse.

**LA THÈSE A ÉTÉ
MICROFILMÉE TELLE QUE
NOUS L'AVONS REÇUE**



National Library
of Canada

Bibliothèque nationale
du Canada

0-315-27080-2

Canadian Theses Division / Division des thèses canadiennes

Ottawa, Canada
K1A 0N4

PERMISSION TO MICROFILM — AUTORISATION DE MICROFILMER

• Please print or type — Ecrire en lettres moulees ou dactylographier

Full Name of Author — Nom complet de l'auteur

Raymond Stanley Dickson

Date of Birth — Date de naissance

December 12, 1957

Country of Birth — Lieu de naissance

Canada

Permanent Address — Residence fixe

12 Glenwood Avenue,
Saskatoon, Sask.
S7L 4A6

Title of Thesis — Titre de la thèse

Structural and Reactivity Studies on Binuclear Metal Complexes

University — Université

University of Alberta

Degree for which thesis was presented — Grade pour lequel cette thèse fut présentée

M.Sc.

Year this degree conferred — Année d'obtention de ce grade

1984

Name of Supervisor — Nom du directeur de thèse

Dr. Martin Cowie

Permission is hereby granted to the NATIONAL LIBRARY OF CANADA to microfilm this thesis and to lend or sell copies of the film.

The author reserves other publication rights, and neither the thesis nor extensive extracts from it may be printed or otherwise reproduced without the author's written permission.

L'autorisation est, par la présente, accordée à la BIBLIOTHÈQUE NATIONALE DU CANADA de microfilmer cette thèse et de prêter ou de vendre des exemplaires du film.

L'auteur se réserve les autres droits de publication, ni la thèse ni de longs extraits de celle-ci ne doivent être imprimés ou autrement reproduits sans l'autorisation écrite de l'auteur.

Date

April 19, 1984

Signature

Raymond Stanley Dickson

THE UNIVERSITY OF ALBERTA
STRUCTURAL AND REACTIVITY STUDIES ON
BINUCLEAR METAL COMPLEXES

by

Raymond Stanley Dickson

A THESIS
SUBMITTED TO THE FACULTY OF GRADUATE STUDIES AND RESEARCH
IN PARTIAL FULFILMENT OF THE REQUIREMENTS FOR THE DEGREE
OF MASTER OF SCIENCE

DEPARTMENT OF CHEMISTRY

EDMONTON, ALBERTA

SPRING, 1984

THE UNIVERSITY OF ALBERTA
FACULTY OF GRADUATE STUDIES AND RESEARCH

The undersigned certify that they have read, and recommend to the Faculty of Graduate Studies and Research, for acceptance, a thesis entitled STRUCTURAL AND REACTIVITY STUDIES ON BINUCLEAR METAL COMPLEXES submitted by RAYMOND STANLEY DICKSON in partial fulfilment of the requirements for the degree of Master of Science in Chemistry.

Martin Curie

Supervisor

David T. Lynch

Joseph L. St.

Date... April 18, 1984

ABSTRACT

This thesis describes the synthesis and characterization of some diphosphine-bridged, binuclear rhodium complexes which contain bridging acetylene ligands, and some chemistry of these complexes with selected small molecules. The X-ray crystal structure of an unusual iron-palladium-bonded heterobinuclear complex is also reported.

The complexes $[\text{Rh}_2\text{X}_2(\mu\text{-RCCR})(\text{DPM})_2]$ (1: $\text{X} = \text{Cl}$, $\text{R} = \text{CF}_3$; 2: $\text{X} = \text{I}$, $\text{R} = \text{CF}_3$; 3: $\text{X} = \text{Cl}$, $\text{R} = \text{CO}_2\text{CH}_3$; $\text{DPM} = \text{bis}(\text{diphenylphosphino})\text{methane}$) were synthesized by the reaction of $[\text{RhCl}(\text{C}_8\text{H}_{12})]_2$ and two equivalents of DPM with the appropriate activated acetylene, $\text{CF}_3\text{C}_2\text{CF}_3$ (hexafluoro-2-butyne, HFB) or $\text{CH}_3\text{O}(\text{O})\text{CC}_2\text{C}(\text{O})\text{OCH}_3$ (dimethylacetylenedicarboxylate, DMA), followed by halide metathesis of 1 with KI to obtain 2. The crystal structure of $[\text{Rh}_2\text{Cl}_2(\mu\text{-HFB})(\text{DPM})_2]$ (1) was determined to establish the mode of acetylene binding in this complex (space group P4_3 , $a = 21.283(1) \text{ \AA}$, $c = 14.255(1) \text{ \AA}$, $Z = 4$; 5243 unique reflections; $R = 0.040$, $R_w = 0.055$). The complex was shown to be a distorted "A-frame" complex, having a metal-metal bond ($\text{Rh}(1)\text{-Rh}(2) = 2.7447(9) \text{ \AA}$), two terminal chloride ligands and a bridging acetylene moiety coordinated parallel to the metal-metal axis, as a so-called cis-dimetallated olefin. Most parameters of this group

suggested sp^2 hybridization of the central two carbon atoms.

The reactions of compounds 1, 2 and 3 with CO and SO_2 were reversible and gave products in which these small molecules had inserted into the Rh-Rh bonds. Protonation by the strong acids CF_3SO_3H and $HBF_4 \cdot (C_2H_5)_2O$ also occurred reversibly at the metal-metal bonds and was most probably accompanied by anion coordination at one metal centre.

However, methyl isocyanide (CNMe) reacted quite differently, yielding complexes in which the isocyanide ligands are bound terminally. Although all of compounds 1 - 3 reacted with CNMe in a rather analogous manner there were some subtle differences observed. Stepwise addition of CNMe to compound 1 yielded two unsymmetrical, isomeric 1:1 adducts, $[Rh_2Cl_2(CNMe)(\mu-HFB)(DPM)_2]$, followed by a 2:1 adduct, $[Rh_2Cl(CNMe)_2(\mu-HFB)(DPM)_2][Cl]$, and finally by a 4:1 adduct $[Rh(CNMe)_4(\mu-HFB)(DPM)_2][Cl]_2$. The iodo analogue species 2 gave analogous products except that the isomer ratio of the 1:1 adduct differed and a second symmetric 2:1 adduct, $[Rh_2I_2(CNMe)_2(\mu-HFB)(DPM)_2]$, was also observed. With the DMA-bridged species 3 only one 1:1 adduct was observed and all other products were analogous to the reactions of compound 1.

The unsymmetrical 2:1 adduct of compound 1 was isolated as the BF_4^- salt, $[Rh_2Cl(CNMe)_2(\mu-HFB)-$

(DPM)₂][BF₄]. Its X-ray crystal structure determination (space group P2₁/n, a = 16.366(3) Å, b = 18.685(3) Å, c = 20.425(4) Å, β = 104.35(1)°, Z = 4; 6800 unique observations; R_s = 0.059, R_w = 0.097) showed that the metal-metal bonded complex retained the cis-dimetallated olefinic binding mode of the acetylene group; one metal had a terminal chloro ligand whereas the other had two terminal CNMe groups.

[(PPh₃)PdFe(SC₅H₄)₂] was prepared and crystallized as the hemitoluene solvate by Mr. T.G. Rucker, Dr. B.W. Hames and Dr. Dietmar Seyferth at M.I.T., via the reaction of Pd(PPh₃)₄ with Fe(C₅H₄)₂S₃. The X-ray crystal structure (space group C2/c, a = 39.258(5) Å, b = 10.548(2) Å, c = 13.612(4) Å, β = 101.69(2)°, Z = 8; 3255 unique observed reflections; R = 0.040, R_w = 0.046) showed that the compound had an unusual iron-palladium dative-bonded structure (Fe→Pd = 2.878(1) Å) with the palladium chelated at trans positions by the two cyclopentadienethiolato sulfurs. The triphenylphosphine ligand is attached to the palladium trans to the metal-metal bond. The tilt angle found between the two cyclopentadienethiolate rings was only 19.6°, about half of those observed for other Cp₂ML_n compounds.

ACKNOWLEDGMENTS

The work in this thesis would not have been possible without the many people who gave me their support and encouragement throughout my life and my years of graduate studies.

In the scientific sphere, my special thanks go to:

Dr. Martin Cowie, my supervisor, not only for teaching me chemistry and crystallography, but also for his long-suffering work on my thesis and the papers we have published, and for the hospitality I have enjoyed in his home;

Dr. Dietmar Seyferth, Dr. Barry Hames and Mr. Tom Rucker for the crystals of $[(PPh_3)PdFe(SC_5H_4)_2] \cdot 0.5C_6H_5CH_3$;

Dr. Joel Mague for his preprints of relevant work and helpful discussion of spectra;

Dr. Alan Sanger for loans of deuterated solvents and other chemicals;

Dr. Richard Ball for one X-ray data collection, the use of his crystallographic computer programs and many valuable consultations;

all the people who have passed through the research group, especially Dr. Steve Dwight and Michele Gauthier for teaching me by example, how to do research, Dr. Timothy Southern for his experienced advice, Bruce Sutherland, Dr.

Ian McKeer and John Gibson for good companionship and Dr. Barry Hames for his continuing work on the isocyanide reactions;

the people in the service labs, particularly Dr. Tom Nakashima and his NMR lab technicians for running multitudes of spectra, teaching me how to run the machines and for some feverish consultations over the telephone when the machine went down;

and the Natural Sciences and Engineering Research Council for two years of scholarship financial support.

In the aspect of life in general, my special thanks go to:

my family, especially my mother for raising me and giving me moral support even when she didn't understand exactly what I was working on, and my brothers, Lawrence for his comprehension of the trials of graduate studies and research and his compassion for a fellow sufferer, and Tom for his willingness to discuss almost anything and for picking me up when I was low;

everyone in the University of Alberta Mixed Chorus for being my friends and giving me a place to sing;

everyone in the Ignatius Loyola Society for the Advancement of Learning for some memorable nights of discussion, dining and drinking;

and the clergy and people of All Saints' Anglican Cathedral, particularly the Venerable Edwin Thain for his teaching and inspiration, the choirmasters, Dr. Hugh Bancroft and Jeremy Spurgeon, the choir, and the people in the young adults' group, All Saints' Alive, for the fellowship I have enjoyed with them during my stay in Edmonton.

TABLE OF CONTENTS

CHAPTER	PAGE
I. Introduction.....	1
References.....	14
II. The Synthesis and Characterization of Some Binuclear Rhodium Complexes Containing Bridging Acetylene Ligands and the X-ray Crystal Structure of $[\text{Rh}_2\text{Cl}_2(\mu\text{-CF}_3\text{C}_2\text{CF}_3)(\text{Ph}_2\text{PCH}_2\text{PPh}_2)_2]$	28
Introduction.....	28
Experimental.....	32
Preparation of Compounds.....	33
X-ray Data Collection.....	36
Structure Solution and Refinement.....	37
Results	41
Discussion.....	51
Description of Structure.....	54
References.....	66
III Some Reactions of $[\text{Rh}_2\text{X}_2(\mu\text{-acetylene})(\text{DPM})_2]$ Complexes with Small Molecules and the X-ray Crystal Structure of One Product, $[\text{Rh}_2\text{Cl}(\text{CNMe})_2(\mu\text{-CF}_3\text{C}_2\text{CF}_3)(\text{DPM})_2][\text{BF}_4]$	71
Introduction.....	71
Experimental.....	73
Protonation of Compounds 1, 2 and 3.....	74

Reactions of Compounds 1, 2 and 3 with CO and SO ₂	75
Reactions of Compounds 1, 2 and 3 with CNMe..	78
Preparation of [Rh ₂ Cl(CNMe) ₂ (μ-HFB)-(DPM) ₂][BF ₄], 15b.....	79
Preparation of [Rh ₂ (CNMe) ₄ (μ-HFB)-(DPM) ₂][BF ₄] ₂ , 16b.....	80
X-Ray Data Collection on Compound 15b.....	81
Structure Solution and Refinement.....	82
Results	86
Description of Structure of Compound 15b....	101
Discussion of Results.....	112
Protonation Reactions.....	112
Reactions with CO and SO ₂	117
Reactions with CNMe.....	123
Conclusions.....	140
References.....	144
IV The Structure of a Novel Heterobinuclear Compound, [(PPh ₃) ₂ POFe(SC ₅ H ₄) ₂]·0.5C ₆ H ₅ CH ₃	148
Introduction.....	148
X-ray Data Collection.....	151
Structure Solution and Refinement.....	152
Results	155
Description of Structure.....	164
References.....	176

LIST OF TABLES

TABLE	Description	PAGE
I	Solvents and Drying Agents.....	32
II	Summary of Crystal Data and Intensity Collection Details for $[\text{Rh}_2\text{Cl}_2(\mu\text{-HFB})(\text{DPM})_2]$	41
III	Positional and Thermal Parameters for the Non-Group Atoms of $[\text{Rh}_2\text{Cl}_2(\mu\text{-HFB})(\text{DPM})_2]$	43
IV	Derived Parameters for the Rigid-Group Atoms of $[\text{Rh}_2\text{Cl}_2(\mu\text{-HFB})(\text{DPM})_2]$	44
V	Idealized Positional and Thermal Parameters for the Hydrogen Atoms of $[\text{Rh}_2\text{Cl}_2(\mu\text{-HFB})(\text{DPM})_2]$	45
VI	Selected Distances (Å) in $[\text{Rh}_2\text{Cl}_2(\mu\text{-HFB})(\text{DPM})_2]$	46
VII	Selected Angles (Deg) in $[\text{Rh}_2\text{Cl}_2(\mu\text{-HFB})(\text{DPM})_2]$	47
VIII	Least-Squares Plane Calculations for $[\text{Rh}_2\text{Cl}_2(\mu\text{-HFB})(\text{DPM})_2]$	50
IX	$^{31}\text{P}\{^1\text{H}\}$ NMR Spectral Parameters for Compounds 1, 2 and 3 and Related Complexes.....	52
X	Spectral Data for Reactions of Compounds 1, 2 and 3 with H^+ , CO and SO_2	86
XI	Spectral Data for Reactions of Compound 1 2 and 3 with CNMe	87
XII	Molar Conductivities for the Stepwise Addition of CNMe to $[\text{Rh}_2\text{X}_2(\mu\text{-RC}_2\text{R})(\text{DPM})_2]$	89

XIII	Summary of Crystal Data and Intensity Collection Details for $[\text{Rh}_2\text{Cl}(\text{CNMe})_2(\mu\text{-HFB})(\text{DPM})_2][\text{BF}_4]$	90
XIV	Positional and Thermal Parameters for the Non- Group Atoms of $[\text{Rh}_2\text{Cl}(\text{CNMe})_2(\mu\text{-HFB})(\text{DPM})_2][\text{BF}_4]$	92
XV	Derived Parameters for the Rigid-Group Atoms of $[\text{Rh}_2\text{Cl}(\text{CNMe})_2(\mu\text{-HFB})(\text{DPM})_2][\text{BF}_4]$	93
XVI	Idealized Positional and Thermal Parameters for the Hydrogen Atoms of $[\text{Rh}_2\text{Cl}(\text{CNMe})_2(\mu\text{-HFB})-$ $(\text{DPM})_2][\text{BF}_4]$	94
XVII	Selected Distances (Å) in $[\text{Rh}_2\text{Cl}(\text{CNMe})_2(\mu\text{-HFB})-$ $(\text{DPM})_2][\text{BF}_4]$	95
XVIII	Selected Angles (Deg) in $[\text{Rh}_2\text{Cl}(\text{CNMe})_2(\mu\text{-HFB})-$ $(\text{DPM})_2][\text{BF}_4]$	97
XIX	Least-Squares Plane Calculations for $[\text{Rh}_2\text{Cl}(\text{CNMe})_2(\mu\text{-HFB})(\text{DPM})_2][\text{BF}_4]$	100
XX	Summary of Crystal Data and Intensity Collection Details for $[(\text{PPh}_3)\text{PdFe}(\text{SC}_5\text{H}_4)_2] \cdot 0.5\text{C}_6\text{H}_5\text{CH}_3$	155
XXI	Atomic Positional Parameters ($\times 10^4$) and Thermal Parameters ($\times 10^2$) for the Non-Group Atoms of $[(\text{PPh}_3)\text{PdFe}(\text{SC}_5\text{H}_4)_2] \cdot 0.5\text{C}_6\text{H}_5\text{CH}_3$	157
XXII	Parameters for the Rigid-Group Atoms of $[(\text{PPh}_3)\text{PdFe}(\text{SC}_5\text{H}_4)_2] \cdot 0.5\text{C}_6\text{H}_5\text{CH}_3$	158
XXIII	Idealized Positional and Thermal Parameters for the Hydrogen Atoms of $[(\text{PPh}_3)\text{PdFe}(\text{SC}_5\text{H}_4)_2] \cdot 0.5\text{C}_6\text{H}_5\text{CH}_3$	159

XXIV	Least Squares Plane Calculations for	
	$[(PPh_3)PdFe(SC_5H_4)_2] \cdot 0.5C_6H_5CH_3$160
XXV	Selected Distances (Å) in	
	$[(PPh_3)PdFe(SC_5H_4)_2] \cdot 0.5C_6H_5CH_3$161
XXVI	Selected Angles (Deg) in	
	$[(PPh_3)PdFe(SC_5H_4)_2] \cdot 0.5C_6H_5CH_3$162

LIST OF FIGURES

FIGURE	Title of Figure	PAGE
1.	Orbital Symmetry Analogies for σ -Basic- π -Acidic Ligands.....	3
2.	Stereoview of the Unit Cell of $[\text{Rh}_2\text{Cl}_2(\mu\text{-HFB})\text{-}(\text{DPM})_2]$	55
3.	Perspective View of $[\text{Rh}_2\text{Cl}_2(\mu\text{-HFB})(\text{DPM})_2]$	56
4.	Representation of the Equatorial Plane of $[\text{Rh}_2\text{Cl}_2(\mu\text{-HFB})(\text{DPM})_2]$	57
5.	Stereoview of the Unit Cell of $[\text{Rh}_2\text{Cl}_2(\text{CNMe})_2(\mu\text{-HFB})(\text{DPM})_2][\text{BF}_4]$	102
6.	Perspective View of $[\text{Rh}_2\text{Cl}(\text{CNMe})_2(\mu\text{-HFB})\text{-}(\text{DPM})_2]^+$	103
7.	Representation of the Equatorial Plane of $[\text{Rh}_2\text{Cl}(\text{CNMe})_2(\mu\text{-HFB})(\text{DPM})_2]^+$	104
8.	161.92 MHz $^{31}\text{P}\{^1\text{H}\}$ NMR Spectrum of $[\text{Rh}_2\text{I}_2(\mu\text{-HFB})(\text{DPM})_2] + \sim 1.3 \text{ CNMe}$	126
9.	Scheme for Reactions of $[\text{Rh}_2\text{X}_2(\mu\text{-RC}_2\text{R})(\text{DPM})_2]$ with CNMe.....	138
10.	Stereoview of the Unit Cell of $[(\text{PPh}_3)\text{PdFe}(\text{SC}_5\text{H}_5) \cdot 0.5\text{C}_6\text{H}_5\text{CH}_3]$	165
11.	Perspective View of $[(\text{PPh}_3)\text{PdFe}(\text{SC}_5\text{H}_4)_2]$	166

LIST OF ABBREVIATIONS AND SYMBOLS

Chemical Abbreviations and Symbols

CNMe	methyl isocyanide
DMA	dimethyl acetylenedicarboxylate
DPM	bis(diphenylphosphino)methane
HFB	hexafluoro-2-butyne
IR	infrared
L	general two-electron ligand
Me	methyl
NMR	nuclear magnetic resonance
Ph	phenyl
R	general monovalent organic group
^t Bu	tertiary butyl
X	general halogen
{ }	for NMR spectra, bracketed nuclei are decoupled

Crystallographic Abbreviations and Symbols

a, b, c,	respective lengths of x, y and z axes of unit cell
B	isotropic thermal parameter
F _c	calculated structure factor
F _o	observed structure factor
p	ignorance factor, accounting for equipment inaccuracies in intensity measurement

ABBREVIATIONS AND SYMBOLS (continued)

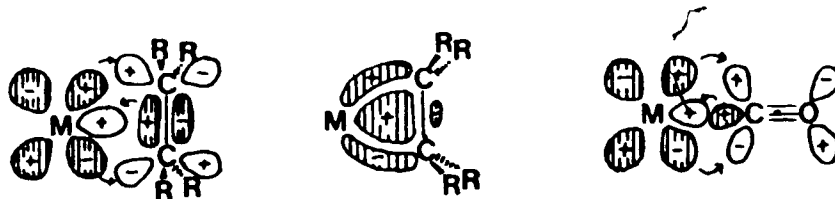
R	residual factor
R_w	weighted residual factor
$U_{n_1 n_2}$	anisotropic thermal parameter
w	weighting factor applied to structure factor
Z	number of formula weights per unit cell
Å	Angstrom units, 10^{-10} m
° or deg	degrees
β	angle between a and c axes of monoclinic unit cell
2θ	angle between incident beam and diffracted beam
k	reciprocal of scaling factor used to bring F_o to absolute units
σ	standard deviation
ω	diffractometer angle, describing deviation of crystal rotation about vertical axis from θ (see 2θ above).

Introduction

The chemistry of small unsaturated molecules such as CO,^{1,2} NO,^{1,3,4} SO₂,^{5,6} acetylenes^{7,8} and olefins^{9,10} with transition metal complexes has received considerable attention over the last decade and a half. This interest is partly due to the novel chemistry displayed by these systems,¹⁻¹¹ and partly due to the relevance of much of this chemistry to important chemical processes which are catalyzed by transition metal complexes.^{1,8,12} Much has been learned, for example, about the natures of transient intermediates in catalytic processes by studying somewhat similar, but less labile, metal complexes which display related chemistry.¹³⁻¹⁵ Using such model systems, information has been obtained on aspects such as the small-molecule coordination modes¹¹ and the transformations of the coordinated small molecules that are likely to be part of catalytic reaction mechanisms.¹²

The mode of coordination of a substrate to a metal is one aspect which is of great importance in understanding metal-centred chemical processes. Considerable attention has therefore been directed towards determining these

coordination modes and trying to rationalize the bonding involved. In the cases of unsaturated substrates such as CO, olefins and acetylenes, one of the most generally useful models for rationalizing the bonding of these ligands to transition metals is that of Dewar,¹⁶ Chatt and Duncanson.¹⁷ Although this model was originally proposed for the binding of alkenes, it can readily be extended to other unsaturated molecules. In this model of alkene



coordination, the filled π orbital on the alkene donates electron density into some empty metal orbital of σ symmetry, while simultaneously a filled π -symmetry metal d orbital donates electron density into the empty π^* alkene orbital. The extension of this σ -donor- π -acceptor bonding model to alkynes is obvious, and differs only slightly when applied to the bonding of carbon monoxide and other σ -base- π -acid ligands which bind to metals by only one atom (e.g. CNR, NO⁺, SO₂, PR₃; see Figure 1).

For alkenes and alkynes, the orbitals formed on complexation resemble those of cyclopropane and cyclopropene, respectively,⁹ so it is not surprising that

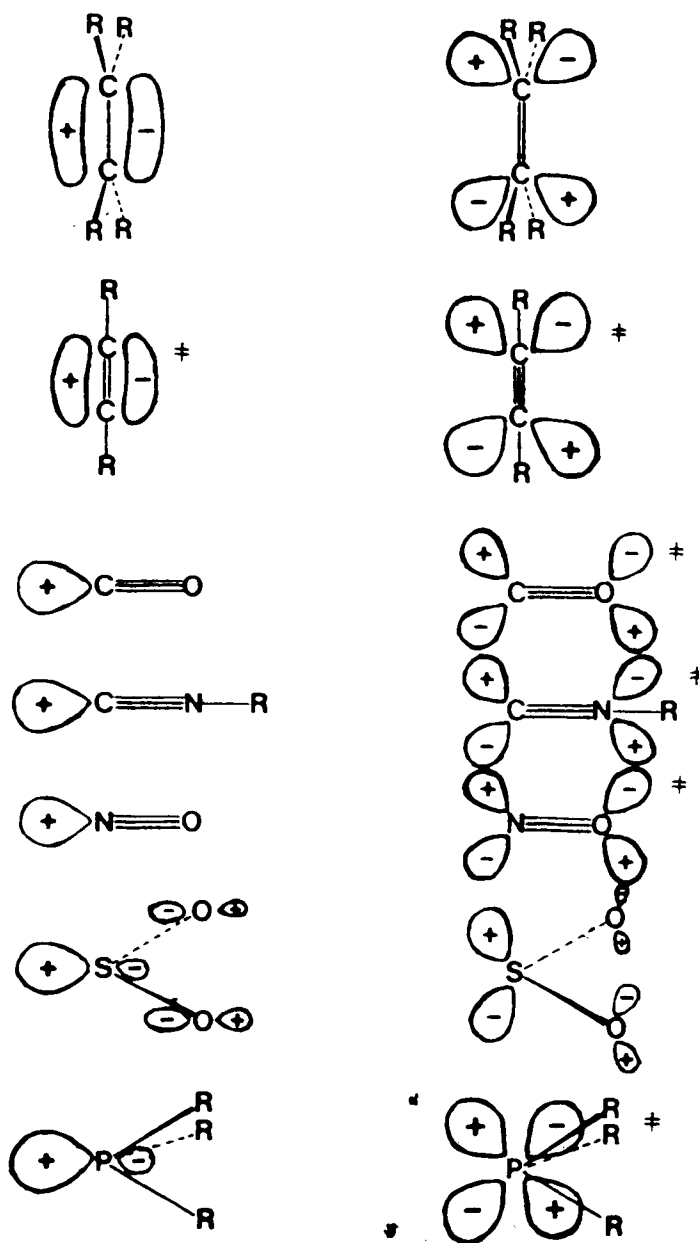
Filled σ orbitals*Empty π orbitals*

Figure 1. Orbital Symmetry Analogies for σ -Basic- π -Acidic Ligands.

*Symmetries are given with respect to the metal-ligand axis.

#There is another orbital similar to the one depicted, but out of the plane of the diagram.

complexation of these molecules is accompanied by lengthening of the carbon-carbon multiple bonds and bending of the substituents away from the metal.⁹ From another point of view, these ligands lose electron density from their highest occupied bonding orbitals and gain electron density in relatively low-energy anti-bonding orbitals, so they resemble their first electronically-excited states in having their coordinated multiple bonds weakened and their substituents bent back, away from their former planar or linear geometries.¹⁸ These geometry changes also resemble those which would be seen during addition reactions of these molecules involving bond order reduction (e.g. hydrogenation, hydroformylation, polymerization), thus rationalizing the activity of transition metals and their complexes in catalysis of such reactions; not only would coordination to the metal bring the reactants together, but would also activate the substrate by bringing it closer to the transition state.

In order to obtain structural information about the mode of coordination of a substrate molecule in a reactive metal complex, it is often necessary to stabilize the substrate adduct to a degree which will allow the appropriate study to be made. Several approaches can be taken to achieve this, including changing the metal, the ancillary ligands on the metal or the substituents on the

substrate molecule, in order to obtain an isolable analogue of the labile intermediate of interest. For example, $[\text{RhCl}(\text{N}_2)(\text{PPh}_3)_2]$, an intermediate in some azide-induced substitution reactions of $[\text{RhCl}(\text{CO})(\text{PPh}_3)_2]$, is highly unstable at room temperature and difficult to isolate even at low temperature,¹⁹ but both $[\text{IrCl}(\text{N}_2)(\text{PPh}_3)_2]$ ²⁰ and $[\text{RhCl}(\text{N}_2)(\text{P}(\text{cyclohexyl})_3)_2]$ ²¹ have been isolated and have reasonable stabilities at room temperature. Thus changing from the second-row metal rhodium to the third-row iridium or changing from the triphenylphosphine ligand to the bulkier tricyclohexylphosphine stabilizes this type of complex.

A common approach to stabilization of acetylene and olefin complexes is to substitute "activated" olefins and acetylenes for the "unactivated" ones in more common catalytic use. Two types of substituent generally lead to more stable low-valent Group VIII metal complexes:^{7,22}

- (1) Electronegative substituents (e.g. $-\text{CF}_3$, $-\text{F}$), which withdraw electron density inductively from the bound carbons, encouraging metal π -back donation and
- (2) π -conjugating substituents (e.g. $-\text{CN}$, $-\text{CO}_2\text{CH}_3$), which delocalize the substrate electron density and lower the π^* orbital energy, thereby also increasing the π -back donation from the metal. This increased back donation helps bind the unsaturated ligand more strongly to the metal, and also

results in a greater geometry change from the free state to the coordinated state for molecules with such substituents. In this thesis, both the ancillary ligands and the acetylene substituents will be varied in order to stabilize desired products; changing the metal from rhodium to iridium has been investigated by others within this group.²³

At the outset, most of the emphasis in the chemistry of small molecules with transition metals dwelt on mononuclear metal complexes²⁴ (i.e. complexes containing one metal centre). However, as more was understood about these simpler single-metal systems, increasing attention was turned to polynuclear metal complexes, which have a greater potential for chemical diversity;²⁵ not only can the metals in a polynuclear compound function independently, in a manner analogous to mononuclear species, they can interact with the substrate molecule in a cooperative manner, which is not possible in the mononuclear case. It is this cooperative interaction which has aroused the most interest in multicentre metal systems. Structurally, we see the greater diversity possible for multinuclear metal complexes with the ubiquitous carbonyl ligand.²⁶ In monometallic complexes, only the terminal end-on carbonyl ligand, bound through the carbon atom, is known, whereas in polymetallic complexes a

variety of further geometries and coordination modes is possible. Obviously, geometries in which carbonyls bridge two or three metals, which are common in multicentre complexes, are not possible with mononuclear species. But even within the common doubly-bridged case a variety of geometries has been observed. The commonest case has the carbonyl bound solely through carbon to each of the two metal centres concerned, in a range of geometries from totally symmetric through to very unsymmetrical cases in which the two metal-carbon distances are quite different, though still within range for significant interaction. Even within the symmetrically bridged case there are two possibilities: the common one, in which there is an accompanying metal-metal bond, and one that has only been observed recently, in which there is no accompanying metal-metal bond.²⁷⁻³⁰ Asymmetric bridging modes include the semi-bridging carbonyl,²⁶ in which the carbon is bound closer to one metal than to the other and the C-O bond is roughly perpendicular to the metal-metal axis, the σ - π carbonyl,³¹ in which the CO group is σ -bound through carbon to one metal and side-on bound to another metal, and the so-called "isocarbonyl",^{32,33} in which the CO group is bound to one or two metals through the carbon and to another metal through oxygen.

Apart from the increased diversity in the chemistry of polynuclear species, the presence of more than one metal centre has considerable relevance from a catalytic viewpoint. Some transformations that occur in multinuclear species may not be possible in similar mononuclear species,²⁵ owing to the necessity for more than one metal site to act on the substrate(s) in a cooperative manner. Also, it is not unreasonable to assume that, if one metal centre activates a substrate molecule, more than one centre will cause increased activation. This latter aspect can be seen in the ways that acetylenes bind to metals. The mononuclear "metallocyclopropene" bonding mode has already been mentioned. In binuclear complexes, acetylenes are usually found in one of two coordination modes:^{8,34} the acetylene may bind parallel to the metal-metal axis, in which case it may be described as a cis-dimetallated olefin since the structural parameters of the ligand are similar to those in free olefins, or more commonly, the acetylene may bind perpendicular to the metal-metal axis, resulting in a quasi-tetrahedral geometry of the two metal atoms and the two acetylenic carbons, in what is called the $\mu_2-\eta^2$ coordination mode. As discussed previously, coordination of an acetylene is accompanied by lengthening of the C-C multiple bond and bending back of the substituents,⁹ and as a natural extension we might assume that the coordination

of the acetylene molecule by a greater number of metals should cause further C-C bond lengthening and greater bend-back of the substituents. These general trends are observed, though other factors are sometimes involved which may obscure the trend. For example, most mononuclear acetylene complexes show C-C distances of 1.22(3) Å to 1.32(4) Å and bend-back angles of 12° to 43°. ^{9,35} In the cis-dimetalated olefinic coordination mode the C-C distances range from 1.27(3) Å to 1.34(1) Å and the bend-back angles have increased to 51(1)°-57.5(8)°. ³⁴ The perpendicular $\mu_2-\eta^2$ mode exhibits C-C distances similar to, though somewhat longer than, those for the parallel mode (1.27(2) Å - 1.42(1) Å), accompanied by smaller bend-back angles than for the parallel model (29.8(5)° - 50(1)°). ^{8,34} This trend of increasing C-C bond distances and bend-back angles with increasing number of bound metals continues for acetylenes bound to three ³⁶⁻⁴⁰ and four ⁴¹ metals (C-C distances: 1.33(3) Å - 1.44(1) Å; bend-back angles: 49(1)° - 62(1)°). Thus, a greater structural activation is possible for polynuclear complexes through cooperative action of the metal centres.

An additional consideration in polymetallic chemistry is the possibility of metal-metal bonding, which again permits chemistry not observed with mononuclear species. ²⁵ For example, insertion reactions resulting in

metal-metal bond rupture and de-insertion reactions resulting in metal-metal bond formation are possible only in polynuclear compounds. Many types of chemistry observed with mononuclear complexes change when performed in the presence of metal-metal bonds, or sites where metal-metal bonds may be formed. For example, in photolysis, excitation involving the metal-metal bonding and antibonding orbitals may occur. In substitution reactions, metal-metal bonding sites are available for electrophilic attack by the incoming ligand. In oxidative addition and reductive elimination reactions, oxidation state changes of one unit on each of adjacent metals may be accomplished through metal-metal bond formation or rupture. Though this brief overview has concentrated on metal-metal single bonds, similar considerations apply to metal-metal multiple bonds. Thus, metal-metal bonds are large contributors to the potential reactivity of polynuclear complexes.

The simplest of the polynuclear metal complexes are the binuclear ones. These can display much of the chemistry observed for higher-order polynuclear species,²⁵ yet are often more convenient to study than the more complex species. In fact, some higher-order complexes, especially trinuclear and tetranuclear species with a reactive pair of adjacent metals, can be considered as reactive binuclear complexes bridged by one or two nearly inert metals.

In studying binuclear complexes, it is often advantageous to have strongly bound, robust bridging groups^{25,42} which permit the complex to remain structurally intact during metal-metal bond formation or rupture. Such a ligand should therefore be chosen to have sufficient flexibility to allow the metals to assume either "normal" non-bonded contact distances or metal-metal bonded distances. With the above criteria in mind, a common ligand of choice is bis(diphenylphosphino)methane^{25,43,44} (DPM); its bite distance (ca. 3.0 Å) is intermediate between normal bonded and non-bonded metal-metal distances, and it is flexible enough to allow a significant range of metal-metal distances to be spanned (a range from 3.492(1) Å⁴⁵ to 2.138(1) Å⁴⁶ has been observed in DPM-bridged complexes). In addition, it is closely related to PPh₃ and even more closely to PMePh₂, allowing ready comparison with the large body of mononuclear chemistry which utilizes these ligands.^{43,47,48}

Unlike its higher homologue bis(diphenylphosphino)ethane (DPE) which almost invariably binds as a chelate,⁴³ DPM has a greater tendency to bridge the metals when in binuclear complexes,^{25,43,44} although many complexes with chelating DPM are also known.^{43,44} The majority of binuclear DPM complexes studied to date have two bridging DPM groups with the phosphorus atoms attached to each metal

in mutually trans positions. Most of these are complexes of the heavier Group VIII metals (rhodium,^{29,30,44,49-93} iridium,^{23,44,51-53,57,59,61,88,90,94} palladium^{27,86,88,95-115} and platinum^{44,85-87,113,114,116-164}); the well-established catalytic activity of these metals and their complexes in a variety of processes¹² makes these metals an obvious choice for study. Furthermore, complexes of these metals, in their common 16-electron configuration, exhibit a strong tendency to undergo oxidative addition or simple ligand addition reactions;^{11,47,48} such complexes are ideally suited to investigations of such small molecule additions.

Our group has, for the past six years, been involved in the investigation of the chemistry of $\text{Rh}_2(\text{DPM})_2$ ^{29,51,58,72-80} and $\text{Ir}_2(\text{DPM})_2$ ²³ systems with small molecules, analogous to the previous studies of $\text{RhCl}(\text{PPh}_3)_3$ ⁴⁷ and $\text{IrCl}(\text{CO})(\text{PPh}_3)_2$.⁴⁸ At the time when this project was undertaken, however, there had been few reports of chemistry of such complexes with unsaturated organic ligands,^{58,165} in spite of the obvious catalytic implications of such reactions. However, several such reports have been published during the course of this work.^{23,29,30,44,54,61,68,70,79,80,83,88} Some investigations in the sub-area of acetylene complexes constitute the next two chapters of this thesis.

The final chapter of this thesis reports the structural determination of a novel heterobinuclear compound synthesized by the group of Professor Dietmar Seyferth at M.I.T. Our group has recently become interested in heterobinuclear chemistry for a number of reasons, and is engaged in attempts to synthesize mixed-metal DPM-bridged dimers. One reason for the recent increase of interest in heteronuclear compounds is that they have a wider potential range of ligand reactions and binding modes than homonuclear complexes, due to the different characteristics and affinities of the metals.¹⁶⁶ For instance, the only known examples of isocarbonyl bonding have been found in heteronuclear complexes^{32,33} (mostly d-block-main group heterometallic compounds), demonstrating the possibility of tailoring different metal sites to react specifically with different moieties. Also, heterometallic metal-metal bonds and their reactivities are of interest, because of the differences in radii, polarizability and available orbitals among metals, which may induce unusual patterns in photochemistry, bond strengths and general reactivity.¹⁶⁷

References

1. Eisenberg, R.; Hendriksen, D.E. Adv. Catal. 1979, **28**, 79.
2. Cotton, F.A.; Wilkinson, G. "Advanced Inorganic Chemistry", 4th edition, Wiley, New York, 1980, pp. 1049-1070, 1257-1260.
3. Johnson, B.F.G.; McCleverty, J.A. Prog. Inorg. Chem. 1966, **7**, 277.
4. McCleverty, J.A. Chem. Rev. 1979, **79**, 53.
5. Mingos, D.M.P. Transition Met. Chem. 1978, **3**, 1.
6. Kubas, G.J. Inorg. Chem. 1979, **18**, 182.
7. Otsuka, S.; Nakamura, A. Adv. Organomet. Chem. 1976, **14**, 245.
8. Muetterties, E.L.; Pretzer, W.R.; Thomas, M.G.; Beier, B.F.; Thorn, D.L.; Day, V.W.; Anderson, A.B. J. Am. Chem. Soc. 1978, **100**, 2090.
9. Ittel, S.D.; Ibers, J.A. Adv. Organomet. Chem. 1976, **14**, 33.
10. Cotton, F.A.; Wilkinson, G. "Advanced Inorganic Chemistry", 4th edition, Wiley, New York, 1980, pp. 1147-1151.
11. Cotton, F.A.; Wilkinson, G. "Advanced Inorganic Chemistry", 4th edition, Wiley, New York, 1980, pp. 1119-1172, 1234-1263.

12. Cotton, F.A.; Wilkinson, G. "Advanced Inorganic Chemistry", 4th edition, Wiley, New York, 1980, pp. 1265-1307.
13. Vaska, L.; DiLuzio, J.W. J. Am. Chem. Soc. 1961, 83, 2784.
14. Vaska, L.; DiLuzio, J.W. J. Am. Chem. Soc. 1962, 84, 679.
15. Cotton, F.A.; Wilkinson, G. "Advanced Inorganic Chemistry", 4th edition, Wiley, New York, 1980, pp. 1292-1293.
16. Dewar, M.J.S. Bull. Soc. Chim. Fr. 1951, 18, C71.
17. Chatt, J.; Duncanson, L.A. J. Chem. Soc. 1953, 2939.
18. Orgel, L.E. "Introduction to Transition-Metal Chemistry", Methuen, London, p. 137.
19. Ukhin, L.Yu.; Shvetsov, Yu.A.; Khidekel, M.L. Izv. Akad. Nauk. SSSR, Ser. Khim. 1967, 957.
20. Collman, J.P.; Kubota, M.; Vastine, F.D.; Sun, J.Y.; Kang, J.W. J. Am. Chem. Soc. 1968, 90, 5430.
21. Van Gaal, H.L.M.; Van den Bekerom, F.L.A. J. Organomet. Chem. 1977, 134, 237.
22. Guggenberger, L.J.; Cramer, R. J. Am. Chem. Soc. 1972, 94, 3779.
23. Cowie, M.; Sutherland, B.R., submitted to Organometallics.

24. Cotton, F.A.; Wilkinson, G. "Advanced Inorganic Chemistry", 4th edition, Wiley, New York, 1980, pp. 1080-1082.
25. (a) Chisholm, M.H. in "Reactivity of Metal-Metal Bonds", ed. M.H. Chisholm, ACS Symposium Series 1981, 155, p. 17.
(b) Chisholm, M.H.; Rothwell, I.P. Prog. Inorg. Chem. 1982, 29, 1.
26. Cotton, F.A.; Wilkinson, G. "Advanced Inorganic Chemistry", 4th edition, Wiley, New York, 1980, pp. 1050-1061.
27. (a) Colton, R.; McCormick, M.J.; Pannan, C.D. J. Chem. Soc., Chem. Commun. 1977, 823.
(b) Colton, R.; McCormick, M.J.; Pannan, C.D. Aust. J. Chem. 1978, 31, 1425.
28. Brown, M.P.; Keith, A.N.; Manojlovic-Muir, Lj.; Muir, K.W.; Puddephatt, R.J.; Seddon, K.R. Inorg. Chim. Acta 1979, 34, L223.
29. (a) Cowie, M.; Southern, T.G. J. Organomet. Chem. 1980, 193, C46.
(b) Cowie, M.; Southern, T.G. Inorg. Chem. 1982, 21, 246.
30. (a) Mague, J.T.; DeVries, S.H. Inorg. Chem. 1982, 21, 1632.
(b) Mague, J.T. Inorg. Chem. 1983, 22, 45.

31. Commons, C.J.; Hoskins, B.F. Aust. J. Chem. 1975, **28**, 1663.
32. Ulmer, S.W.; Skarstad, P.M.; Burlitch, J.M.; Hughes, R.G. J. Am. Chem. Soc. 1973, **95**, 4469.
33. Tilley, T.D.; Andersen, R.A. J. Am. Chem. Soc. 1982 **104**, 1772.
34. Hoffman, D.M.; Hoffmann, R.; Fisel, C.R. J. Am. Chem. Soc. 1982, **104**, 3858.
35. Farrar, D.H.; Payne, N.C. J. Organomet. Chem. 1981, **220**, 239 and 251.
36. Ferraris, G.; Gervasio, G. J. Chem. Soc., Dalton Trans. 1973, 1933.
37. Pierpont, C.G. Inorg. Chem. 1977, **16**, 636.
38. Blount, J.F.; Dahl, L.F.; Hoogzand, C.; Hubel, W. J. Am. Chem. Soc. 1966, **88**, 292.
39. Dodge, R.P.; Schomacker, V. J. Organomet. Chem. 1965, **3**, 274.
40. Trinh-Toan; Broach, R.W.; Gardner, S.A.; Rausch, M.D.; Dahl, L.F. Inorg. Chem. 1977, **16**, 279.
41. Dahl, L.F.; Smith, D.L. J. Am. Chem. Soc. 1962, **84**, 2450.
42. Poilblanc, R. Inorg. Chim. Acta 1982, **62**, 75.
43. McAuliffe, C.A.; Levasor, W. "Phosphine, Arsine and Stibine Complexes of the Transition Metals", Elsevier, Amsterdam, 1979, p. 213 and p. 271.

44. Puddephatt, R.J. Chem. Soc. Rev. 1983, 12, 99.
45. Balch, A.L.; Lee, C.-L.; Lindsay, C.H.; Olmstead, M.M. J. Organomet. Chem. 1979, 177, C22.
46. Abbott, E.H.; Bose, K.S.; Cotton, F.A.; Hall, W.T.; Sekutowski, J.C. Inorg. Chem. 1978, 17, 3240.
47. Jardine, F.H. Prog. Inorg. Chem. 1981, 28, 63.
48. Vaska, L. Acc. Chem. Res. 1968, 1, 335.
49. Hieber, W.; Kummer, R. Chem. Ber. 1967, 100, 148.
50. Mague, J.T.; Mitchener, J.P. Inorg. Chem. 1969, 8, 119.
51. Cowie, M.; Mague, J.T.; Sanger, A.R. J. Am. Chem. Soc. 1978, 100, 3628.
52. Mague, J.T.; Sanger, A.R. Inorg. Chem. 1979, 18, 2060.
53. Mague, J.T.; DeVries, S.H. Inorg. Chem. 1980, 19, 3743.
54. Mague, J.T. Inorg. Chem. 1983, 22, 1158.
55. Sanger, A.R. J. Chem. Soc., Chem. Commun. 1975, 893.
56. Sanger, A.R. J. Chem. Soc., Dalton Trans. 1977, 120.
57. Sanger, A.R. J. Chem. Soc., Dalton Trans. 1977, 1971.
58. Cowie, M.; Dwight, S.K.; Sanger, A.R. Inorg. Chim. Acta 1978, 31, L407.
59. Sanger, A.R. Prepr.-Can. Symp. Cat. 1979, 6, 37.
60. Sanger, A.R. J. Chem. Soc., Dalton Trans. 1981, 228.
61. Sanger, A.R. Can. J. Chem. 1982, 60, 1363.

62. Balch, A.L. J. Am. Chem. Soc. 1976, **98**, 8049.
63. Balch, A.L.; Tulyathan, B. Inorg. Chem. 1977, **16**, 2840.
64. Balch, A.L.; Labadie, J.W.; Delker, G. Inorg. Chem. 1979, **18**, 1224.
65. Olmstead, M.M.; Lindsay, C.H.; Benner, L.S.; Balch, A.L. J. Organomet. Chem. 1979, **179**, 289.
66. Balch, A.L.; Benner, L.S. Inorg. Synth. 1982, **21**, 47.
67. Kubiak, C.P.; Eisenberg, R. J. Am. Chem. Soc. 1977, **99**, 6129.
68. Kubiak, C.P.; Eisenberg, R. J. Am. Chem. Soc. 1980, **102**, 3637.
69. Kubiak, C.P.; Eisenberg, R. Inorg. Chem. 1980, **19**, 2726.
70. Kubiak, C.P.; Woodcock, C.; Eisenberg, R. Inorg. Chem. 1982, **21**, 2119.
71. Woodcock, C.; Eisenberg, R. Organometallics 1982, **1**, 886.
72. Cowie, M. Inorg. Chem. 1979, **18**, 286.
73. Cowie, M.; Dwight, S.K. Inorg. Chem. 1979, **18**, 2700.
74. Cowie, M.; Dwight, S.K. Inorg. Chem. 1980, **19**, 209.
75. Cowie, M.; Dwight, S.K. Inorg. Chem. 1980, **19**, 2500.
76. Cowie, M.; Dwight, S.K. Inorg. Chem. 1980, **19**, 2508.
77. Cowie, M.; Dwight, S.K. J. Organomet. Chem. 1980, **198**, C20.

78. Cowie, M.; Dwight, S.K. J. Organomet. Chem. 1981, **214**, 233.
79. Cowie, M.; Dickson, R.S. Inorg. Chem. 1981, **20**, 2682.
80. McKeer, I.R.; Cowie, M. Inorg. Chim. Acta 1982, **65**, L107.
81. Yaneff, P.V.; Powell, J. J. Organomet. Chem. 1979, **179**, 101.
82. Van der Ploeg, A.F.M.J.; Van Koten, G. Inorg. Chim. Acta 1981, **51**, 225.
83. Fryzuk, M.D. Inorg. Chim. Acta 1981, **54**, L265.
84. Fordyce, W.A.; Crosby, G.A. J. Am. Chem. Soc. 1982, **104**, 985.
85. McEwan, D.M.; Pringle, P.G.; Shaw, B.L. J. Chem. Soc., Chem. Commun. 1982, 859.
86. Pringle, P.G.; Shaw, B.L. J. Chem. Soc., Chem. Commun. 1982, 956.
87. Pringle, P.G.; Shaw, B.L. J. Chem. Soc., Chem. Commun. 1982, 1313.
88. Langrick, C.R.; Pringle, P.G.; Shaw, B.L. Inorg. Chim. Acta 1983, **76**, L263.
89. Cooper, G.R.; Hutton, A.T.; McEwan, D.M.; Pringle, P.G.; Shaw, B.L. Inorg. Chim. Acta 1983, **76**, L267.
90. Hutton, A.T.; Pringle, P.G.; Shaw, B.L. Organometallics 1983, **2**, 1889.

91. Fukuzumi, S.; Nishizawa, N.; Tanaka, T. Bull. Chem. Soc. Jpn. 1982, 55, 2886.
92. Fukuzumi, S.; Nishizawa, N.; Tanaka, T. Bull. Chem. Soc. Jpn. 1982, 55, 2892.
93. Mondal, J.O.; Young, K.G.; Blake, D.M. J. Organomet. Chem. 1982, 240, 447.
94. Kubiak, C.P.; Woodcock, C.; Eisenberg, R. Inorg. Chem. 1980, 19, 2733.
95. Holloway, R.G.; Penfold, B.R.; Colton, R.; McCormick, M.J. J. Chem. Soc., Chem. Commun. 1976, 485.
96. Olmstead, M.M.; Hope, H.; Benner, L.S.; Balch, A.L. J. Am. Chem. Soc. 1977, 99, 5502.
97. Benner, L.S.; Balch, A.L.; J. Am. Chem. Soc. 1978, 100, 6099.
98. Benner, L.S.; Olmstead, M.M.; Hope, H.; Balch, A.L. J. Organomet. Chem. 1978, 153, C31.
99. Balch, A.L.; Benner, L.S.; Olmstead, M.M. Inorg. Chem. 1979, 18, 2996.
100. Brant, P.; Benner, L.S.; Balch, A.L. Inorg. Chem., 1979, 18, 3422.
101. Olmstead, M.M.; Benner, L.S.; Hope, H.; Balch, A.L. Inorg. Chim. Acta 1979, 32, 193.
102. Lindsay, C.H.; Benner, L.S.; Balch, A.L. Inorg. Chem. 1980, 19, 3503.

103. Lindsay, C.H.; Balch, A.L. Inorg. Chem. 1981, 20, 2267.
104. Balch, A.L.; Hunt, C.T.; Lee, C.-L.; Olmstead, M.M.; Farr, J.P. J. Am. Chem. Soc. 1981, 103, 3764.
105. Lee, C.-L.; Hunt, C.T.; Balch, A.L. Inorg. Chem. 1981, 20, 2498.
106. Olmstead, M.M.; Farr, J.P.; Balch, A.L. Inorg. Chim. Acta 1981, 52, 47.
107. Hunt, C.T.; Balch, A.L. Inorg. Chem. 1982, 21, 1242.
108. Hunt, C.T.; Balch, A.L. Inorg. Chem. 1982, 21, 1641.
109. Lee, C.-L.; Hunt, C.T.; Balch, A.L. Organometallics 1982, 1, 824.
110. Rattray, A.D.; Sutton, D. Inorg. Chim. Acta 1978, 27, L85.
111. Taylor, S.T.; Maitlis, P.M. J. Am. Chem. Soc. 1978, 100, 4700.
112. Hughes, J.G.; Robson, R. Inorg. Chim. Acta 1979, 35, 87.
113. Pringle, P.G.; Shaw, B.L. J. Chem. Soc., Chem. Commun. 1982, 81.
114. Pringle, P.G.; Shaw, B.L. J. Chem. Soc., Dalton Trans. 1983, 889.
115. Grossel, M.C.; Brown, M.P.; Nelson, C.D.; Yavari, A.; Kallas, E.; Moulding, R.P.; Seddon, K.R. J. Organomet. Chem. 1982, 232, C13.

116. Appleton, T.G.; Bennett, M.A.; Tomkins, I.B. J. Chem. Soc., Dalton Trans. 1976, 439.
117. Brown, M.P.; Puddephatt, R.J.; Rashidi, M. Inorg. Chim. Acta 1976, 19, L33.
118. Brown, M.P.; Puddephatt, R.J.; Rashidi, M.; Seddon, K.R. Inorg. Chim. Acta 1977, 23, L27.
119. Brown, M.P.; Puddephatt, R.J.; Rashidi, M.; Manojlovic-Muir, I.; Muir, K.W.; Solomun, T.; Seddon, K.R. Inorg. Chim. Acta 1977, 23, L33.
120. Brown, M.P.; Puddephatt, R.J.; Rashidi, M.; Seddon, K.R. J. Chem. Soc., Dalton Trans. 1977, 951.
121. Brown, M.P.; Puddephatt, R.J.; Rashidi, M.; Seddon, K.R. J. Chem. Soc., Dalton Trans. 1978, 516.
122. Brown, M.P.; Fisher, J.R.; Franklin, S.J.; Puddephatt, R.J.; Seddon, K.R. J. Organomet. Chem. 1978, 161, C46.
123. Brown, M.P.; Puddephatt, R.J.; Rashidi, M.; Seddon, K.R. J. Chem. Soc., Dalton Trans. 1978, 1540.
124. Brown, M.P.; Fisher, J.R.; Franklin, S.J.; Puddephatt, R.J.; Seddon, K.R. J. Chem. Soc., Chem. Commun. 1978, 749.
125. Brown, M.P.; Fisher, J.R.; Puddephatt, R.J.; Seddon, K.R. Inorg. Chem. 1979, 18, 2808.
126. Brown, M.P.; Franklin, S.J.; Puddephatt, R.J.; Thomson, M.A.; Seddon, K.R. J. Organomet. Chem. 1979, 178, 281.

127. Brown, M.P.; Fisher, J.R.; Manojlovic-Muir, Lj.;
Muir, K.W.; Puddephatt, R.J.; Thomson, M.A.; Seddon,
K.R. J. Chem. Soc., Chem. Commun. 1979, 931.
128. Brown, M.P.; Cooper, S.J.; Puddephatt, R.J.; Thomson,
M.A.; Seddon, K.R. J. Chem. Soc., Chem. Commun. 1979,
1117.
129. Brown, M.P.; Fisher, J.R.; Mills, A.J.; Puddephatt,
R.J.; Thomson, M.A. Inorg. Chim. Acta 1980, 44, 271.
130. Brown, M.P.; Cooper, S.J.; Frew, A.A.;
Manojlovic-Muir, Lj.; Muir, K.W.; Puddephatt, R.J.;
Thomson, M.A. J. Organomet. Chem. 1980, 198, C33.
131. Cooper, S.J.; Brown, M.P.; Puddephatt, R.J. Inorg.
Chem. 1981, 20, 1374.
132. Brown, M.P.; Cooper, S.J.; Frew, A.A.;
Manojlovic-Muir, Lj.; Muir, K.W.; Puddephatt, R.J.;
Seddon, K.R.; Thomson, M.A. Inorg. Chem. 1981, 20,
1500.
133. Bancroft, G.M.; Chan, T.; Puddephatt, R.J.; Brown,
M.P. Inorg. Chim. Acta 1981, 53, L119.
134. Puddephatt, R.J.; Thomson, M.A.; Manojlovic-Muir,
Lj.; Muir, K.W.; Frew, A.A.; Brown, M.P. J. Chem.
Soc., Chem. Commun. 1981, 805.
135. Brown, M.P.; Fisher, J.R.; Hill, R.H.; Puddephatt,
R.J.; Seddon, K.R. Inorg. Chem. 1981, 20, 3516.

136. Brown, M.P.; Fisher, J.R.; Franklin, S.J.;
Puddephatt, R.J.; Thomson, M.A. Adv. Chem. Ser. 1982,
196, 231.
137. Brown, M.P.; Cooper, S.J.; Frew, A.A.;
Manojlovic-Muir, Lj.; Muir, K.W.; Puddephatt, R.J.;
Thomson, M.A. J. Chem. Soc., Dalton Trans. 1982,
299.
138. Azam, K.A.; Brown, M.P.; Cooper, S.J.; Puddephatt,
R.J. Organometallics 1982, 1, 1183.
139. Fisher, J.R.; Mills, A.J.; Sumner, S.; Brown, M.P.;
Thomson, M.A.; Puddephatt, R.J.; Frew, A.A.;
Manojlovic-Muir, Lj.; Muir, K.W. Organometallics
1982, 1, 1421.
140. Azam, K.A.; Puddephatt, R.J.; Brown, M.P.; Yavari, A.
J. Organomet. Chem. 1982, 234, C31.
141. Puddephatt, R.J.; Azam, K.A.; Hill, R.H.; Brown,
M.P.; Nelson, C.D.; Moulding, R.P.; Seddon, K.R.;
Grossel, M.C. J. Am. Chem. Soc. 1983, 105, 5642.
142. Hill, R.H.; Puddephatt, R.J. Inorg. Chim. Acta 1981,
54, L277.
143. Puddephatt, R.J.; Thomson, M.A. Inorg. Chem. 1982,
21, 725.
144. Azam, K.A.; Frew, A.A.; Manojlovic-Muir, Lj.; Muir,
K.W.; Puddephatt, R.J. J. Chem. Soc., Chem. Commun.
1982, 614.

145. Hill, R.H.; DeMayo, P.; Puddephatt, R.J. Inorg. Chem. 1982, **21**, 3642.
146. Puddephatt, R.J.; Thomson, M.A. J. Organomet. Chem. 1982, **238**, 231.
147. Azam, K.A.; Puddephatt, R.J. Organometallics 1983, **2**, 1396.
148. Hill, R.H.; Puddephatt, R.J. Organometallics 1983, **2**, 1472.
149. Hill, R.H.; Puddephatt, R.J. J. Am. Chem. Soc. 1983, **105**, 5797.
150. Grossel, M.C.; Moulding, R.P.; Seddon, K.R. Inorg. Chim. Acta 1982, **64**, L275.
151. Grossel, M.C.; Moulding, R.P.; Seddon, K.R. J. Organomet. Chem. 1983, **247**, C32.
152. Manojlovic-Muir, Lj.; Muir, K.W.; Solomun, T. Acta Crystallogr., Sect. B 1979, **B35**, 1237.
153. Manojlovic-Muir, Lj.; Muir, K.W.; Solomun, T. J. Organomet. Chem. 1979, **179**, 479.
154. Frew, A.A.; Manojlovic-Muir, Lj.; Muir, K.W. J. Chem. Soc., Chem. Commun. 1980, 624.
155. Manojlovic-Muir, Lj.; Muir, K.W. J. Chem. Soc., Chem. Commun. 1982, 1155.
156. Chin, C.-S.; Sennett, M.S.; Wier, P.J.; Vaska, L. Inorg. Chim. Acta 1978, **31**, L443.

157. Anderson, G.K.; Clark, H.C.; Davies, J.A. J. Organomet. Chem. 1981, **210**, 135.
158. Cameron, T.S.; Gardner, P.A.; Grundy, K.R. J. Organomet. Chem. 1981, **212**, C19.
159. Morris, R.H.; Foley, H.C.; Targos, T.S.; Geoffroy, G.L. J. Am. Chem. Soc. 1981, **103**, 7337.
160. Geoffroy, G.L. ACS Symp. Ser. 1982, **198**, 347.
161. Pringle, P.G.; Shaw, B.L. J. Chem. Soc., Chem. Commun. 1982, 581.
162. McDonald, W.S.; Pringle, P.G.; Shaw, B.L. J. Chem. Soc., Chem. Commun. 1982, 861.
163. McEwan, D.M.; Pringle, P.G.; Shaw, B.L. J. Chem. Soc., Chem. Commun. 1982, 1240.
164. Blagg, A.; Hutton, A.T.; Pringle, P.G.; Shaw, B.L. Inorg. Chim. Acta 1983, **76**, L265.
165. Nutt, M.O. M.S. Thesis, Tulane University, 1969.
166. Gladfelter, W.L.; Geoffroy, G.L. Adv. Organomet. Chem. 1980, **18**, 207.
167. Fawcett, J.P.; Poe, A.J.; Sharma, K.R. J. Am. Chem. Soc. 1976, **98**, 1401.

Chapter II

The Synthesis and Characterization of Some Binuclear Rhodium Complexes Containing Bridging Acetylene Ligands, and the X-ray Crystal Structure of $[\text{Rh}_2\text{Cl}_2(\mu\text{-CF}_3\text{C}_2\text{CF}_3)(\text{Ph}_2\text{PCH}_2\text{PPh}_2)_2]$.

Introduction

A major theme in the research interests of this group has concerned the chemistry of small molecules with transition metal complexes.¹⁻¹² In particular, our efforts over the past six years have concentrated on such chemistry in complexes with metals held in close proximity to each other by bridging DPM ligands. In such complexes, we encounter the possibility of cooperative binding and activation of substrate molecules by both metals, as was briefly discussed in Chapter I. Cooperativity of metals has important implications for reactions catalysed by multinuclear complexes.

At the time that this work was undertaken, the chemistry of similar binuclear complexes with small molecules such as CO, SO₂ and H₂ was being actively studied by several other groups (most notably those of Professors

Balch, Eisenberg, Mague and Puddephatt),¹³ yet little had been reported regarding the chemistry of olefins and acetylenes with these binuclear complexes.¹⁴⁻¹⁶ We therefore undertook the present study into binuclear rhodium-acetylene complexes. Since this work was started, several studies involving acetylene coordination in similar binuclear rhodium,^{7,8,17-21} iridium,^{11,21} palladium^{22,23} and platinum²³⁻²⁵ complexes have been reported or are known to be underway. We were particularly interested in complexes in which the acetylene molecule was simultaneously coordinated to both metals, and, more specifically, in such complexes that were also coordinatively unsaturated, having as few ancillary ligands as possible. Such coordinative unsaturation is important for the subsequent reactivity of these compounds.²⁶

Complexes of the type $[\text{Rh}_2\text{X}_2(\mu\text{-acetylene})(\text{DPM})_2]$ were chosen as a reasonable starting point for these studies. Such species would be analogues of two closely related series of complexes prepared and studied in this group, namely $[\text{Rh}_2\text{X}_2(\mu\text{-CO})(\text{DPM})_2]$ ^{4-7,9,10,12} and $[\text{Rh}_2\text{X}_2(\mu\text{-SO}_2)(\text{DPM})_2]$ ², and to two of the few similar acetylene-bridged complexes known at the time, $[\text{Pd}_2\text{Cl}_2(\mu\text{-CF}_3\text{C}_2\text{CF}_3)(\text{DPM})_2]$ ^{15,22} and $[\text{Co}_2(\text{CO})_2(\mu\text{-PhC}_2\text{Ph})(\text{Ph}_2\text{AsCH}_2\text{AsPh}_2)_2]$.²⁷ One aspect of interest in binuclear, acetylene-bridged complexes concerns their acetylene binding modes; the two

possibilities commonly encountered are seen in these palladium and cobalt systems. In $[\text{Pd}_2\text{Cl}_2(\mu\text{-CF}_3\text{C}_2\text{CF}_3)(\text{DPM})_2]$ the acetylene group is bound parallel to the Pd-Pd axis, and may be regarded as a cis-dimetalated olefin, while in $[\text{Co}_2(\text{CO})_2(\mu\text{-PhC}_2\text{Ph})\text{-}(\text{Ph}_2\text{AsCH}_2\text{AsPh}_2)_2]$ the acetylene is bound perpendicular to the Co-Co bond, in a pseudotetrahedral geometry. What the factors are that favour one acetylene binding mode over the other are not clear, although it is naturally of interest to establish these factors and to determine how the different binding modes affect the subsequent chemistry of the acetylene moiety.²⁸⁻³²

One of the proposed species, $[\text{Rh}_2\text{Cl}_2(\mu\text{-CF}_3\text{C}_2\text{CF}_3)\text{-}(\text{DPM})_2]$, would be very similar to the known complex $[\text{Pd}_2\text{Cl}_2(\mu\text{-CF}_3\text{C}_2\text{CF}_3)(\text{DPM})_2]$,^{15,22} differing only in the metals. It was therefore of interest to compare these compounds, especially with regard to the binding of the acetylene ligands. There are two obvious structural possibilities for the rhodium complex, which has two electrons less than the palladium analogue; like the palladium species, it could have the acetylene bound as a cis-dimetalated olefin, but this time accompanied by a metal-metal bond, or it could have the acetylene bound perpendicular to the metal-metal axis, with no metal-metal bond present.

This chapter describes the preparation and characterization of some $[\text{Rh}_2\text{X}_2(\mu\text{-acetylene})(\text{DPM})_2]$ complexes, including the X-ray structural determination for one of these compounds, which was carried out in order to establish unambiguously the acetylene binding mode in these species. Some of the subsequent chemistry of these species will be presented in Chapter III.

Experimental

All non-aqueous solvents were deoxygenated and dried, either by distilling them over the appropriate drying agents under an atmosphere of N_2 (see Table I) or, for the cases

Table I. Solvents and Drying Agents

$CHCl_3$	P_2O_5
CH_2Cl_2	P_2O_5
THF	Na/benzophenone
CH_3OH	CH_3ONa
Et_2O	molecular sieves
C_6H_6	molecular sieves

of ether and benzene, by placing them over molecular sieves and bubbling a stream of N_2 through them. Water was also deoxygenated by bubbling a stream of N_2 through it. All reactions were routinely performed under Schlenk conditions using an atmosphere of either N_2 or the reactant gas. Bis(diphenylphosphino)methane (Strem), hydrated rhodium chloride (Research Organic/Inorganic Chemicals or

Engelhard), hexafluoro-2-butyne (Pierce Chemicals or PCR Research Chemicals), dimethyl acetylenedicarboxylate (Aldrich) and potassium iodide (BDH) were used as received. $[\text{RhCl}(\text{C}_8\text{H}_{12})]_2$ was prepared by the reported procedure.³³ Infrared spectra were run as Nujol mulls on KBr plates utilizing Perkin-Elmer 467 or Nicolet 7199 IR spectrometers, and $^{31}\text{P}\{^1\text{H}\}$ spectra were run at 36.4 MHz on a Bruker HFX-90 NMR spectrometer at -40°C .

Preparation of Compounds

i) $[\text{Rh}_2\text{Cl}_2(\mu\text{-CF}_3\text{C}_2\text{CF}_3)(\text{DPM})_2]$, 1: 200 mg (0.406 mmol) of $[\text{RhCl}(\text{C}_8\text{H}_{12})]_2$ and 302 mg (0.786 mmol) of ground bis(diphenylphosphino)methane (DPM) were dissolved in 10 mL of CH_2Cl_2 and a stream of gaseous hexafluoro-2-butyne (HFB) was passed over the stirring solution. The orange solution turned dark green almost immediately, but was left under an atmosphere of HFB for several hours. A green solid was precipitated in about 75% yield by the addition of diethyl ether. The infrared spectrum showed an acetylene stretch at 1638 cm^{-1} but was otherwise rather uninformative. The molar conductivity of a 1.00 mM solution of 1 in CH_2Cl_2 was $0.9\ \Omega^{-1}\text{ cm}^2\text{ mol}^{-1}$, the $^{31}\text{P}\{^1\text{H}\}$ NMR spectrum displayed a resonance at 7.5 ppm (positive chemical shifts are downfield of H_3PO_4) with a splitting of 112.0 Hz between

the two major peaks and the ^{19}F NMR spectrum contained one sharp singlet at -49.93 ppm (positive chemical shifts are downfield of CFCl_3). The ^1H NMR spectrum contained a complex multiplet in the phenyl region (7.03 - 7.62 ppm δ , 40 H) and two higher-field multiplets corresponding to two methylene hydrogen resonances (3.59 ppm δ , 2H; 2.92 ppm δ , 2H). Elemental analyses were consistent with the above formulation. (Found: C, 52.78; H, 3.49; F, 9.07; Cl, 8.01. Calculated for $\text{Rh}_2\text{Cl}_2\text{P}_4\text{F}_6\text{C}_{54}\text{H}_{44}$: C, 53.71; H, 3.67; F, 9.44; Cl, 5.87.)

ii) $[\text{Rh}_2\text{I}_2(\mu\text{-CF}_3\text{C}_2\text{CF}_3)(\text{DPM})_2]$, 2: 200 mg (0.166 mmol) of $[\text{Rh}_2\text{Cl}_2(\mu\text{-HFB})(\text{DPM})_2]$ and 300 mg (1.81 mmol) of KI were placed in a flask under N_2 , then 10 mL CH_2Cl_2 and 10 mL CH_3OH were added. The colour of the resulting suspension changed from green to dark brown within 15 minutes. This mixture was stirred overnight, then most of the solvent was removed by a stream of N_2 . The brown powder was dissolved in 10 mL CH_2Cl_2 , then KCl and KI were removed by two extractions with 10 mL of water. CH_2Cl_2 and residual water were removed by N_2 stream, then by vacuum. Samples for elemental analysis and conductivity were recrystallized from CH_2Cl_2 /ether. The infrared spectrum showed an acetylene stretch at 1635 cm^{-1} , the molar conductivity of a 1.00 mM solution in CH_2Cl_2 was $\leq 0.4\ \Omega^{-1}\text{ cm}^2\text{ mol}^{-1}$, and the

$^{31}\text{P}\{^1\text{H}\}$ NMR spectrum showed a resonance centred at 9.1 ppm with a major-doublet splitting of 110.0 Hz. The ^{19}F NMR spectrum showed a sharp singlet at -50.03 ppm and the ^1H NMR spectrum consisted of three sets of peaks as for 1 (complex multiplet, 6.97-7.70 ppm, 40H; multiplet, 4.14 ppm, 2H; multiplet, 3.22 ppm, 2H). Elemental analysis was consistent with the above formulation. (Found: C, 46.69; H, 3.20; F, 8.03; I, 14.27. Calculated for $\text{Rh}_2\text{I}_2\text{P}_4\text{F}_6\text{C}_{54}\text{H}_{44}$: C, 46.65; H, 3.29; F, 8.20; I, 18.25.)

iii) $[\text{Rh}_2\text{Cl}_2(\mu\text{-CH}_3\text{O}_2\text{CC}_2\text{CO}_2\text{CH}_3)(\text{DPM})_2]$, 3: 100 μL (0.813 mmol) of $\text{CH}_3\text{O}_2\text{CC}_2\text{CO}_2\text{CH}_3$ (DMA) was added to a flask containing 200 mg (0.406 mmol) $[\text{RhCl}(\text{C}_8\text{H}_{12})]_2$ and 302 mg (0.786 mmol) DPM under N_2 . Three mL of CH_2Cl_2 was added immediately, whereupon the solution became dark green. After stirring for 15 minutes, 10 mL of ether was added to the suspension and the light green solid was filtered off and recrystallized from CH_2Cl_2 /ether. The infrared spectrum showed a broad organic carboxylate stretch at 1705 cm^{-1} and a stretch attributed to the coordinated acetylene moiety at 1610 cm^{-1} . The conductivity of a 1.00 mM CH_2Cl_2 solution was $\leq 0.4 \Omega^{-1} \text{cm}^2 \text{mol}^{-1}$ and the $^{31}\text{P}\{^1\text{H}\}$ NMR spectrum showed a resonance centred at 8.6 ppm with a separation of 115.0 Hz between the two major peaks. The ^1H NMR spectrum revealed a sharp singlet at 2.64 ppm

attributable to the two equivalent DMA methyl groups as well as DPM phenyl and methylene resonances in the appropriate regions (complex multiplet, 7.01-7.70 ppm, 40H; multiplet, 3.64 ppm, 2H; multiplet, 2.87 ppm, 2H). Elemental analyses were consistent with the above formulation. (Found: C, 55.33; H, 4.25; Cl, 6.14. Calculated for $\text{Rh}_2\text{Cl}_2\text{P}_4\text{O}_4\text{C}_{56}\text{H}_{50}$: C, 56.64; H, 4.24; Cl, 5.97.)

X-ray Data Collection

Crystals of $[\text{Rh}_2\text{Cl}_2(\mu\text{-HFB})(\text{DPM})_2]$, 1, suitable for a single-crystal X-ray study were obtained by the slow diffusion of diethyl ether into a saturated CH_2Cl_2 solution of 1 under an atmosphere of HFB. One of these dark green crystals was mounted in air on a glass fibre. Preliminary film data showed that the crystal belonged to the tetragonal system with diffraction symmetry $4/m$ and extinctions $(00l:l \neq 4n)$, characteristic of space groups $P4_1$ and $P4_3$. Accurate cell parameters were obtained by a least-squares analysis of 12 carefully centred reflections chosen from diverse regions of reciprocal space ($50^\circ < 2\theta < 65^\circ$, $\text{CuK}\alpha$ radiation) and obtained using a narrow X-ray source. See Table II for pertinent crystal and data collection details. The width at half height of several

strong reflections (ω scan, open counter) lay in the range 0.08-0.09°.

Data were collected on an automated Picker four-circle diffractometer equipped with a scintillation counter and pulse height analyser tuned to accept 90% of the $\text{CuK}\alpha$ peak. Background counts were measured at both ends of the scan range with crystal and counter stationary. The intensities of three standard reflections were measured every 100 reflections throughout the data collection. A second set of four standards was monitored twice a day. No significant decay in any of the standards was observed over the course of the data collection. The intensities of 5944 unique reflections ($3^\circ \leq 2\theta \leq 120^\circ$) were measured using $\text{CuK}\alpha$ radiation and the data were processed in the usual manner, correcting for Lorentz and polarization effects. The standard deviations in the measured F^2 values were calculated using a value of 0.05 for p .³⁴ A total of 5243 reflections had $F_o^2 > 3\sigma(F_o^2)$ and were used in subsequent calculations. Absorption corrections were applied to the data using Gaussian integration.³⁵

Structure Solution and Refinement.

The structure was solved in space group $P4_1$, using a sharpened Patterson synthesis to locate the two independent

Rh atoms. Subsequent refinements and difference Fourier syntheses led to the location of all remaining non-hydrogen atoms. In the full-matrix least-squares refinements the function which was minimized was

$$D = \sum_{hkl} w_{hkl} (|F_o| - |kF_c|)^2$$

where k is the inverse of the scale factor used to bring the data to absolute units and w is the weighting factor and equals $1/\sigma^2(F_o(hkl))^2$. Atomic scattering factors were taken from Cromer and Waber's tabulation³⁶ for all atoms except hydrogen for which the values of Stewart et al³⁷ were used. Anomalous dispersion terms³⁸ for Rh, Cl, P and F were included in F_c . All phenyl ring carbon atoms were refined as rigid groups having idealized D_{6h} symmetry and C-C distances of 1.392 Å. The carbon atoms were given independent isotropic thermal parameters. The hydrogen atoms were included as fixed contributions and not refined. Their idealized positions were calculated from the geometries of their attached carbon atoms using a C-H distance of 0.95 Å. These hydrogen atoms were assigned isotropic thermal parameters of 1 Å² greater than those of their attached carbon atoms. All other non-group atoms were refined individually with anisotropic thermal parameters. Initial refinements were carried out in space

group $P4_1$, converging to $R = 0.056$ and $R_w = 0.082$.³⁹ Refining in the enantiomeric space group $P4_3$ resulted in the significantly improved crystallographic residuals $R = 0.044$ and $R_w = 0.062$, indicating that the latter was probably the correct choice. Since both of the possible space groups are polar and, with atoms displaying high anomalous scattering, can give rise to polar dispersion errors,^{40,41} significant differences in bond lengths were observed between the two space groups. In $P4_3$ the chemically equivalent P-C_{phenyl} distances, for example, showed a narrower range (1.822(5) to 1.844(5) Å) than those in $P4_1$ (1.808(7) to 1.852(7) Å), offering further confirmation that $P4_3$ is the correct choice. At this stage of refinement a comparison of the observed and calculated structure amplitudes of strong, low angle reflections suggested that they suffered from extinction effects. Application of an isotropic secondary extinction correction⁴² yielded $R = 0.040$ and $R_w = 0.055$ and greatly improved the agreement between $|F_o|$ and $|F_c|$ in the affected reflections. The highest 20 residual peaks on a final electron density difference map (0.78 - 0.50 eÅ⁻³) were all in the vicinities of the phenyl groups. A typical carbon atom on earlier Fourier syntheses had an electron density of about 2.3 eÅ⁻³.

The final positional and thermal parameters of the non-hydrogen atoms and the group atoms are given in Tables III and IV, respectively. The idealized hydrogen parameters are given in Table V and a listing of the observed and calculated structure factor amplitudes is available.⁴³

Results

Table II. Summary of Crystal Data and Intensity Collection
Details for $[\text{Rh}_2\text{Cl}_2(\mu\text{-HFB})(\text{DPM})_2]$

compound	$[\text{Rh}_2\text{Cl}_2(\mu\text{-HFB})(\text{DPM})_2]$
formula weight	1207.5
formula	$\text{Rh}_2\text{Cl}_2\text{P}_4\text{F}_6\text{C}_{54}\text{H}_{44}$
cell parameters	
a, Å	21.283(1) Å
c, Å	14.255(1) Å
z	4
v, Å ³	6457.3
density, g/cm ³	1.242 (calculated), 1.244 (measured by flotation)
space group	$P4_3$
crystal dimensions, mm	0.28x0.40x0.42 [†]
crystal shape	tetragonal prism with 20 faces of the forms: {100}, {110}, {101}, {111}, {310}, {410}, {122}, {113}.
crystal volume, mm ³	0.0213
temperature, °C	23
radiation	Cu K α
μ , cm ⁻¹	63.587

(continued...)

Table II. (continued)

range in absorption correction factors	0.179-0.341
receiving aperture, mm	3x4 (at 30 cm from crystal)
takeoff angle, deg	3.0
scan speed, deg/min	2 in 2θ
scan range, deg	0.95 below $K\alpha_1$ to 0.95 above $K\alpha_2$
background counting times, s	10, $2.5^\circ < 2\theta < 61^\circ$; 20, $61^\circ < 2\theta < 95^\circ$; 40, $95^\circ < 2\theta < 120^\circ$,
2θ limits, deg	$2.5 < 2\theta < 120$
unique data measured	5944
unique data used	5243
$(F_o^2 > 3\sigma(F_o^2))$	
final number of parameters varied	278
error in observation of unit weight (GOF)	1.530
R	0.040
R_w	0.055

Table III. Positional and Thermal Parameters for the Non-Group Atoms of $[\text{Rh}_2\text{Cl}_2(\mu\text{-HFB})(\text{DPM})_2]$.

Atom	^a			^b			U11	U22	U33	U12	U13	U23
	x	y	z	U11	U22	U33	U12	U13	U23	U12	U13	U23
Rh(1)	-0.00175(3)	0.28686(3)	0	4.62(4)	3.64(4)	4.55(4)	-0.08(3)	0.01(3)	0.08(3)	-0.08(3)	0.01(3)	0.08(3)
Rh(2)	0.06543(3)	0.37793(3)	0.09233(6)	5.45(4)	3.74(4)	4.13(4)	0.15(3)	-0.16(3)	-0.24(3)	0.15(3)	-0.16(3)	-0.24(3)
Cl(1)	-0.0941(1)	0.2242(1)	-0.0144(2)	5.8(1)	5.0(1)	7.6(2)	-0.9(1)	-1.1(1)	0.3(1)	-0.9(1)	-1.1(1)	0.3(1)
Cl(2)	0.0686(1)	0.4453(1)	0.2252(2)	9.4(2)	5.6(1)	5.3(2)	0.8(1)	-0.9(1)	-1.4(1)	0.8(1)	-0.9(1)	-1.4(1)
P(1)	-0.0545(1)	0.3638(1)	-0.0838(2)	5.2(1)	4.1(1)	4.4(1)	-0.0(1)	-0.2(1)	0.3(1)	-0.0(1)	-0.2(1)	0.3(1)
P(2)	0.0258(1)	0.46142(10)	0.0027(2)	5.8(1)	3.8(1)	4.3(1)	-0.24(9)	-0.0(1)	0.2(1)	-0.24(9)	-0.0(1)	0.2(1)
P(3)	0.0434(1)	0.2027(1)	0.0739(2)	4.7(1)	3.8(1)	4.8(1)	0.18(9)	0.1(1)	-0.0(1)	0.18(9)	0.1(1)	-0.0(1)
P(4)	0.1156(1)	0.3027(1)	0.1819(2)	6.3(2)	4.3(1)	5.0(2)	0.5(1)	-1.1(1)	-0.4(1)	0.5(1)	-1.1(1)	-0.4(1)
F(1)	0.1158(4)	0.3113(3)	-0.2223(4)	17.2(7)	7.0(4)	5.6(4)	-1.8(4)	4.1(4)	0.0(3)	-1.8(4)	4.1(4)	0.0(3)
F(2)	0.0458(3)	0.2424(3)	-0.1952(4)	8.6(4)	9.3(4)	7.1(4)	-1.4(4)	0.2(3)	-3.1(4)	-1.4(4)	0.2(3)	-3.1(4)
F(3)	0.1389(3)	0.2282(3)	-0.1460(5)	8.4(4)	7.9(4)	9.1(5)	1.9(3)	2.1(4)	-1.3(4)	1.9(3)	2.1(4)	-1.3(4)
F(4)	0.1757(3)	0.4098(3)	-0.1192(5)	8.2(4)	9.4(5)	9.4(5)	-2.4(4)	1.7(4)	2.0(4)	-2.4(4)	1.7(4)	2.0(4)
F(5)	0.2161(3)	0.3251(3)	-0.0660(6)	6.2(4)	8.2(4)	17.9(8)	0.6(3)	2.7(5)	-2.4(5)	0.6(3)	2.7(5)	-2.4(5)
F(6)	0.2028(3)	0.4041(3)	0.0220(5)	6.4(4)	8.7(4)	10.6(5)	-2.7(3)	0.3(4)	-1.3(4)	-2.7(3)	0.3(4)	-1.3(4)
C(1)	0.0942(5)	0.2734(4)	-0.1563(8)	7.9(7)	5.2(6)	5.3(6)	0.1(5)	0.8(6)	0.1(5)	0.1(5)	0.8(6)	0.1(5)
C(2)	0.0784(4)	0.3056(4)	-0.0668(7)	5.5(5)	4.4(5)	5.5(6)	0.8(4)	0.8(5)	-0.0(4)	0.8(4)	0.8(5)	-0.0(4)
C(3)	0.1117(4)	0.3474(4)	-0.0207(6)	4.3(5)	4.9(5)	5.3(6)	0.4(4)	-0.7(4)	-0.2(4)	0.4(4)	-0.7(4)	-0.2(4)
C(4)	0.1758(5)	0.3714(5)	-0.0448(8)	6.7(6)	5.4(6)	6.3(7)	0.8(5)	1.2(6)	-0.7(5)	0.8(5)	1.2(6)	-0.7(5)
C(5)	-0.0070(4)	0.4328(4)	-0.1082(6)	6.0(5)	3.8(4)	4.3(5)	-0.4(4)	0.2(4)	0.5(4)	-0.4(4)	0.2(4)	0.5(4)
C(6)	0.1244(4)	0.2278(4)	0.1228(6)	4.5(5)	3.9(4)	4.4(5)	0.4(4)	-0.1(4)	0.3(4)	0.4(4)	-0.1(4)	0.3(4)

^a Estimated standard deviations in the least significant figures are given in parentheses in this and all subsequent tables.

^b The form of the thermal ellipsoid is: $\exp[-2\pi i \{a^*U11h + b^*U22k + c^*U33l + 2a^*b^*U12hk + 2a^*c^*U13hl + 2b^*c^*U23kl\}]$. The quantities given in the table are the thermal coefficients $\times 10^3$.

Table IV. Derived Parameters for the Rigid Group Atoms of $[\text{Rh}_2\text{Cl}_2(\mu\text{-HFB})(\text{DPM})_2]$.

Atom	x	y	z	B(A ²)	Atom	x	y	z	B(A ²)
C(11)	-0.0831(8)	0.3406(3)	-0.1992(9)	4.3(2)	C(151)	0.0720(4)	0.1380(3)	-0.0032(5)	3.7(2)
C(12)	-0.0479(3)	0.3525(3)	-0.280(1)	5.2(2)	C(152)	0.1298(3)	0.1081(3)	0.0052(5)	4.3(2)
C(13)	-0.0696(8)	0.3323(4)	-0.3667(5)	6.2(3)	C(153)	0.1468(2)	0.0614(3)	-0.0583(4)	4.8(2)
C(14)	-0.1264(8)	0.3004(3)	-0.3734(9)	6.3(3)	C(154)	0.1058(4)	0.0446(3)	-0.1302(5)	5.6(2)
C(15)	-0.1616(3)	0.2885(3)	-0.293(1)	6.3(3)	C(155)	0.0479(3)	0.0746(3)	-0.1386(5)	5.5(2)
C(16)	-0.1400(8)	0.3086(4)	-0.2059(5)	5.3(2)	C(156)	0.0310(2)	0.1213(3)	-0.0751(4)	4.4(2)
C(21)	-0.1254(5)	0.3945(3)	-0.0281(4)	4.3(2)	C(161)	0.0106(5)	0.1636(3)	0.1737(6)	4.3(2)
C(22)	-0.1589(6)	0.4427(3)	-0.0711(6)	6.3(3)	C(162)	-0.0473(4)	0.1839(3)	0.2072(6)	5.1(2)
C(23)	-0.2126(4)	0.4669(3)	-0.0386(7)	7.0(3)	C(163)	-0.0740(5)	0.1554(3)	0.2855(4)	6.0(3)
C(24)	-0.2328(5)	0.4427(3)	0.0570(4)	7.6(3)	C(164)	-0.0427(5)	0.1065(3)	0.3304(6)	7.1(3)
C(25)	-0.1994(6)	0.3945(3)	0.1000(6)	6.8(3)	C(165)	0.0153(4)	0.0861(3)	0.2969(6)	7.2(3)
C(26)	-0.1457(4)	0.3703(3)	0.0574(7)	5.2(2)	C(166)	0.0420(5)	0.1147(3)	0.2186(4)	5.9(3)
C(31)	0.0867(3)	0.5169(3)	-0.0337(8)	4.1(2)	C(171)	0.1958(6)	0.3224(5)	0.2167(9)	5.3(2)
C(32)	0.1348(5)	0.5713(3)	0.0288(8)	5.3(2)	C(172)	0.2475(7)	0.2945(5)	0.1735(7)	7.1(3)
C(33)	0.1820(3)	0.5731(4)	0.0027(4)	7.3(3)	C(173)	0.3081(6)	0.3113(5)	0.2005(8)	10.7(5)
C(34)	0.1810(3)	0.6006(3)	-0.0859(8)	7.3(3)	C(174)	0.3170(6)	0.3559(5)	0.2706(9)	13.8(6)
C(35)	0.1328(5)	0.5862(3)	-0.1484(8)	7.0(3)	C(175)	0.2654(7)	0.3838(5)	0.3137(7)	19.0(9)
C(36)	0.0857(3)	0.5444(4)	-0.1223(4)	5.7(2)	C(176)	0.2048(6)	0.3670(5)	0.2868(8)	11.8(6)
C(41)	-0.0358(3)	0.5133(3)	0.0470(4)	3.7(2)	C(181)	0.0793(8)	0.2822(4)	0.2942(8)	5.3(2)
C(42)	-0.0515(4)	0.5670(3)	-0.0034(4)	5.5(2)	C(182)	0.0197(6)	0.3053(4)	0.3153(8)	6.2(3)
C(43)	-0.0985(3)	0.6069(3)	0.0294(6)	6.4(3)	C(183)	-0.0102(7)	0.2869(4)	0.3976(5)	8.4(4)
C(44)	-0.1298(3)	0.5929(3)	0.1126(4)	6.0(3)	C(184)	0.0194(8)	0.2454(4)	0.4588(8)	9.0(4)
C(45)	-0.1140(4)	0.5392(3)	0.1630(4)	5.4(2)	C(185)	0.0789(6)	0.2223(4)	0.4377(9)	9.8(4)
C(46)	-0.0670(3)	0.4983(3)	0.1302(6)	4.6(2)	C(186)	0.1088(7)	0.2407(4)	0.3553(5)	8.5(4)

Rigid Group Parameters

Ring	a			b		
	Xc	Yc	Zc	Delta	Epsilon	Eta
Ring1	-0.1048(2)	0.3205(2)	-0.2863(4)	4.196(4)	1.322(9)	3.813(9)
Ring2	-0.1791(2)	0.4186(2)	0.0144(4)	-0.741(4)	0.859(6)	5.760(6)
Ring3	0.1338(2)	0.5587(2)	-0.0598(4)	4.005(4)	2.160(7)	1.392(7)
Ring4	-0.0828(2)	0.5531(2)	0.0798(3)	-0.549(4)	0.926(5)	5.488(4)
Ring5	0.0889(2)	0.0913(2)	-0.0667(3)	-0.762(4)	2.531(6)	1.732(5)
Ring6	-0.0160(2)	0.1350(2)	0.2520(4)	-0.721(4)	0.661(6)	0.620(6)
Ring7	0.2564(3)	0.3392(3)	0.2436(5)	2.332(6)	3.134(9)	0.38(1)
Ring8	0.0493(3)	0.2638(3)	0.3765(4)	-0.881(5)	0.709(9)	0.459(9)

a

b

Xc, Yc and Zc are the fractional coordinates of the centroid of the rigid group.
 The rigid group orientation angles Delta, Epsilon and Eta (radians) are the angles by which the rigid body is rotated with respect to a set of axes X, Y and Z. The origin is the centre of the ring; X is parallel to a*, Z is parallel to c and Y is parallel to the line defined by the intersection of the plane containing a* and b* with the plane containing b and c.

Table V. Idealized Positional and Thermal Parameters for the Hydrogen Atoms of
 $[\text{Rh}_2\text{Cl}_2(\mu\text{-HFB})(\text{DPM})_2]$.

Atom	x	y	z	B(A ²)	Atom	x	y	z	B(A ²)
H(1C5)	-0.0320	0.4646	-0.1362	4.74	H(45)	-0.1353	0.5298	0.2198	6.35
H(2C5)	0.0262	0.4221	-0.1501	4.74	H(46)	-0.0563	0.4628	0.1647	5.60
H(1C6)	0.1544	0.2317	0.0737	4.35	H(52)	0.1577	0.1195	0.0545	5.26
H(2C6)	0.1389	0.1971	0.1662	4.35	H(53)	0.1862	0.0409	-0.0523	5.76
H(12)	-0.0092	0.3743	-0.2748	6.21	H(54)	0.1174	0.0128	-0.1734	6.54
H(13)	-0.0455	0.3403	-0.4214	7.19	H(55)	0.0201	0.0633	-0.1877	6.32
H(14)	-0.1412	0.2865	-0.4328	7.32	H(56)	-0.0084	0.1419	-0.0809	5.46
H(15)	-0.2005	0.2666	-0.2976	7.32	H(62)	-0.0687	0.2174	0.1762	5.95
H(16)	-0.1642	0.3006	-0.1511	6.32	H(63)	-0.1135	0.1696	0.3082	6.94
H(22)	-0.1449	0.4590	-0.1301	7.15	H(64)	-0.0609	0.0872	0.3838	8.02
H(23)	-0.2353	0.4997	-0.0587	7.99	H(65)	0.0365	0.0527	0.3275	8.04
H(24)	-0.2694	0.4593	0.0854	8.66	H(66)	0.0814	0.1005	0.1955	6.90
H(25)	-0.2132	0.3782	0.1581	7.68	H(72)	0.2416	0.2638	0.1254	8.06
H(26)	-0.1229	0.3375	0.0867	6.09	H(73)	0.3434	0.2924	0.1711	11.72
H(32)	0.1354	0.5126	0.0893	6.31	H(74)	0.3580	0.3676	0.2890	14.45
H(33)	0.2147	0.5830	0.0452	8.35	H(75)	0.2709	0.4144	0.3611	20.08
H(34)	0.2131	0.6290	-0.1040	8.23	H(76)	0.1691	0.3858	0.3154	13.06
H(35)	0.1321	0.6047	-0.2091	7.89	H(82)	-0.0003	0.3336	0.2732	7.10
H(36)	-0.0527	0.5344	-0.1651	6.52	H(83)	-0.0508	0.3025	0.4116	9.33
H(42)	-0.0302	0.5765	-0.0603	6.40	H(84)	-0.0011	0.2327	0.5147	9.92
H(43)	-0.1093	0.6436	-0.0051	7.33	H(85)	0.0991	0.1940	0.4793	10.78
H(44)	-0.1618	0.6202	0.1349	6.91	H(86)	0.1496	0.2250	0.3409	9.33

Table VI. Selected Distances (Å) in $[\text{Rh}_2\text{Cl}_2(\mu\text{-HFB})(\text{DPM})_2]$

Bonding Distances			
Rh(1)-Rh(2)	2.7447(9)	C(4)-F(4)	1.34(1)
Rh(1)-Cl(1)	2.384(2)	C(4)-F(5)	1.34(1)
Rh(2)-Cl(2)	2.377(2)	C(4)-F(6)	1.31(1)
Rh(1)-P(1)	2.318(2)	P(1)-C(5)	1.816(8)
Rh(1)-P(3)	2.345(2)	P(2)-C(5)	1.831(9)
Rh(2)-P(2)	2.346(2)	P(3)-C(6)	1.823(8)
Rh(2)-P(4)	2.309(2)	P(4)-C(6)	1.813(8)
Rh(1)-C(2)	1.994(9)	P(1)-C(11)	1.822(5)
Rh(2)-C(3)	1.997(9)	P(1)-C(21)	1.826(5)
C(2)-C(3)	1.315(12)	P(2)-C(31)	1.828(5)
C(1)-C(2)	1.49(1)	P(2)-C(41)	1.827(5)
C(3)-C(4)	1.50(1)	P(3)-C(51)	1.826(5)
C(1)-F(1)	1.32(1)	P(3)-C(61)	1.844(5)
C(1)-F(2)	1.34(1)	P(4)-C(71)	1.827(7)
C(1)-F(3)	1.35(1)	P(4)-C(81)	1.830(6)
Nonbonding Distances			
P(1)-P(2)	2.959(3)	Cl(2)-H(76)	2.80
P(3)-P(4)	2.981(3)	Cl(2)-H(46)	2.82
Cl(1)-H(56)	2.70	H(72)-H(1C6)	2.11
Cl(1)-H(62)	2.78	H(12)-H(2C5)	2.18
Cl(2)-H(32)	2.80		

Table VII. Selected Angles (Deg) in $[\text{Rh}_2\text{Cl}_2(\mu\text{-HFB})(\text{DPM})_2]$

Bond Angles			
P(1)-Rh(1)-Rh(2)	90.02(6)	C(21)-P(1)-C(5)	104.7(4)
P(3)-Rh(1)-Rh(2)	94.71(6)	C(31)-P(2)-C(41)	102.5(3)
P(2)-Rh(2)-Rh(1)	94.95(6)	C(31)-P(2)-C(5)	103.9(4)
P(4)-Rh(2)-Rh(1)	90.94(6)	C(41)-P(2)-C(5)	103.0(4)
P(1)-Rh(1)-P(3)	174.87(9)	C(51)-P(3)-C(61)	104.0(3)
P(2)-Rh(2)-P(4)	173.03(9)	C(51)-P(3)-C(6)	102.7(3)
Cl(1)-Rh(1)-Rh(2)	149.97(7)	C(61)-P(3)-C(6)	103.3(4)
Cl(2)-Rh(2)-Rh(1)	145.39(8)	C(71)-P(4)-C(81)	102.2(4)
P(1)-Rh(1)-Cl(1)	87.21(8)	C(71)-P(4)-C(6)	103.3(4)
P(3)-Rh(1)-Cl(1)	89.68(8)	C(81)-P(4)-C(6)	103.9(4)
P(2)-Rh(2)-Cl(2)	89.28(9)	Rh(1)-P(1)-C(11)	115.8(2)
P(4)-Rh(2)-Cl(2)	87.96(9)	Rh(1)-P(1)-C(21)	115.4(2)
P(1)-Rh(1)-C(2)	91.5(3)	Rh(1)-P(1)-C(5)	113.6(3)
P(3)-Rh(1)-C(2)	88.3(3)	Rh(2)-P(2)-C(31)	112.9(2)
P(2)-Rh(2)-C(3)	89.1(2)	Rh(2)-P(2)-C(41)	121.8(2)
P(4)-Rh(2)-C(3)	89.6(2)	Rh(2)-P(2)-C(5)	110.8(3)
Cl(1)-Rh(1)-C(2)	140.9(3)	Rh(1)-P(3)-C(51)	115.3(2)
Cl(2)-Rh(2)-C(3)	145.6(3)	Rh(1)-P(3)-C(61)	119.0(2)
C(2)-Rh(1)-Rh(2)	69.0(3)	Rh(1)-P(3)-C(6)	110.8(3)
C(3)-Rh(2)-Rh(1)	68.9(2)	Rh(2)-P(4)-C(71)	115.1(3)

(continued...)

Table VII (continued)

Rh(1)-C(2)-C(3)	111.0(7)	Rh(2)-P(4)-C(81)	117.0(3)
Rh(2)-C(3)-C(2)	111.0(7)	Rh(2)-P(4)-C(6)	113.6(3)
Rh(1)-C(2)-C(1)	120.8(7)	P(1)-C(5)-P(2)	108.4(4)
Rh(2)-C(3)-C(4)	121.6(7)	P(3)-C(6)-P(4)	110.1(4)
C(1)-C(2)-C(3)	128.3(9)	P(1)-C(11)-C(12)	120.9(4)
C(4)-C(3)-C(2)	127.4(9)	P(1)-C(11)-C(16)	119.0(4)
F(1)-C(1)-C(2)	114.0(8)	P(1)-C(21)-C(22)	119.6(4)
F(2)-C(1)-C(2)	114.0(8)	P(1)-C(21)-C(26)	120.4(4)
F(3)-C(1)-C(2)	112.9(9)	P(2)-C(31)-C(32)	118.8(4)
F(4)-C(4)-C(3)	112.9(9)	P(2)-C(31)-C(36)	121.2(4)
F(5)-C(4)-C(3)	112.6(8)	P(2)-C(41)-C(42)	119.4(4)
F(6)-C(4)-C(3)	114.5(8)	P(2)-C(41)-C(46)	120.6(4)
F(1)-C(1)-F(2)	105.8(9)	P(3)-C(51)-C(52)	121.8(3)
F(1)-C(1)-F(3)	105.0(9)	P(3)-C(51)-C(56)	118.1(3)
F(2)-C(1)-F(3)	104.2(8)	P(3)-C(61)-C(62)	121.3(4)
F(4)-C(4)-F(5)	105.7(9)	P(3)-C(61)-C(66)	118.6(4)
F(4)-C(4)-F(6)	104.6(8)	P(4)-C(71)-C(72)	121.4(7)
F(5)-C(4)-F(6)	105.9(9)	P(4)-C(71)-C(76)	118.6(7)
C(11)-P(1)-C(21)	102.3(3)	P(4)-C(81)-C(82)	119.3(5)
C(11)-P(1)-C(5)	103.5(4)	P(4)-C(81)-C(86)	120.5(5)

(continued...)

Table VII (continued)

Torsion Angles			
P(1)-Rh(1)-Rh(2)-P(2)	-6.16(8)	C(51)-P(3)-Rh(1)-C1(1)	73.7(2)
P(3)-Rh(1)-Rh(2)-P(4)	-4.43(9)	C(61)-P(3)-Rh(1)-C1(1)	-50.9(3)
P(1)-Rh(1)-Rh(2)-P(4)	177.56(9)	C(31)-P(2)-Rh(2)-C1(2)	78.8(3)
P(2)-Rh(2)-Rh(1)-P(3)	171.85(8)	C(41)-P(2)-Rh(2)-C1(2)	-43.8(3)
C(5)-P(1)-P(3)-C(6)	13.1(4)	C(71)-P(4)-Rh(2)-C1(2)	-66.1(4)
C(5)-P(2)-P(4)-C(6)	10.3(4)	C(81)-P(4)-Rh(2)-C1(2)	53.9(3)
C(11)-P(1)-P(3)-C(51)	16.0(3)	C(11)-P(1)-Rh(1)-C(2)	83.4(4)
C(21)-P(1)-P(3)-C(61)	11.5(4)	C(21)-P(1)-Rh(1)-C(2)	-157.1(4)
C(31)-P(2)-P(4)-C(71)	12.4(4)	C(51)-P(3)-Rh(1)-C(2)	-67.2(3)
C(41)-P(2)-P(4)-C(81)	10.6(4)	C(61)-P(3)-Rh(1)-C(2)	168.2(4)
C(1)-C(2)-C(3)-C(4)	-2.8(1.6)	C(31)-P(2)-Rh(2)-C(3)	-66.9(3)
Rh(1)-C(2)-C(3)-Rh(2)	-3.4(8)	C(41)-P(2)-Rh(2)-C(3)	170.6(4)
C1(1)-Rh(1)-Rh(2)-C1(2)	5.3(2)	C(71)-P(4)-Rh(2)-C(3)	79.6(4)
C(11)-P(1)-P(2)-C(31)	-19.3(5)	C(81)-P(4)-Rh(2)-C(3)	-160.4(4)
C(21)-P(1)-P(2)-C(41)	-11.7(3)	C(5)-P(1)-Rh(1)-C(2)	-36.1(4)
C(51)-P(3)-P(4)-C(71)	-11.2(6)	C(5)-P(2)-Rh(2)-C(3)	49.2(4)
C(61)-P(3)-P(4)-C(81)	-5.7(4)	C(6)-P(3)-Rh(1)-C(2)	48.8(4)
C(11)-P(1)-Rh(1)-C1(1)	-57.5(3)	C(6)-P(4)-Rh(2)-C(3)	-39.3(4)
C(21)-P(1)-Rh(1)-C1(1)	62.0(3)		

Table VIII. Least-Squares Planes Calculations^a for $[\text{Rh}_2\text{Cl}_2(\mu\text{-HFB})(\text{DPM})_2]$.

plane no.	equation	Plane no.	equation
1	$-0.4482X + 0.7081Y - 0.5457Z - 4.3442 = 0$	3	$-0.4534X + 0.7049Y - 0.5455Z - 4.3207 = 0$
2	$-0.4200X + 0.7420Y - 0.5225Z - 4.6334 = 0$	4	$-0.4469X + 0.7078Y - 0.5471Z - 4.3422 = 0$

Distances from Planes (Å)								
plane no.	Rh(1)	Rh(2)	Cl(1)	Cl(2)	Cl(3)	Cl(4)		
1	-0.0045(5)	0.0089(7)	0.045(2)	-0.040(3)	0.093(10)	0.033(9)	-0.013(9)	-0.076(10)
2					0.606(10)	-0.010(9)	0.009(9)	-0.006(10)
3	0.0000(5)	0.0001(7)			0.087(10) ^b	0.027(9)	-0.025(9)	-0.096(10) ^b
4	-0.0041(5)	0.0088(7)	0.043(2)	-0.043(3)		0.037(9) ^b	-0.009(9) ^b	

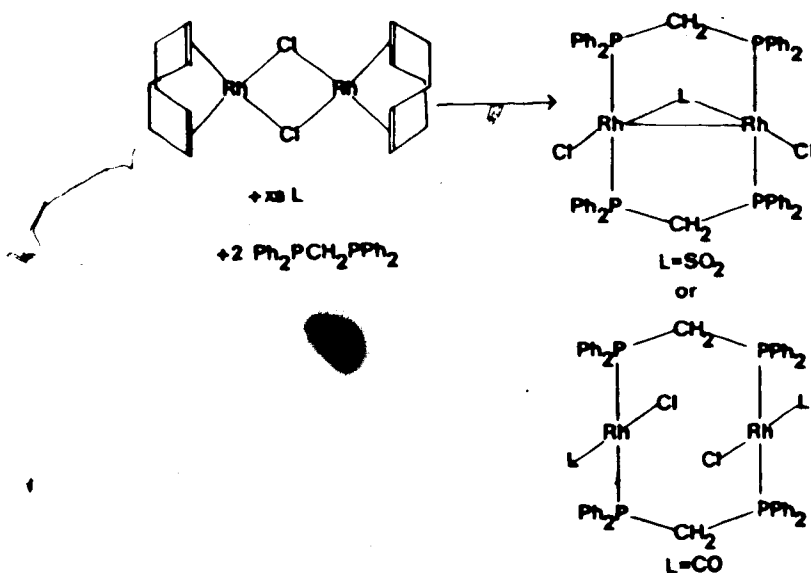
Dihedral Angles Between Planes (Deg)			
plane no.	angle	plane no.	angle
1		2	0.12
2	2.86	3	3.15
3	0.35	4	0.42

^aX, Y and Z are orthogonal coordinates in A with X along the a axis, Y in the ab plane, and Z along the c* axis.

^bNot included in least-squares plane calculations.

Discussion

Based on the group's previous success in preparing complexes of the type $[\text{Rh}_2\text{X}_2(\mu\text{-L})(\text{DPM})_2]$ ($\text{L} = \text{CO}, \text{SO}_2$) or their precursors via the reaction diagrammed below, we



attempted the preparation of the acetylene-bridged analogues by a modification of the same route. This method has only proven successful for acetylenes having strong electron-withdrawing groups (i.e., $-\text{CF}_3$ or $-\text{CO}_2\text{CH}_3$ groups). In the other cases tried, largely uncharacterized complexes were obtained,⁴⁴ whose $^{31}\text{P}\{^1\text{H}\}$ NMR spectra were in the region normally associated with chelating DPM ligands in similar complexes.^{44,45}

The $^{31}\text{P}\{^1\text{H}\}$ NMR spectral parameters of the $[\text{Rh}_2\text{X}_2(\mu\text{-acetylene})(\text{DPM})_2]$ species bear a close resemblance to those for the $\mu\text{-CO}$ and $\mu\text{-SO}_2$ analogues. The $^{31}\text{P}\{^1\text{H}\}$ NMR spectra are of the type previously observed for symmetric DPM-bridged species, which are AA'A"A''XX' spin systems. The spectra for such species are dominated by two major peaks, the separations of which (hereafter called J) are tabulated for species 1, 2 and 3 and their $\mu\text{-CO}$ and $\mu\text{-SO}_2$ analogues in Table IX. This value has been calculated to be essentially that of $^1J_{\text{Rh-P}}^{18}$ and is closely comparable among

Table IX. $^{31}\text{P}\{^1\text{H}\}$ NMR Spectral Parameters for 1, 2 and 3 and Related Complexes

	^{31}P NMR		Reference
	δ (ppm)	J(Hz)	
$[\text{Rh}_2\text{Cl}_2(\mu\text{-HFB})(\text{DPM})_2]$, 1	7.5	112.0	This work
$[\text{Rh}_2\text{I}_2(\mu\text{-HFB})(\text{DPM})_2]$, 2	9.1	110.0	This work
$[\text{Rh}_2\text{Cl}_2(\mu\text{-DMA})(\text{DPM})_2]$, 3	8.6	115.0	This work
$[\text{Rh}_2\text{Cl}_2(\mu\text{-CO})(\text{DPM})_2]$	19.8	116.0	4
$[\text{Rh}_2\text{I}_2(\mu\text{-CO})(\text{DPM})_2]$	16.3	113.7	4
$[\text{Rh}_2\text{Cl}_2(\mu\text{-SO}_2)(\text{DPM})_2]$	22.5	115.0	2

all these species. Although we have often used this major-doublet splitting as an empirical indication of whether or not the complex is metal-metal bonded, the values in the present case are ambiguous. Values of J less than 100 Hz have so far indicated the presence of a Rh-Rh bond while values of J greater than 120 Hz have been associated with complexes having no metal-metal bond. Values in the 100-120 Hz region, however, present an ambiguity; $[\text{Rh}_2(\text{CO})_2(\mu\text{-Cl})(\text{DPM})_2]^+$ has a J of 113.4 Hz and lacks a metal-metal bond,^{1,3} while $[\text{Rh}_2\text{Cl}_2(\mu\text{-CO})(\text{DPM})_2]$ has the slightly greater J of 116.0 Hz but has a metal-metal bond.^{4,5} Therefore the acetylene bonding mode cannot be inferred from the ^{31}P NMR spectroscopic data.

The IR information available on parallel and perpendicular binuclear acetylene complexes suggests that the acetylenes in 1 and 2 are bound as cis-dimetallated olefins. For $\mu_2\text{-}\eta^2$ acetylenes, C-C stretching values from 1595 cm^{-1} to 1491 cm^{-1} have been reported;^{46,47} for cis-dimetallated olefins, values from 1643 cm^{-1} to 1639 cm^{-1} have been reported for $\text{CF}_3\text{C}_2\text{CF}_3$ complexes.^{48,49} No other acetylene has had a cis-dimetallated olefinic C-C stretching frequency reported. Thus, the limited number of data make this inference somewhat uncertain, but the X-ray crystal structure, described in the next section, confirms that the acetylene ligand is coordinated parallel to the metal-metal axis and accompanied by a Rh-Rh bond.

Description of Structure

The unit cell of $[\text{Rh}_2\text{Cl}_2(\mu\text{-CF}_3\text{C}_2\text{CF}_3)(\text{DPM})_2]$ consists of four discrete molecules of the complex, in which there are no unusually short intermolecular contacts (see Figure 2 and Table VI). A perspective view of the molecule together with the numbering scheme is presented in Figure 3 (phenyl hydrogens have the same number as their attached carbon atoms), and a representation of the inner coordination sphere in the plane of the rhodium atoms and the acetylene molecule is shown in Figure 4. Distances and angles of interest are contained in Tables VI and VII, respectively, and some least-squares plane calculations are shown in Table VIII.

The complex has a geometry typical of DPM-bridged binuclear complexes, in which the two rhodium atoms are bridged by two transoid DPM ligands. In the equatorial plane, approximately perpendicular to the Rh-P vectors, the metals are bridged by the hexafluoro-2-butyne molecule, which is coordinated as a cis-dimetalated olefin. A terminal chloro ligand on each metal and a rhodium-rhodium bond complete the rhodium coordinations. The molecule has approximately C_{2v} symmetry with the one pseudo mirror plane bisecting the Rh-Rh bond and the other lying in the metal-

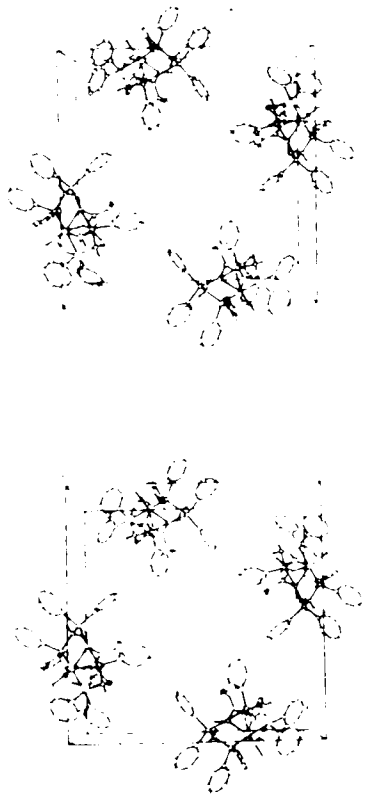


Figure 2. Stereoview of the Unit Cell of $[\text{Rh}_2\text{Cl}_2(\mu\text{-HFB})(\text{DPM})_2]$. As viewed with the title at the bottom, the x-axis is from left to right, the y axis runs from bottom to top and the z-axis comes out of the page. 20% thermal ellipsoids are shown with the exception of the methylene hydrogen atoms, which are drawn artificially small on this and all subsequent drawings.

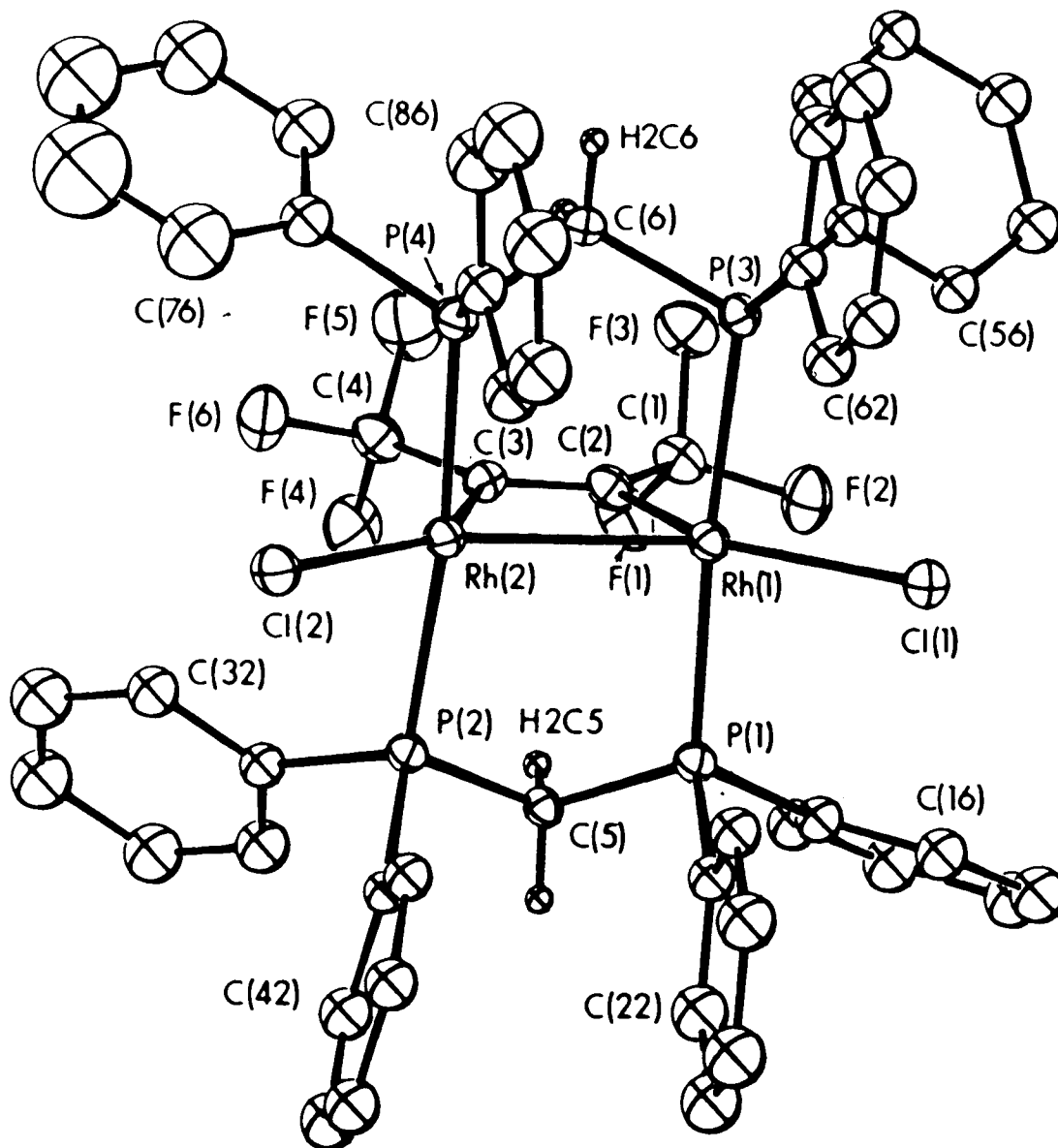


Figure 3. Perspective View of $[\text{Rh}_2\text{Cl}_2(\mu\text{-HFB})(\text{DPM})_2]$. The numbering scheme is as shown; the numbering on the phenyl carbon atoms starts at the carbon bonded to phosphorus and increases sequentially around the ring. 20% thermal ellipsoids are shown.

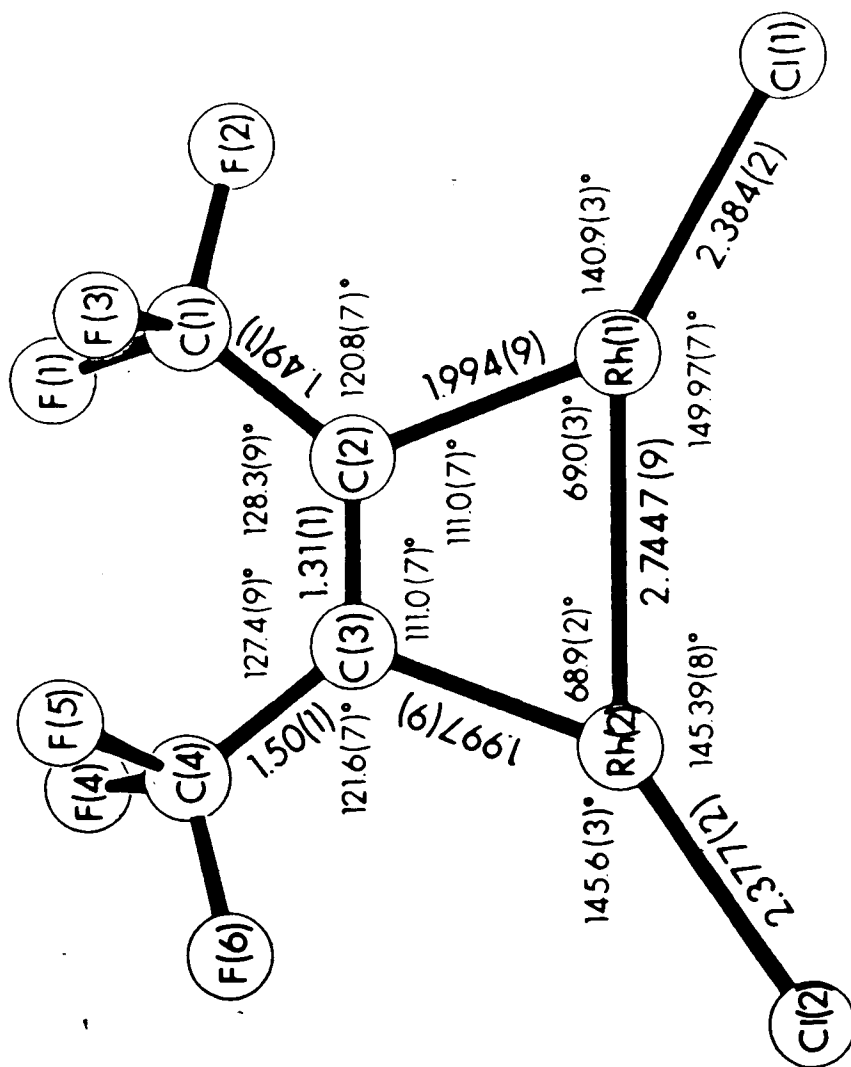


Figure 4. Representation of the Equatorial Plane of $[\text{Rh}_2\text{Cl}_2(\mu\text{-HFB})(\text{DPM})_2]$. Some relevant bond lengths and angles are shown.

acetylene plane. Each rhodium has a somewhat distorted trigonal bipyramidal coordination with the trans phosphines in the axial sites and the chloro ligand, an acetylenic carbon atom and the other metal occupying the three equatorial sites. The major distortion from idealized trigonal bipyramidal geometry results from the acute $\text{C}_{\text{acetylene}}\text{-Rh-Rh}$ angles (Figure 4) and the concomitant larger angles involving the chloro ligands. These acute angles at rhodium are typical for metal-metal bonded complexes which are bridged by acetylenes in the cis-dimetallated olefinic geometry.^{50,51}

Within the DPM framework the parameters are essentially as expected; the Rh-P distances (range, 2.309(2) to 2.346(2) Å) compare well with other determinations as do the phosphorus-carbon distances (both methylene and phenyl). Similarly all angles within the DPM ligand are normal. As is often observed in these systems, the bridging methylene groups of the DPM ligand are both bent in the direction of the bulkier equatorial ligand (the acetylene ligand) allowing the phenyl groups to minimize their non-bonded contacts with this group. All phenyl groups are essentially staggered with regard to the equatorial ligands (as shown by the torsion angles in Table VII), again minimizing non-bonded contacts.

The Rh-Rh distance in the present compound (2.7447(9) Å) is typical for a Rh-Rh single bond; it compares well with other such distances in analogous compounds containing Rh-Rh single bonds (range: 2.731(2) Å¹⁷ to 2.9653(6) Å²⁰) and in particular is close to the values of 2.7566(9) Å for $[\text{Rh}_2\text{Br}_2(\mu\text{-CO})(\text{DPM})_2]$ ⁵ and 2.7838(8) Å in $[\text{Rh}_2\text{Cl}_2(\mu\text{-SO}_2)(\text{DPM})_2]$,² to which it is closely related. This distance can also be contrasted with the very long Pd-Pd (3.492(1) Å) and Rh-Rh (3.3542(9) Å) distances in $[\text{Pd}_2\text{Cl}_2(\mu\text{-HFB})(\text{DPM})_2]$ ^{15,22} and $[\text{Rh}_2\text{Cl}_2(\mu\text{-CO})(\mu\text{-DMA})(\text{DPM})_2]$ ⁷ respectively, in which the bridging acetylene groups are not accompanied by metal-metal bonds. The presence of a Rh-Rh bond in 1 is further substantiated by the intraligand P-P distances (2.959(3) Å and 2.981(3) Å) which are significantly longer than the Rh-Rh distance, suggesting a mutual attraction of the metals. This compression of the Rh-Rh axis is clearly evident in Figure 3.

Both Rh-Cl distances (2.377(2) and 2.384(2) Å) are normal for terminal chlorides and are significantly shorter than those observed in the analogous carbonyl adduct $[\text{Rh}_2\text{Cl}_2(\mu\text{-CO})(\mu\text{-DMA})(\text{DPM})_2]$,⁷ where these bonds are nearly trans to a σ -alkenyl group of high trans influence. In the present compound the rhodium-alkenyl bonds (Rh(1)-C(2) and Rh(2)-C(3)) are inclined to the Rh-Cl bonds by 140.9(3)° and 145.6(3)°, respectively, significantly bent from the trans geometry.

As noted, the coordinated hexafluoro-2-butyne group can be regarded as a cis-dimetalated olefin; all angles about C(2) and C(3) are close to 120° , as expected for sp^2 hybridization of these atoms. The slight distortion from idealized sp^2 hybridization seems to result from the strain imposed by the Rh-Rh bond, which compresses the Rh(1)-C(2)-C(3) and Rh(2)-C(3)-C(2) angles to $110.0(7)^\circ$. In other metal-metal bonded species having similarly bound acetylene ligands similar distortions were observed,^{50,51} whereas when no metal-metal bond is present (as in $[Pd_2Cl_2(\mu-HFB)(DPM)_2]$ and $[Rh_2Cl_2(\mu-CO)(\mu-DMA)(DPM)_2]$) the acetylene ligands are found to approach more closely the undisturbed olefin geometry. In spite of this strain in the acetylene molecule, imposed by the short Rh-Rh distance, the rhodium atoms and the carbon atom framework of the acetylene ligand are quite planar (Table VIII). Based on the observed strain in the molecule, one might expect that the resulting metal-acetylene orbital overlap would be less than in unstrained cases, resulting in less activation of the acetylene. However the other structural parameters in the ligand do not confirm this expectation. The rhodium-acetylene bonds (av. $1.996(9)$ Å) are among the shortest observed for second or third row, acetylene-bridged complexes (range $1.985(12) - 2.12(3)$ Å), suggesting that the acetylene moiety is strongly bound, and the C(2)-C(3) bond

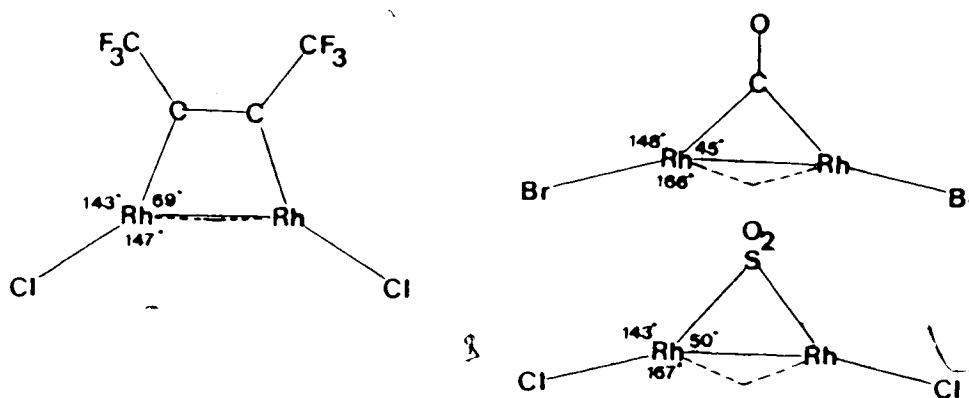
(1.315(12) Å), although somewhat shorter than those in the complexes without metal-metal bonds, is not significantly different, and is still close to that expected for a C-C double bond (1.337(6) Å).⁵² Only the C(1)-C(2)-C(3) and C(4)-C(3)-C(2) angles, at 128.3(9)° and 127.4(9)°, respectively, indicate a slight tendency towards a more linear acetylenic geometry, relative to the species without metal-metal bonds, where comparable angles ranging from 122(1)° to 124.7(11)° have been reported.

The C(1)-C(2) and C(3)-C(4) bonds are exactly as expected for single bonds between an sp² and an sp³ hybridized carbon atom, and agree well with the analogous distances in other binuclear HFB complexes.^{15,50,53} Similarly the C-F distances and all angles at the CF₃ groups are normal.

[Rh₂Cl₂(μ-HFB)(DPM)₂] is now the third member of a series of complexes structurally characterized in this group, each of which contains a rhodium-rhodium bond, terminal halide ligands and a bridging π-acceptor ligand; the other members are [Rh₂Cl₂(μ-SO₂)(DPM)₂]² and [Rh₂Br₂(μ-CO)(DPM)₂].⁵ Structurally these three species are remarkably similar, having very similar Rh-Rh distances, similar rhodium-DPM frameworks and even similar orientations of the DPM phenyl groups. Significantly, all display short bonds between the metals and the bridging

small molecules, implying strong coordination of these groups to the metals. Although the Δ change in the geometries of the CO and SO₂ ligands on coordination is not obvious, the acetylene molecule is obviously structurally activated, resembling as it does a cis-dimetallated olefin (vide supra). Apart from the obvious differences resulting from the different bonding modes of SO₂, CO and CF₃C₂CF₃, the major difference of possible chemical significance in the three related compounds is found in the Rh-Rh-halide angles. In the acetylene complex, these angles (ca. 148°) are significantly smaller than those in the SO₂ and CO complexes (ca. 166°), suggesting that the sideways orientation of the acetylene group and the CF₃ groups may force the two Cl ligands towards each other. Although the Cl and F atoms are well beyond van der Waals contact, the phenyl hydrogen atoms H(32) and H(56) are aimed into the spaces between the CF₃ groups and the Cl groups and may be responsible for transmitting this steric interaction.

Another possibility is that the orientation of the terminal halide ligands with respect to the bridging groups may be determined by electronic factors. In compound 1, the μ -CO complex and the μ -SO₂ complex, the terminal halide-metal-bridging ligand angle has remained nearly constant (near 145° in all three cases).



Considered simplistically, an angle similar to the 145° value above might be thought to lie between the Rh-halide bonds and the orbitals responsible for the metal-metal bond. The dotted lines in the above figures show the directions of these hypothetical orbitals. If the metal-metal bonds in these three species were therefore considered as bent bonds, they would be increasingly bent in the order $1 < \mu\text{-CO} < \mu\text{-SO}_2$. This is consistent with the order of the metal-metal bond lengths ($1 < \mu\text{-CO} < \mu\text{-SO}_2$), with the most linear bond (1) presumably having the best orbital overlap conditions. Hoffman and Hoffmann²⁸ have considered the halide-rhodium-bridging ligand angles in the $\mu\text{-SO}_2$ and $\mu\text{-CO}$ compounds, but concluded that they resulted from "a balance between various trends in the lower filled orbitals". There seems to be no reason obvious to us why values near 145° are favoured.

The previously mentioned additional crowding by the CF_3 groups may also result in chemical differences between the acetylene-bridged species and the SO_2 and CO analogues by blocking the terminal sites of attack (i.e., those between C(2) and Cl(1) and between C(3) and Cl(2) in 1.) Some comparisons in reactivity between 1 and the SO_2 and CO species will be given in Chapter III.

From the outset, the major uncertainty in the $[\text{Rh}_2\text{X}_2(\mu\text{-acetylene})(\text{DPM})_2]$ species has concerned the acetylene coordination mode. This study unambiguously establishes that the acetylene group is bound as a cis-dimetalated olefin accompanied by a Rh-Rh bond. As such the present compound bears a strong resemblance to $[\text{Pd}_2\text{Cl}_2(\mu\text{-CF}_3\text{C}_2\text{CF}_3)(\text{DPM})_2]$ differing only in the metals and in the presence of a metal-metal bond in our Rh species. Essentially all structural differences between these two species are a consequence of this difference in metal-metal bonding. That both above complexes have the cis-dimetalated olefin coordination of their acetylene groups is significant given that their electron counts differ by 2. The fact that this coordination mode is retained for the CO adducts of 1, 2 and 3, $[\text{Rh}_2\text{X}_2(\mu\text{-CO})(\mu\text{-acetylene})(\text{DPM})_2]$, is also significant; in the transformation of $[\text{Cp}_2\text{Rh}_2(\text{CO})_2(\mu\text{-CF}_3\text{C}_2\text{CF}_3)]$ to $[\text{Cp}_2\text{Rh}_2(\mu\text{-CO})(\mu\text{-CF}_3\text{C}_2\text{CF}_3)]$ ^{48,50,54} the acetylene group

rotates with respect to the Rh-Rh bond by ca. 90° and the Rh-Rh bond is retained.

Calculations by Hoffmann and co-workers²⁹⁻³¹ confirm that the cis-dimetalated olefinic coordination of the acetylene ligands is favoured over the perpendicular mode in these compounds for electronic reasons. However, these authors suggest that the favoured acetylene binding mode in $[\text{Rh}_2\text{Cl}_2(\mu\text{-CF}_3\text{C}_2\text{CF}_3)(\text{DPM})_2]$ should have this acetylene twisted significantly from the parallel configuration. This was not observed in the present structural determination. Furthermore, a somewhat less accurate structure determination of this compound in a different space group⁴⁴ (absorption correction not applied; space group $P4_32_12$ or $P4_12_12$) also showed essentially no twisting of the acetylene unit, suggesting that packing considerations are not responsible for the observed orientation in this species. It is, of course, possible that the twisted configuration suggested by Hoffmann and co-workers is only slightly favoured electronically, and that non-bonded forces are enough to result in the non-twisted geometries in the two cases studied. However, we feel that there is no evidence to suggest that any structure other than that in which the acetylene lies essentially parallel to the metal-metal bond is the most favoured one.

References

1. (a) Cowie, M.; Mague, J.T.; Sanger, A.R. J. Am. Chem. Soc. 1978, **100**, 3628.
(b) Cowie, M. Inorg. Chem. 1979, **18**, 286.
2. (a) Cowie, M.; Dwight, S.K.; Sanger, A.R. Inorg. Chim. Acta 1978, **31**, L407.
(b) Cowie, M.; Dwight, S.K. Inorg. Chem. 1980, **19**, 209.
3. Cowie, M.; Dwight, S.K. Inorg. Chem. 1979, **18**, 2700.
4. Cowie, M.; Dwight, S.K. Inorg. Chem. 1980, **19**, 2500.
5. Cowie, M.; Dwight, S.K. Inorg. Chem. 1980, **19**, 2508.
6. (a) Cowie, M.; Dwight, S.K. J. Organomet. Chem. 1980, **198**, C20.
(b) Cowie, M.; Dwight, S.K. J. Organomet. Chem. 1981, **214**, 233.
7. (a) Cowie, M.; Southern, T.G. J. Organomet. Chem. 1980, **193**, C46.
(b) Cowie, M.; Southern, T.G. Inorg. Chem. 1982, **21**, 246.
8. Cowie, M.; Dickson, R.S. Inorg. Chem. 1981, **20**, 2682.
9. (a) McKeer, I.R.; Cowie, M. Inorg. Chim. Acta 1982, **65**, L107.
(b) Cowie, M.; McKeer, I.R. in preparation.

10. Cowie, M.; Sutherland, B.R., accepted by Inorg. Chem.
11. Cowie, M.; Sutherland, B.R., accepted by Inorg. Chem.
12. Cowie, M.; Gibson, J.A.E. Two papers submitted to Organometallics.
13. See Chapter I, References 27-30, 44, 45 and 49-164 for a complete list of references on binuclear doubly-bridged DPM complexes; reference 44 is a review.
14. Nutt, M.O. M.S. Thesis, Tulane University, 1969.
15. Balch, A.L.; Lee, C.-L.; Lindsay, C.H.; Olmstead, M.M. J. Organomet. Chem. 1979, 177, C22.
16. Sanger, A.R. Prepr. - Can. Symp. Cat. 1979, 6, 37.
17. (a) Kubiak, C.P.; Eisenberg, R. J. Am. Chem. Soc. 1980, 102, 3637.
(b) Kubiak, C.P.; Woodcock, C.; Eisenberg, R. Inorg. Chem. 1982, 21, 2119.
18. Mague, J.T.; DeVries, S.H. Inorg. Chem. 1982, 21, 1632.
19. Mague, J.T. Inorg. Chem. 1983, 22, 45.
20. Mague, J.T. Inorg. Chem. 1983, 22, 1158.
21. Sanger, A.R. Can. J. Chem. 1982, 60, 1363.
22. Lee, C.-L.; Hunt, C.T.; Balch, A.L. Inorg. Chem. 1981, 20, 2498.
23. Pringle, P.G.; Shaw, B.L. J. Chem. Soc., Chem. Commun. 1982, 81.
24. Puddephatt, R.J.; Thomson, M.A. Inorg. Chem. 1982, 21,

- 725.
25. Azam, K.A.; Puddephatt, R.J. Organometallics 1983, 2, 1396.
 26. Tolman, C.A. Chem. Soc. Rev. 1972, 1, 337.
 27. Bird, P.H.; Fraser, A.R.; Hall, D.N. Inorg. Chem. 1977, 16, 1923.
 28. Hoffman, D.M.; Hoffmann, R. Inorg. Chem. 1981, 20, 3543.
 29. Hoffman, D.M.; Hoffmann, R. J. Chem. Soc., Dalton Trans. 1982, 1471.
 30. Hoffman, D.M.; Hoffmann, R.; Fisel, C.R. J. Am. Chem. Soc. 1982, 104, 3858.
 31. Hoffmān, D.M.; Hoffmann, R. Organometallics 1982, 1, 1299.
 32. Muetterties, E.L.; Pretzer, W.R.; Thomas, M.G.; Beier, B.F.; Thorn, D.L.; Day, V.W.; Anderson, A.B. J. Am. Chem. Soc. 1978, 100, 2090.
 33. Chatt, J.; Venanzi, L.M. J. Chem. Soc. 1957, 4735.
 34. Doedens, R.J.; Ibers, J.A. Inorg. Chem. 1967, 6, 204.
 35. Besides local programs and modifications, the following programs were used in the solution and refinement of the structure: **FORDAP**, a Fourier summation program by A. Zalkin; **SFLS-5**, for structure factors and least-squares refinement; by C.J. Prewitt; **ORFFE**, for calculation of bond lengths and angles with

- their associated standard deviations, by W. Busing and H.A. Levy; ORTEP, a plotting program by C.K. Johnson; AGNOST, a Northwestern University absorption correction program which includes the Coppens-Leiserowitz-Rabinovich logic for Gaussian integration.
36. Cromer, D.T. and Waber, J.T. "International Tables for X-ray Crystallography," Vol. IV, Kynoch Press, Birmingham, England, 1974, Table 2.2.A.
 37. Stewart, R.F.; Davidson, E.R.; Simpson, W.T. J. Chem. Phys. 1965, **42**, 3175.
 38. Cromer, D.T. and Liberman, D. J. Chem. Phys. 1970, **53**, 1891.
 39. $R = \Sigma ||F_O| - |F_C|| / \Sigma |F_O|$; $R_w = [\Sigma w(|F_O| - |F_C|)^2 / \Sigma w F_O^2]^{1/2}$
 40. Ueki, T.; Zalkin, A.; Templeton, D.H. Acta Crystallogr. 1966, **20**, 836.
 41. Cruickshank, D.W.J.; McDonald, W.S. Acta Crystallogr. 1967, **23**, 9.
 42. Zachariasen, W.H. Acta Crystallogr. 1968, **A24**, 212.
 43. Supplementary material is available from Dr. M. Cowie, Department of Chemistry, University of Alberta, Edmonton, Alberta, Canada T6G 2G2.
 44. Cowie, M.; Dickson, R.S. unpublished results.
 45. Cowie, M.; Dwight, S.K. Inorg. Chem. 1979, **18**, 1209.
 46. Boag, N.M.; Green, M.; Howard, J.A.K.; Spencer, J.L.; Stansfield, R.F.D.; Thomas, M.D.O.; Stone, F.G.A.;

- Woodward, P. J. Chem. Soc., Dalton Trans. 1980, 2182.
47. Restivo, R.J.; Ferguson, G.F.; Ng, T.W.; Carty, A.J.
Inorg. Chem. 1977, 16, 172.
48. Dickson, R.S.; Pain, G.N. J. Chem. Soc., Chem. Commun.
1979, 277.
49. Jarvis, A.C.; Kemmitt, R.D.W.; Russell, D.R.; Tucker,
P.A. J. Organomet. Chem. 1978, 159, 341.
50. Dickson, R.S.; Johnson, S.H.; Kirsch, H.F.; Lloyd,
D.J. Acta Crystallogr., Sect. B 1977, B33, 2057.
51. Koie, Y.; Shinoda, S.; Saito, Y.; Fitzgerald, B.J.;
Pierport, C.G. Inorg. Chem. 1980, 19, 770.
52. "Chemical Rubber Company Handbook of Chemistry and
Physics", 62nd edition, ed. R.C. Weast, CRC Press,
Boca Raton, Florida, 1981, p. F-176.
53. Davidson, J.L.; Harrison, W.; Sharp, D.W.A.; Sim, G.A.
J. Organomet. Chem. 1972, 46, C47.
54. Dickson, R.S.; Pain, G.N.; Mackay, M.F. Acta
Crystallogr., Sect. B 1979, B35, 2321.

Chapter III

Some Reactions of $[\text{Rh}_2\text{X}_2(\mu\text{-acetylene})(\text{DPM})_2]$ Complexes
with Small Molecules and the X-ray Crystal Structure
of One Product, $[\text{Rh}_2\text{Cl}(\text{CNMe})_2(\mu\text{-CF}_3\text{C}_2\text{CF}_3)(\text{DPM})_2][\text{BF}_4]$

Introduction

In Chapter II, we described the synthesis and characterization of the binuclear acetylene-bridged complexes $[\text{Rh}_2\text{X}_2(\mu\text{-RC}_2\text{R})(\text{DPM})_2]$ ($\text{R} = \text{CF}_3$, $\text{X} = \text{Cl}$ (1), I(2); $\text{R} = \text{CO}_2\text{Me}$, $\text{X} = \text{Cl}$ (3)) and showed, by an X-ray structure determination of 1, that the acetylene group in this complex bridges the metals, bound as a cis-dimetalated olefin and accompanied by a rhodium-rhodium bond.¹ Some structural resemblances were also noted between this compound and two other types of compound previously studied in this group, namely $[\text{Rh}_2\text{X}_2(\mu\text{-CO})(\text{DPM})_2]$ ($\text{X} = \text{Cl}$, Br , I)²⁻⁴ and $[\text{Rh}_2\text{X}_2(\mu\text{-SO}_2)(\text{DPM})_2]$ ($\text{X} = \text{Cl}$, Br);^{2,5} all three types of compounds are distorted A-frames having bridging π -acid groups, accompanying Rh-Rh single bonds and terminal halide ligands.

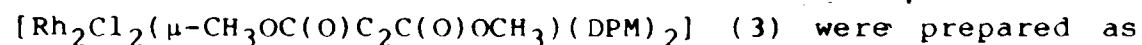
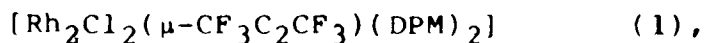
One aspect of interest to us in these complexes regarded their possible Rh-Rh bond reactivities.

$[\text{Rh}_2\text{X}_2(\mu\text{-CO})(\text{DPM})_2]$ ($\text{X} = \text{Cl}$), for example, had been shown to undergo protonation at the Rh-Rh bond⁶ while the three halo derivatives ($\text{X} = \text{Cl}, \text{Br}, \text{I}$) reacted with activated acetylenes with insertion of these groups into the Rh-Rh bond.⁴ In contrast, neither the CO- nor the SO_2 -bridged dihalides showed evidence of Rh-Rh bond reactivity with ligands such as CO, SO_2 or CNR, but usually instead reacted to give complexes with these ligands bound terminally.^{2,3,5,7} Complexes 1, 2 and 3, on the other hand, seemed to be likely candidates for displaying metal-metal bond reactivity with ligands such as CO since the products of such reactions would be exactly the compounds obtained on reacting $[\text{Rh}_2\text{X}_2(\mu\text{-CO})(\text{DPM})_2]$ with the appropriate activated acetylene, $\text{CF}_3\text{C}_2\text{CF}_3$ or $\text{CH}_3\text{OC}(\text{O})\text{C}_2\text{C}(\text{O})\text{OCH}_3$.⁴ This also suggested that compounds 1, 2 and 3 might display metal-metal bond reactivity with other small groups such as CNR, SO_2 and H^+ .

We were also interested in the possibility of ligand insertions (particularly of CO, CNR and SO_2) into the Rh-acetylene bonds of species like compound 1. For these reasons a study was initiated to investigate the chemistry of compound 1 and related complexes with small molecules such as CO, SO_2 and CNMe, and also with H^+ . The results of this study are reported herein.

Experimental

All solvents were purified according to standard procedures⁸ and deaerated with a dinitrogen purge. Reactions were performed in Schlenk apparatus using inert atmosphere techniques. Sodium tetrafluoroborate (Alfa Inorganics), silver tetrafluoroborate (Aldrich), trifluoromethylsulfonic acid (Aldrich), sulfur dioxide (Matheson) and carbon monoxide (Matheson) were used as received.



were prepared as described in Chapter II. Methyl isocyanide (CNMe) was prepared by a literature method⁹ and its purity was ascertained by ¹H NMR spectroscopy. Infrared spectra were obtained as CH₂Cl₂ solutions in KCl cells or as Nujol mulls between either NaCl or KBr plates, using Nicolet MX-1 or 7199 FTIR spectrometers. NMR spectra were obtained at ambient temperature on Bruker WH-200 or WH-400 spectrometers, or at -40°C on a Bruker HFX-90 spectrometer. Conductivities of 1.0 x 10⁻³ M CH₂Cl₂ solutions were measured using a Yellow Springs Instruments Model 31 conductivity bridge and 3401 cell.¹⁰

(a) Protonation of Compounds 1, 2 and 3: A green suspension of $[\text{Rh}_2\text{Cl}_2(\mu\text{-HFB})(\text{DPM})_2]$ (1) (HFB = $\text{CF}_3\text{C}_2\text{CF}_3$) (40 mg, 0.033 mmol) in 1.5 mL CH_2Cl_2 was placed in a 10 mm NMR tube in which a concentric 5 mm sealed insert containing acetone- d_6 was present, and then cooled to -80°C . Addition of 6 μL (0.045 mmol) $\text{CF}_3\text{SO}_3\text{H}$ caused the solid to dissolve yielding a yellow solution. A $^{31}\text{P}\{^1\text{H}\}$ NMR spectrum of the product, $[\text{Rh}_2\text{Cl}_2(\mu\text{-H})(\mu\text{-HFB})(\text{DPM})_2]\text{-}[\text{CF}_3\text{SO}_3]$ (4a), was then obtained at -40°C , revealing a pattern centred at 11.0 ppm which was dominated by two major peaks separated by 92.0 Hz; the observed pattern is typical of AA'A''A'''XX' spin systems.¹¹ The ^1H NMR spectrum of 4a exhibited a multiplet centred at -20.44 ppm ($^1J_{\text{Rh-H}} = 23.4$ Hz; $^2J_{\text{P-H}} = 8.4$ Hz) attributable to a bridging hydride ligand.

Reactions of compounds 2 and 3 with $\text{CF}_3\text{SO}_3\text{H}$ were carried out by the method described above, giving the analogous products 5a and 6a, respectively, and the protonation of compounds 1 - 3 using $\text{HBF}_4 \cdot \text{OEt}_2$, yielding compounds 4b - 6b, was also performed in a similar manner. For the compounds containing the bridging HFB group (4 and 5), the $^{31}\text{P}\{^1\text{H}\}$ NMR spectra were very similar to that reported for 4a (see Table X). However, the $^{31}\text{P}\{^1\text{H}\}$ NMR spectra for the DMA complexes (6a and 6b) differed significantly, most notably in having a larger

splitting between the two major peaks. Hydride resonances in the ^1H NMR spectra were observed for compounds **4b** and **5b**, and resembled that of **4a** (Table X), but no such resonances were observed for complexes **5a**, **6a** or **6b** over a range of temperatures from -80°C to $+20^\circ\text{C}$. The slightly weaker acid $\text{CF}_3\text{CO}_2\text{H}$ failed to protonate compounds **1** - **3**.

When warmed to room temperature, the solutions of **4-6** decomposed within a few hours. All attempts to isolate the protonated species at low temperature were unsuccessful. Spectral data for the protonation reactions are given in Table X.

(b) Reactions of Compounds 1, 2 and 3 with CO and SO_2 : The reactions of the three acetylene-bridged complexes **1**, **2** and **3** with CO to give **7**, **8** and **9**, respectively, were performed by syringing the appropriate volume of CO, at ambient temperature and pressure, into a solution or suspension of the starting complex in CH_2Cl_2 . In a typical reaction this was carried out by adding 0.73 mL of CO (0.028 mmol) to 30 mg of compound **1** (0.025 mmol) in 3 mL CH_2Cl_2 in a 10 mm NMR tube for acquiring the $^{31}\text{P}\{^1\text{H}\}$ NMR spectrum or by adding 0.25 mL of CO (0.0095 mmol) to 10.0 mg of compound **1** (0.0083 mmol) in 1.0 mL CH_2Cl_2 in a 10 mL flask fitted with serum stoppers for observation of the solution infrared spectrum. Spectral

results for the reactions with CO and SO₂ are given in Table X.

The ³¹P{¹H} NMR spectra of the reactions of compounds 1, 2 and 3 with 1 equivalent of CO were observed at -40°C, immediately after the injection of gas into the solution, which had been precooled to -40°C, in attempts to observe possible intermediates. In all three cases the solutions darkened almost immediately, and the precipitation of considerable amounts of dark green or brown solids occurred within a few minutes. The ³¹P{¹H} NMR spectra showed only the symmetric species 7, 8 and 9 (see Table X), and the IR spectra of the isolated solids were identical to those previously reported for the complexes [Rh₂X₂(μ-CO)-(μ-acetylene)(DPM)₂]⁴ (see Table X).

These reactions with 1 equivalent of CO could not be reversed to any observable extent by flushing the solutions with a stream of N₂ at room temperature. Previous experiments with [Rh₂Cl₂(μ-CO)(μ-HFB)(DPM)₂] (7) had shown that an overnight reflux in CHCl₃ with a slow N₂ purge was necessary to produce compound 1.⁴ Similar conditions resulted in the loss of CO from 8 to yield 2, but refluxing [Rh₂Cl₂(μ-CO)(μ-DMA)(DPM)₂] 9, for 48 hours in CHCl₃ caused only partial reversal of this reaction; complete consumption of the complex required refluxing 200 mg of 9 in 50 mL C₆H₆ with a slow N₂ purge for 2 1/2 days. However,

under these conditions some $[\text{Rh}_2\text{Cl}_2(\mu\text{-CO})(\text{DPM})_2]$ was also formed in addition to the expected compound, $[\text{Rh}_2\text{Cl}_2(\mu\text{-DMA})(\text{DPM})_2]$ (3).

The reactions of SO_2 with compounds 1 and 2 to give compounds 10 and 11, respectively, were performed by saturating CH_2Cl_2 solutions of the appropriate complex (100 mg in 5 mL), in 50 or 100 mL flasks, with SO_2 . The initial green solutions turned dark brown almost immediately. After 48 hours under an SO_2 atmosphere $^{31}\text{P}\{^1\text{H}\}$ NMR spectra were run at -40°C and showed two symmetrical species in each case, one due to starting material and the other attributable to the SO_2 adduct (10 or 11). For the reaction yielding 10, about 15% remained as unreacted compound 1, and for 11 about 7% remained as 2, even under these conditions of high SO_2 concentration. Evaporation of these solutions by a nitrogen stream, followed by redissolving of the solids in CH_2Cl_2 , revealed that only the respective starting materials remained.

The reaction of SO_2 with 3 was done in a manner similar to the reactions with CO; that is, 0.73 mL (0.028 mmol at ambient temperature and pressure) SO_2 were injected into a solution of 30 mg (0.025 mmol) of 3 in 1.5 mL CH_2Cl_2 in a 10 mm NMR tube at room temperature. The green solution immediately turned a dark yellow-brown and a dark brown solid began precipitating after a few minutes. A

$^{31}\text{P}\{^1\text{H}\}$ NMR spectrum at -40°C showed only a symmetrical pattern due to 12, which was the only product observed even with an excess of SO_2 . A 20 minute N_2 purge reversed the reaction to the extent that about 15% of compound 12 reverted to 3.

Due to the lability of the SO_2 ligand in compounds 10-12, they could not be isolated as pure solids. A summary of their $^{31}\text{P}\{^1\text{H}\}$ NMR and IR spectral details is given in Table X.

(c) Reactions of Compounds 1, 2 and 3 with CNMe: In a typical experiment 150 mg of compound 1 (0.124 mmol) was suspended in 0.7 mL CD_2Cl_2 in a 5 mm NMR tube. Successive additions of 0.062 mL of a 1.0 M CH_2Cl_2 solution of the isocyanide (0.062 mmol) were made with NMR monitoring of the reaction mixture after each addition. In this manner a series of NMR spectra was obtained ($^{31}\text{P}\{^1\text{H}\}$ at 161.92 MHz, ^{19}F at 376.41 MHz (for 1 and 2) and ^1H at 400.14 MHz) for the reactions of compounds 1, 2 and 3 with CNMe over the range from 0 to 6 equivalents of isocyanide per complex molecule. Typically, matching the $^{31}\text{P}\{^1\text{H}\}$, ^{19}F and ^1H NMR signals arising from a given complex in the reaction sequence was straightforward on the basis of molecular symmetry, signal integration and amount of isocyanide added; where necessary all three spectra were obtained

using the same sample to confirm the assignments, which are given in Table XI. Similar IR monitoring of the reaction sequence was carried out and, where possible, the isocyanide stretching frequencies were assigned (see Table XI). The conductivities of 1.0 mM CH_2Cl_2 solutions of 1, 2 and 3 were also monitored as successive additions of CNMe were made (see Table XII).

Preparation of $[\text{RhCl}(\text{CNMe})_2(\mu\text{-HFB})(\text{DPM})_2][\text{BF}_4]$ (15b):

340 μL (0.35 mmol) of 1.04 M CNMe in CH_2Cl_2 was added with stirring to a suspension of 200 mg (0.166 mmol) of 1 in 10 mL CH_2Cl_2 in a 100 mL 3-necked round bottom flask. Five mL of methanol was added to the green solution, followed by a solution of 100 mg (0.911 mmol) of NaBF_4 in 7 mL of methanol. A stream of N_2 was passed over the stirred solution for about 3 h, reducing its volume to about 8 mL and causing the precipitation of a purple micro-crystalline solid. The light yellow supernatant was removed and the solid was washed twice with 5 mL of methanol. A sample for elemental analysis was recrystallized from CH_2Cl_2 /ether; it analyzed as a hemi-dichloromethane solvate (Found: C, 50.82; H, 3.69; N, 1.86; Cl, 4.98) Calcd. for $\text{Rh}_2\text{Cl}_2\text{P}_4\text{F}_{10}\text{N}_2\text{C}_{58.5}\text{BH}_{51}$: C, 50.79; H, 3.72; N, 2.02; Cl, 5.13.. A 200 MHz ^1H NMR spectrum of this species in CDCl_3 solution confirmed the presence of dichloromethane. This

spectrum also displayed resonances in the phenyl region (δ 6.9 - 8.0, 40H, m), one of two expected DPM methylene resonances (δ 3.72, 2H, m) and two singlets in the region appropriate for the isocyanide methyl protons. One of these singlets was superimposed on a broad multiplet, attributable to the other DPM methylene protons (δ 3.17, 5H) whereas the other was a sharp singlet (δ 3.49, 3H). An IR spectrum of **15b** as a Nujol mull revealed two isocyanide stretches at 2244 and 2216 cm^{-1} .

Preparation of $[\text{Rh}_2(\text{CNMe})_4(\mu\text{-HPB})(\text{DPM})_2][\text{BF}_4]_2$ (**16b**):

The preparation of compound **16b** was similar to that for **15b**, except that 0.70 mL (0.73 mmol) of the 1.04 M CNMe solution was added to a suspension of 200 mg (0.166 mmol) **1**. The resultant product was a yellow powder which was only slightly soluble in methanol or methylene chloride. The ^1H NMR spectrum (see Table XI) revealed the presence of four CNMe groups per complex molecule. Two isocyanide stretches were observed at 2234 and 2217 cm^{-1} in the IR spectrum of a CH_2Cl_2 solution of **16b**.

Analysis. Found: C, 48.89; H, 3.91; N, 3.49; Cl, <1%.
Calcd for $\text{Rh}_2\text{P}_4\text{N}_4\text{F}_{14}\text{C}_{62}\text{B}_2\text{H}_{56}$: C, 50.51; H, 3.83; N, 3.80; Cl, 0.00.

X-ray Data Collection on Compound 15b.

Dark purple crystals of $[\text{Rh}_2\text{Cl}(\text{CNMe})_2(\mu\text{-HFB})\text{-}(\text{DPM})_2][\text{BF}_4]$ (15b) were obtained by slow diffusion of diethyl ether into a CH_2Cl_2 solution of the complex. A suitable crystal was mounted on a glass fibre. Preliminary film data showed that the crystal belonged to the monoclinic system, and had systematic absences ($h0l$: $h + l$ odd; $0k0$: k odd) characteristic of the space group $P2_1/n$, a non-standard setting of $P2_1/c$. Accurate cell parameters were obtained by a least-squares analysis of the setting angles of 12 carefully centred reflections chosen from diverse regions of reciprocal space ($50^\circ < 2\theta < 60^\circ$, $\text{CuK}\alpha$ radiation) and obtained using a narrow X-ray source. See Table XIII for pertinent crystal data and details of intensity collection. The widths at half-height of several strong low-angle reflections (ω scan, open counter) lay in the range $0.20 - 0.26^\circ$. Data were collected on a Picker four-circle automated diffractometer equipped with a scintillation counter and a pulse height analyser tuned to accept 90% of the $\text{CuK}\alpha$ peak. Background counts were measured at both ends of the scan range with both crystal and counter stationary. The intensities of three standard reflections were measured every 100 reflections during the data collection, and second set of four standards was

monitored twice a day. No significant decay of these standards was observed over the course of the data collection. The intensities of 9428 unique reflections ($3^\circ < 2\theta < 120^\circ$) were measured and processed in the usual way, using a value of 0.05 for p .¹² Of these 6800 had $F_O^2 > 3\sigma(F_O^2)$ and were used in subsequent calculations. Absorption corrections were applied to the data using Gaussian integration.¹³

Structure Solution and Refinement.

The structure was solved by using a sharpened Patterson synthesis to locate the two independent Rh atoms. Subsequent refinements and difference Fourier syntheses led to the location of all atoms of the anion and cation including hydrogens. Atomic scattering factors were taken from Cromer and Waber's tabulation¹⁴ for all atoms except hydrogen, for which the values of Stewart et al¹⁵ were used. Anomalous dispersion terms¹⁶ for Rh, Cl and P were included in F_C . The carbon atoms of all phenyl rings were refined as rigid groups having D_{6h} symmetry and 1.392 Å C-C distances, but with independent isotropic thermal parameters. All hydrogen atoms located were included as fixed contributions and were not refined. The idealized positions of the phenyl and methylene hydrogens were

calculated from the geometries about the attached carbon atom using C-H distances of 0.95 Å. The methyl hydrogens were located approximately from difference Fourier maps, then idealized such that the methyl carbon atoms had C_{3v} symmetry with C-H bond lengths of 0.95 Å. All other non-group atoms were refined independently with anisotropic thermal parameters. Since the geometry of the tetrafluoroborate anion appeared to be irregular and its fluorine atoms all exhibited large thermal parameters, these atoms were removed from the refinements. However, a subsequent difference Fourier map, phased on the model without these atom contributions, reaffirmed their positions and showed the rather diffuse nature of the peaks so these atoms were reinserted and refinement was continued as previously. At this time a region of electron density ($0.99 - 2.33 \text{ eÅ}^{-3}$) was located remote from the anion or complex cation. Although both CH_2Cl_2 and Et_2O were observed in ^1H NMR spectra of the solid redissolved in CDCl_3 and the presence of CH_2Cl_2 was suggested by the elemental analysis, all attempts to assign the electron density to disordered CH_2Cl_2 , Et_2O or both were unsuccessful. In all attempts, the peaks did not fit any simple disorder pattern, yielding chemically unreasonable geometries and badly behaved thermal parameters. In any case, the refinements involving the various disordered

solvent models did not cause a significant change in the parameters associated with either the anion or cation as compared to the results in refinements without these disordered groups so this electron density was left unaccounted for in subsequent refinements. In the final difference Fourier map the top five residual peaks ($0.99 - 2.33 \text{ eA}^{-3}$) were associated with the assumed disordered solvent molecule(s) and the next twenty ($0.46 - 0.94 \text{ eA}^{-3}$) were in the vicinities of the metals, the tetrafluoroborate anion and the phenyl rings. A typical carbon atom on earlier Fourier syntheses had a peak intensity of ca. 2.9 eA^{-3} . The final model with 367 parameters varied converged to $R = 0.054$ and $R_w = 0.097$.¹⁷ No doubt the refinement suffers from our inability to adequately assign the portion of electron density which we assume corresponds to disordered solvent. The absorption coefficient used was the one assuming no solvent was present. With partial occupancy of solvent (as suggested by crystal density measurements and the elemental analysis) the absorption coefficient is not sufficiently different to result in a significant variation in the correction applied, so this should produce no adverse effects in the refinements.

The final positional and thermal parameters of the non-hydrogen atoms and the group atoms are given in Tables XIV and XV, respectively. The idealized hydrogen

parameters are given in Table XVI and a listing of the observed and calculated structure factor amplitudes is available.¹⁸

Results

Table X. Spectral Data^a for Reactions of Compounds 1, 2 and 3 with H⁺, CO and SO₂.

Complex	³¹ P(¹ H) NMR ^b		Infrared ν(cm ⁻¹) assignment
	δ(ppm)	J(Hz) ^c	
1 [Rh ₂ Cl ₂ (μ-HFB)(DPM) ₂]	7.5	111.9	1642 w (C≡C)
2 [Rh ₂ I ₂ (μ-HFB)(DPM) ₂]	9.1	110.0	1635 w (C≡C)
3 [Rh ₂ Cl ₂ (μ-DMA)(DPM) ₂]	8.6	115.0	1615 w (C≡C) 1705 br,m (CO ₂ Me)
4 [Rh ₂ Cl ₂ (μ-H)(μ-HFB)(DPM) ₃] ⁺	11.0	92.0	
5 [Rh ₂ I ₂ (μ-H)(μ-HFB)(DPM) ₂] ⁺	14.5	93.3	
6 [Rh ₂ Cl ₂ (μ-H)(μ-DMA)(DPM) ₂] ⁺	9.9	109.5	
7 [Rh ₂ Cl ₂ (μ-CO)(μ-HFB)(DPM) ₂]	8.9	131.8	1705 m (CO)
8 [Rh ₂ I ₂ (μ-CO)(μ-HFB)(DPM) ₂]	9.5	131.0	1690 m (CO)
9 [Rh ₂ Cl ₂ (μ-CO)(μ-DMA)(DPM) ₂]	11.0	140.6	1720 m (CO) 1660 m (¹³ CO) 1700 br, m (CO ₂ Me)
10 [Rh ₂ Cl ₂ (μ-SO ₂)(μ-HFB)(DPM) ₂]	16.0	130.1	1140(w), 1030(w) (SO ₂)
11 [Rh ₂ I ₂ (μ-SO ₂)(μ-HFB)(DPM) ₂]	18.5	127.9	1128(m), 1072(w) (SO ₂)
12 [Rh ₂ Cl ₂ (μ-SO ₂)(μ-DMA)(DPM) ₂]	13.0	135.5	1162(m), 1068(w) (SO ₂)

^a For compounds 4a (CF₃SO₃⁻ anion) and 4b (BF₄⁻ anion) the ¹H NMR spectra show a triplet of quintets at δ = -20.4 ppm (¹J_{Rh-H} = 23.4 Hz; ²J_{P-H} = 8.4 Hz) and for 5b (BF₄⁻ anion) a broad unresolved resonance is observed at δ = -21.4 ppm.

^b Spectra were run on a Bruker HFX-90 spectrometer.

^c J is the splitting between the two major lines of the AA'A'A'' XX' spectra.

Table XI. Spectral Data for Reactions of Compounds 1, 2 and 3 with CNMe.

Compound	¹ H	NMR (δ, ppm) 19F	³¹ P (1H)	Infrared ν(CN), cm ⁻¹
1. [Rh ₂ Cl ₂ (μ-HFB)(DPM) ₂] ^b	7.03-7.62(m), 4OH, C ₆ H ₅ 3.59(m), 2H, CH ₂ 2.92(m), 2H, CH ₂	-49.93(s)	6.76(112)	
13. [Rh ₂ Cl ₂ (CNMe) ₂ (μ-HFB)(DPM) ₂]	3.32(s), 3H, CH ₃	-47.11(11.5)(q)	12.15(122)(32)	2192
	2.98(s), 3H, CH ₃	-47.88(11.5)(q)	-0.11(102)(36)	
		-48.67(br.s)	9.55(124)(36)	2212
			2.67(94)(36)	
15a. [Rh ₂ Cl ₂ (CNMe) ₂ (μ-HFB)(DPM) ₂][Cl]	3.62(s), 3H, CH ₃	-47.62(11.2)(q)	11.67(119)(34)	2229, 2192
	3.38(s), 3H, CH ₃	-48.73(11.2)(q)	7.70(87)(31)	
	3.50(s), 3H, CH ₃			2244, 2216
	3.18(br), 5H, CH ₂ , CH ₃			
16a. [Rh ₂ (CNMe) ₄ (μ-HFB)(DPM) ₂][Cl] ₂	3.44(sh), 6H, CH ₃	-51.12(s)	10.46(90)	2216(br)
	3.04(s), 6H, CH ₃			
16b. [Rh ₂ (CNMe) ₄ (μ-HFB)(DPM) ₂][BF ₄] ₂	3.07(sh), 6H, CH ₃	-51.05(s)	11.57(89)	2234, 2217
	3.06(s), 6H, CH ₃			
2. [Rh ₂] ₂ (μ-HFB)(DPM) ₂	6.97-7.70(m), 4OH, C ₆ H ₅ 4.14(m), 2H, CH ₂ 3.22(m), 2H, CH ₂	-50.03(s)	8.78(110)	
17. [Rh ₂] ₂ (CNMe) ₂ (μ-HFB)(DPM) ₂	3.44(s), 3H, CH ₃	-48.05(11.6)(q)	9.59(119)(30)	2182
		-47.03(11.6)(q)	-0.16(99)(30)	
18. [Rh ₂] ₂ (CNMe) ₂ (μ-HFB)(DPM) ₂	2.94(s), 3H, CH ₃	-47.03(11.0)(q)	14.23(92)(31)	
		-47.83(11.0)(q)	6.21(113)(32)	

(continued...)

Table XI. (continued)

19. $[\text{Rh}_2\text{I}(\text{CMe})_2(\mu\text{-HFB})(\text{DPM})_2][\text{I}]$	3.59(s), 3H, CH ₃	-47.24(11.1)(q)	11.42(119)(31)
	3.37(s), 3H, CH ₃	-48.62(11.1)(q)	7.69(85)(31)
20. $[\text{Rh}_2\text{I}_2(\text{CMe})_2(\mu\text{-HFB})(\text{DPM})_2]$	2.89(s), 6H, CH ₃	-48.17(s)	18.76(93)
16c. $[\text{Rh}_2(\text{CMe})_4(\mu\text{-HFB})(\text{DPM})_2][\text{I}]_2$	3.07(sh), 6H, CH ₃	-51.05(s)	11.57(89)
	3.06(s), 6H, CH ₃		2211(br)
3. $[\text{Rh}_2\text{Cl}_2(\mu\text{-DMA})(\text{DPM})_2]$	7.01-7.70(m), 4OH, C ₆ H ₅		8.07(116)
	3.64(m), 2H, CH ₂		
	2.87(m), 2H, CH ₂		
	2.64(s), 6H, CH ₃ (DMA)		
21. $[\text{Rh}_2\text{Cl}_2(\text{CMe})_2(\mu\text{-DMA})(\text{DPM})_2]$	2.97(s), 3H, CH ₃ (CMe)		12.41(127)(26)
	2.74(s), 3H, CH ₃ (DMA)		3.71(96)(38)
	2.26(s), 3H, CH ₃ (DMA)		
22. $[\text{Rh}_2\text{Cl}(\text{CMe})_2(\mu\text{-DMA})(\text{DPM})][\text{Cl}]$	3.62(s), 3H, CH ₃ (CMe)		13.43(120)(34)
	3.22(s), 3H, CH ₃ (CMe)		10.21(88)(33)
	2.81(s), 3H, CH ₃ (DMA)		
	2.41(s), 3H, CH ₃ (DMA)		
23. $[\text{Rh}_2(\text{CMe})_4(\mu\text{-DMA})(\text{DPM})_2][\text{Cl}]_2$	3.68(s), 6H, CH ₃ (CMe)		11.96(94)
	2.92(s), 6H, CH ₃ (CMe)		2201, 2218(sh)
	2.77(s), 6H, CH ₃ (DMA)		

^a Spectra were run on Bruker WH-400 spectrometer.

^b The slight differences between ³¹P NMR parameters quoted here and those in Table I for compounds 1-3 result because of the different instruments used.

Table XII. Molar Conductivities^a for the Stepwise Addition of CNMe to $[\text{Rh}_2\text{X}_2(\mu\text{-RC}_2\text{R})(\text{DPM})_2]^\text{b}$.

Stoichiometry ^c	Conductivity ($\Lambda_M, \Omega^{-1}\text{cm}^2\text{mol}^{-1}$)		
	Compound 1	2	3
0:1	0.9	<0.4	<0.4
0.5:1	1.6	0.4	4.1
1:1	2.8	6.2	9.7
1.5:1	6.8	10.5	24.5
2:1	12.4	11.8	31.0
2.5:1	16.8	12.9	33.9
3:1	20.0	14.6	32.3
3.5:1	22.9	14.8	31.6
4:1	22.7	14.8	31.6

^a 1.0 mM solutions of the complexes in CH_2Cl_2

^b Complex 1, X = Cl, R = CF_3 ; 2, X = I, R = CF_3 ; 3 X = Cl, R = CO_2Me .

^c Moles of CNMe per mole of complex.

Table XIII.. Summary of Crystal Data and Intensity

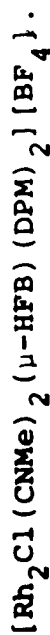
Collection Details for $[\text{Rh}_2\text{Cl}(\text{CNMe})_2(\mu\text{-HFB})\text{-}(\text{DPM})_2][\text{BF}_4]$

compound	$[\text{Rh}_2\text{Cl}(\text{CNMe})_2(\mu\text{-CF}_3\text{C}_2\text{CF}_3)(\text{DPM})_2][\text{BF}_4]$
formula weight	1341.0
formula	$\text{Rh}_2\text{ClP}_4\text{F}_{10}\text{N}_2\text{C}_{58}\text{BH}_{50}$
space group	$C_{2h}^5 - P2_1/n$ (non-standard setting of $P2_1/c$)
cell parameters	
a, Å	16.366(3)
b, Å	18.685(3)
c, Å	20.425(4)
β , °	104.35(1)
V, Å ³	6051.1
Z	4
density, g cm ⁻³	1.472 (calculated) 1.521 (measured by flotation) ^a
crystal dimensions, mm	0.41 x 0.31 x 0.47
crystal shape	monoclinic prism with faces of the forms {010}, {011}, {111} and {212}
crystal volume, mm ³	0.0125
temperature, °C	23
radiation	CuK α

μ , cm^{-1}	65.407
range in absorption correction factors	0.258-0.417
receiving aperture, mm	3.5 x 4.5 (at 30 cm from crystal)
take off angle, deg	5.0
scan speed, deg min^{-1}	2.0 in 2θ
scan range, deg	1.00 below $K\alpha_1$ to 1.00 above $K\alpha_2$
background counting times, s	10, $3^\circ < 2\theta < 60^\circ$; 20, $60^\circ < 2\theta < 78^\circ$; 40, $78^\circ < 2\theta < 120^\circ$
2θ limits, deg	$3 < 2\theta < 120$
unique data measured	9428
unique data used	6800
final number of parameters varied	367
error in observation of unit weight (GOF)	2.009
R	0.059
R_w	0.097

^aSee the text for an explanation of the poor agreement between the calculated and observed densities.

Table XIV. Positional and Thermal Parameters for the Non-Group Atoms of



Atom	x	y	z	U ₁₁	U ₂₂ ^a	U ₃₃	U ₁₂	U ₁₃	U ₂₃
Rh(1)	0.10197(3)	0.17210(3)	-0.06387(3)	3.30(3)	3.55(3)	4.04(3)	-0.41(2)	0.80(2)	0.06(2)
Rh(2)	0.20603(3)	0.23677(3)	-0.09089(3)	2.81(3)	3.48(3)	4.31(3)	-0.38(2)	0.51(2)	0.14(2)
C1	0.1238(2)	0.0821(1)	0.0185(1)	8.2(2)	9.0(1)	5.6(1)	0.7(1)	2.6(1)	1.1(1)
P(1)	0.1497(1)	0.0920(1)	-0.1356(1)	3.8(1)	3.6(1)	4.4(1)	-0.40(8)	0.91(8)	0.07(8)
P(2)	0.2573(1)	0.2058(1)	-0.1690(1)	3.3(1)	4.0(1)	4.6(1)	-0.32(8)	0.92(8)	-0.04(8)
P(3)	0.0391(1)	0.2430(1)	-0.0023(1)	3.3(1)	4.3(1)	4.6(1)	-0.47(8)	0.95(9)	-0.23(9)
P(4)	0.1428(1)	0.3631(1)	-0.0314(1)	3.4(1)	3.8(1)	5.2(1)	-0.15(8)	0.75(8)	-0.08(8)
F(1)	0.0944(3)	0.2641(3)	-0.1773(4)	3.5(3)	8.7(4)	12.4(5)	-0.2(3)	-0.2(3)	-1.1(4)
F(2)	0.0670(3)	0.1538(3)	-0.1691(3)	4.7(3)	6.8(3)	7.9(4)	-2.5(3)	-0.1(3)	0.8(3)
F(3)	0.0497(4)	0.2108(4)	-0.2542(3)	6.9(4)	14.7(6)	4.4(3)	-4.7(4)	-0.5(3)	-0.6(3)
F(4)	0.0005(3)	0.3647(3)	-0.2371(3)	5.8(3)	7.7(4)	8.0(4)	2.4(3)	1.3(3)	2.7(3)
F(5)	0.0739(3)	0.2991(3)	-0.2849(3)	7.1(4)	8.4(4)	4.5(3)	0.3(3)	1.0(3)	0.4(3)
F(6)	0.1310(3)	0.3869(3)	-0.2226(3)	7.4(4)	6.0(3)	7.2(4)	-1.5(3)	0.8(3)	2.1(3)
F(7)	0.549(1)	0.2828(8)	0.0537(9)	34(2)	18(1)	28(2)	-8(2)	-2(2)	-6(1)
F(8)	0.4675(6)	0.3581(1)	0.0188(6)	7.7(6)	46(2)	18(1)	5(1)	-0.2(7)	5(1)
F(9)	0.5615(9)	0.3731(7)	0.1178(6)	24(1)	19(1)	12.8(9)	4(1)	-2.8(9)	-5.1(8)
F(10)	0.5984(9)	0.3691(1)	0.0267(9)	19(1)	39(2)	31(2)	-12(1)	14(1)	-7(2)
N(1)	0.3362(4)	0.2161(4)	0.0390(4)	4.7(4)	5.5(4)	5.5(5)	-0.2(3)	-0.0(4)	0.2(4)
N(2)	0.3228(5)	0.4022(4)	-0.1113(4)	5.7(5)	5.2(4)	8.6(6)	-1.5(4)	3.2(4)	-0.3(4)
C(1)	-0.0393(5)	0.2143(5)	0.1877(4)	3.9(4)	5.8(5)	5.3(6)	-0.3(4)	0.1(4)	0.3(4)
C(2)	0.0506(4)	0.2330(4)	-0.1498(4)	2.5(4)	4.6(4)	4.5(5)	-0.6(3)	0.3(3)	-0.5(4)
C(3)	0.0860(4)	0.2853(4)	-0.1664(4)	3.3(4)	3.9(4)	4.3(4)	-0.2(3)	0.4(3)	0.3(3)
C(4)	0.0756(5)	0.3336(5)	-0.2260(5)	4.4(5)	5.6(5)	5.5(5)	0.3(4)	0.5(4)	0.6(4)
C(5)	0.2888(5)	0.2390(4)	-0.0085(4)	3.6(4)	4.2(4)	5.1(5)	-0.7(3)	1.1(4)	-0.3(4)
C(6)	0.3960(8)	0.1827(7)	0.0957(6)	8.5(8)	9.2(9)	7.1(7)	1.5(7)	-3.2(6)	1.0(7)
C(7)	0.2785(5)	0.3556(5)	-0.1075(4)	3.9(4)	5.1(5)	4.9(5)	0.0(4)	1.1(4)	-0.0(4)
C(8)	0.3805(8)	0.4580(7)	-0.1145(8)	10.4(9)	7.8(8)	15(1)	-4.7(7)	3.8(9)	0.3(8)
C(9)	0.1829(4)	0.1359(4)	-0.2040(4)	3.6(4)	3.9(4)	4.2(4)	-0.6(3)	0.7(3)	-0.4(3)
C(10)	0.0393(4)	0.3374(4)	-0.0262(4)	3.2(4)	4.5(4)	5.0(5)	0.1(3)	0.8(3)	-0.1(4)
B	0.540(1)	0.354(1)	0.056(1)	8(1)	11(1)	12(2)	-4.9(10)	-1(1)	-1(1)

^a Estimated standard deviations in the least significant figure(s) are given in parentheses in this and all subsequent tables.

^b The form of the thermal ellipsoid is: $\exp[-2\pi^2 \{a^*U_{11}h^2 + b^*U_{22}k^2 + c^*U_{33}l^2 + 2a^*b^*U_{12}hk + 2a^*c^*U_{13}hl + 2b^*c^*U_{23}kl\}]$. The quantities given in the table are the thermal coefficients $\times 10^3$.

Table XV. Derived Parameters for the Rigid-Group Atoms of $[\text{Rh}_2\text{Cl}(\text{CNMe})_2(\mu\text{-HFB})(\text{DPM})_2][\text{BF}_4]$

Atom	x	y	z	B(A ²)	Atom	x	y	z	B(A ²)
C(11)	0.2388(3)	0.0323(3)	-0.1015(3)	3.6(1)	C(15)	0.079(1)	0.2443(4)	0.0895(7)	3.6(2)
C(12)	0.2941(4)	0.0472(3)	-0.0394(4)	4.1(2)	C(16)	0.0269(4)	0.2664(4)	0.1302(6)	4.4(2)
C(13)	0.3667(3)	0.0061(3)	-0.0169(3)	5.7(2)	C(17)	0.0590(9)	0.2723(4)	0.200(1)	5.7(2)
C(14)	0.3839(3)	-0.0497(3)	-0.0565(3)	5.8(2)	C(18)	0.143(1)	0.2560(4)	0.2287(7)	6.5(2)
C(15)	0.3286(4)	-0.0645(3)	-0.1187(4)	5.3(2)	C(19)	0.1953(4)	0.2339(4)	0.1881(6)	6.0(2)
C(16)	0.2560(3)	-0.0235(3)	-0.1412(3)	4.6(2)	C(20)	0.1632(9)	0.2281(4)	0.119(1)	4.7(2)
C(21)	0.0664(4)	0.0307(3)	-0.1775(4)	3.1(1)	C(21)	-0.0721(3)	0.2208(3)	-0.0155(2)	3.8(2)
C(22)	0.0306(6)	-0.0126(3)	-0.1366(2)	3.9(2)	C(22)	-0.0919(3)	0.1483(3)	-0.0151(3)	4.7(2)
C(23)	-0.0339(5)	-0.0598(3)	-0.1657(4)	4.7(2)	C(23)	-0.1757(4)	0.1269(2)	-0.0268(4)	6.2(2)
C(24)	-0.0626(4)	-0.0639(3)	-0.2357(4)	4.5(2)	C(24)	-0.2398(3)	0.1778(3)	-0.0388(2)	7.0(3)
C(25)	-0.0268(6)	-0.0206(3)	-0.2766(2)	4.1(2)	C(25)	-0.2200(3)	0.2502(3)	-0.0391(3)	6.3(2)
C(26)	0.0377(5)	0.0266(3)	-0.2475(4)	3.8(2)	C(26)	-0.1362(4)	0.2717(2)	-0.0275(4)	4.8(2)
C(31)	0.3618(3)	0.1654(3)	-0.1410(2)	3.6(2)	C(27)	0.202(1)	0.3853(4)	0.0548(8)	3.8(2)
C(32)	0.4242(4)	0.2001(3)	-0.0827(3)	4.4(2)	C(28)	0.1594(7)	0.4098(4)	0.1017(6)	5.5(2)
C(33)	0.5073(4)	0.1763(3)	-0.0793(3)	5.6(2)	C(29)	0.204(1)	0.4272(4)	0.1670(4)	6.8(3)
C(34)	0.5281(3)	0.1179(3)	-0.1143(2)	5.9(2)	C(30)	0.292(1)	0.4202(4)	0.1853(8)	6.6(3)
C(35)	0.4657(4)	0.0832(3)	-0.1626(3)	5.7(2)	C(31)	0.3342(7)	0.3957(4)	0.1384(6)	5.8(2)
C(36)	0.3826(4)	0.1069(3)	-0.1760(3)	4.2(2)	C(32)	0.289(1)	0.3783(4)	0.0732(4)	4.5(2)
C(41)	0.2761(7)	0.2510(3)	-0.2443(4)	3.2(1)	C(33)	0.1304(4)	0.4528(3)	-0.0688(3)	3.7(2)
C(42)	0.2299(3)	0.2332(3)	-0.3091(5)	3.9(2)	C(34)	0.0563(4)	0.4721(3)	-0.1155(3)	4.7(2)
C(43)	0.2534(7)	0.2604(3)	-0.3652(2)	4.9(2)	C(35)	0.0503(4)	0.5386(3)	-0.1472(3)	6.1(2)
C(44)	0.3231(7)	0.3054(4)	-0.3565(4)	4.9(2)	C(36)	0.1183(4)	0.5857(3)	-0.1322(3)	6.2(2)
C(45)	0.3693(3)	0.3231(3)	-0.2917(5)	4.8(2)	C(37)	0.1924(4)	0.5663(3)	-0.0854(3)	6.0(2)
C(46)	0.3458(7)	0.2959(3)	-0.2356(2)	4.1(2)	C(38)	0.1984(4)	0.4999(3)	-0.0538(3)	4.9(2)

Rigid Group Parameters

	Xc	Yc	Zc	Delta	Epsilon	Eta
Ring1	0.3113(3)	-0.0087(2)	-0.0790(2)	-0.682(4)	2.435(5)	0.788(4)
Ring2	0.0019(2)	-0.0166(2)	-0.2066(2)	0.790(3)	1.850(5)	2.017(4)
Ring3	0.4450(3)	0.1416(2)	-0.1277(2)	-0.662(4)	2.925(5)	0.416(4)
Ring4	0.2896(2)	0.2782(2)	-0.3004(2)	0.918(4)	1.817(6)	3.786(5)
Ring5	0.1111(3)	0.2502(2)	0.1591(2)	-1.258(4)	2.19(1)	6.03(1)
Ring6	-0.1560(3)	0.1993(2)	-0.0271(2)	3.091(4)	0.061(4)	5.990(3)
Ring7	0.2468(3)	0.4028(2)	0.1201(2)	-1.226(4)	2.86(1)	5.52(1)
Ring8	0.1243(3)	0.5192(2)	-0.1005(2)	0.410(4)	2.751(4)	4.476(4)

^a Xc, Yc and Zc are the fractional coordinates of the centroid of the rigid group

^b The rigid group orientation angles Delta, Epsilon and Eta (radians) are the angles by which the rigid body is rotated with respect to a set of axes X, Y and Z. The origin is the centre of the ring; X is parallel to a^{*}, Z is parallel to c and Y is parallel to the line defined by the intersection of the plane containing a^{*} and b^{*} with the plane containing b and c.

Table XVI. Idealized Positional and Thermal Parameters for the Hydrogen Atoms of $[\text{Rh}_2\text{Cl}(\text{CNMe})_2(\mu\text{-HFB})(\text{DPM})_2](\text{BF}_4)$.

Atom	x	y	z	B(A ²)	Atom	x	y	z	B(A ²)
H(1C9)	0.1254	0.1556	-0.2352	4.12	H(42)	0.1821	0.2028	-0.3151	4.91
H(2C9)	0.2094	0.1020	-0.2270	4.12	H(43)	0.2219	0.2484	-0.4094	5.91
H(1C10)	0.0220	0.3661	0.0062	4.39	H(44)	0.3395	0.3237	-0.3947	5.94
H(2C10)	0.0005	0.3442	-0.0692	4.39	H(45)	0.4173	0.3533	-0.2856	5.85
H(1C6)	0.4107	0.2308	0.1280	8.36	H(46)	0.3775	0.3078	-0.1913	5.09
H(2C6)	0.4466	0.1775	0.0840	8.36	H(52)	-0.0308	0.2771	0.1103	5.44
H(3C6)	0.3754	0.1535	0.1167	8.36	H(53)	0.0231	0.2872	0.2274	6.64
H(1C8)	0.4102	0.4715	-0.0709	9.80	H(54)	0.1650	0.2605	0.2761	7.29
H(2C8)	0.3501	0.4884	-0.1371	9.80	H(55)	0.2529	0.2238	0.2077	6.99
H(3C8)	0.4190	0.4422	-0.1399	9.80	H(56)	0.1990	0.2138	0.0907	5.71
H(12)	0.2824	0.0860	-0.0125	5.15	H(62)	-0.0480	0.1135	-0.0072	5.63
H(13)	0.4042	0.0167	0.0256	6.67	H(63)	-0.1890	0.0773	-0.0263	7.29
H(14)	0.4328	-0.0777	-0.0408	6.68	H(64)	-0.2968	0.1630	-0.0462	7.89
H(15)	0.3396	-0.1029	-0.1452	6.47	H(65)	-0.2636	0.2848	-0.0470	7.27
H(16)	0.2177	-0.0337	-0.1832	5.52	H(66)	-0.1227	0.3210	-0.0279	5.86
H(22)	0.0500	-0.0098	-0.0889	4.91	H(72)	0.0994	0.4149	0.0885	6.48
H(23)	-0.0584	-0.0894	-0.1378	5.70	H(73)	0.1747	0.4440	0.1984	7.78
H(24)	-0.1067	-0.0862	-0.2556	5.51	H(74)	0.3217	0.4318	0.2298	7.74
H(25)	-0.0465	-0.0234	-0.3245	5.11	H(75)	0.3934	0.3904	0.1512	6.83
H(26)	0.0619	0.0563	-0.2755	4.75	H(76)	0.3181	0.3612	0.0413	5.55
H(32)	0.4097	0.2398	-0.0688	5.27	H(82)	0.0098	0.4399	-0.1262	5.73
H(33)	0.5494	0.1893	-0.0458	6.58	H(83)	-0.0005	0.5517	-0.1796	7.03
H(34)	0.5842	0.1010	-0.1047	7.01	H(84)	0.1138	0.6311	-0.1540	7.05
H(35)	0.4794	0.0433	-0.1867	6.64	H(85)	0.2382	0.5988	-0.0751	6.89
H(36)	0.3398	0.0838	-0.2097	5.25	H(86)	0.2485	0.4870	-0.0218	5.96

Table XVII. Selected Distances (Å) in $[\text{Rh}_2\text{Cl}(\text{CNMe})_2(\mu\text{-HFB})\text{-}(\text{DPM})_2][\text{BF}_4]$

Bonding Distances			
Rh(1)-Rh(2)	2.7091(8)	C(4)-F(4)	1.342(9)
Rh(1)-Cl	2.400(2)	C(4)-F(5)	1.360(10)
Rh(1)-P(1)	2.301(2)	C(4)-F(6)	1.338(9)
Rh(1)-P(3)	2.302(2)	P(1)-C(9)	1.815(8)
Rh(2)-P(2)	2.371(2)	P(2)-C(9)	1.821(7)
Rh(2)-P(4)	2.384(2)	P(3)-C(10)	1.831(8)
Rh(1)-C(2)	2.025(8)	P(4)-C(10)	1.821(7)
Rh(2)-C(3)	2.067(7)	P(1)-C(11)	1.831(4)
Rh(2)-C(5)	2.009(9)	P(1)-C(21)	1.823(4)
Rh(2)-C(7)	1.972(8)	P(2)-C(31)	1.835(4)
C(2)-C(3)	1.322(10)	P(2)-C(41)	1.838(4)
C(1)-C(2)	1.523(10)	P(3)-C(51)	1.827(5)
C(3)-C(4)	1.486(11)	P(3)-C(61)	1.822(5)
C(5)-N(1)	1.162(10)	P(4)-C(71)	1.826(5)
C(7)-N(2)	1.148(10)	P(4)-C(81)	1.833(5)
C(6)-N(1)	1.389(12)	B-F(7)	1.35(2)
C(8)-N(2)	1.420(12)	B-F(8)	1.25(2)
C(1)-F(1)	1.349(10)	B-F(9)	1.27(2)
C(1)-F(2)	1.309(9)	B-F(10)	1.27(2)
C(1)-F(3)	1.329(10)		

Table XVII (continued)

Non Bonded Distances			
P(1)-P(2)	2.961(3)	Cl-H(12)	2.82
P(3)-P(4)	2.982(3)	C(5)-H(76)	2.50
Rh(1)-C(3)	2.902(7)	C(5)-H(32)	2.58
Rh(2)-C(2)	2.660(7)	H(1C10)-H(72)	2.05
Rh(1)-F(2)	3.033(5)	H(2C9)-H(36)	2.10
Rh(2)-F(6)	3.369(5)	R(1) ^a -H(73) ^b	2.59
F(6)-C(7)	2.981(10)	R(2) ^a -H(34) ^c	2.61
Cl-H(62)	2.79		
Cl-H(22)	2.82	R(3) ^a -H(3C6)	2.61

a. R(1), R(2) and R(3) are 3 of the 5 most intense residual Fourier peaks.

b. H(73) of the molecule at (1-x, -y, -z).

c. H(34) of the molecule at ($\frac{1}{2}$ -x, y- $\frac{1}{2}$, $\frac{1}{2}$ -z).

Table XVIII. Selected Angles (Deg) in $[\text{Rh}_2\text{Cl}(\text{CNMe})_2(\mu\text{-HFB})\text{-}(\text{DPM})_2][\text{BF}_4]$.

Bond Angles			
P(1)-Rh(1)-Rh(2)	92.56(5)	Rh(1)-P(1)-C(9)	112.2(2)
P(3)-Rh(1)-Rh(2)	94.37(5)	Rh(1)-P(1)-C(11)	121.6(2)
P(2)-Rh(2)-Rh(1)	93.49(5)	Rh(1)-P(1)-C(21)	111.5(2)
P(4)-Rh(2)-Rh(1)	92.22(5)	Rh(2)-P(2)-C(9)	110.5(2)
P(1)-Rh(1)-P(3)	172.61(7)	Rh(2)-P(2)-C(31)	118.8(2)
P(2)-Rh(2)-P(4)	168.34(7)	Rh(2)-P(2)-C(41)	118.4(2)
Cl-Rh(1)-Rh(2)	130.35(6)	Rh(1)-P(3)-C(10)	111.6(3)
Cl-Rh(1)-P(1)	88.57(7)	Rh(1)-P(3)-C(51)	120.6(2)
Cl-Rh(1)-P(3)	88.91(8)	Rh(1)-P(3)-C(61)	110.9(2)
Cl-Rh(1)-C(2)	163.1(2)	Rh(2)-P(4)-C(10)	112.1(3)
P(1)-Rh(1)-C(2)	90.2(2)	Rh(2)-P(4)-C(71)	117.8(2)
P(3)-Rh(1)-C(2)	90.2(2)	Rh(2)-P(4)-C(81)	115.7(2)
P(2)-Rh(2)-C(3)	85.9(2)	C(9)-P(1)-C(11)	101.9(3)
P(4)-Rh(2)-C(3)	86.0(2)	C(9)-P(1)-C(21)	104.8(3)
C(5)-Rh(2)-C(3)	159.1(3)	C(11)-P(1)-C(21)	103.2(3)
C(7)-Rh(2)-C(3)	105.3(3)	C(9)-P(2)-C(31)	107.3(3)
C(2)-Rh(1)-Rh(2)	66.6(2)	C(9)-P(2)-C(41)	103.4(3)
C(3)-Rh(2)-Rh(1)	73.5(2)	C(31)-P(2)-C(41)	96.5(3)
C(5)-Rh(2)-Rh(1)	85.7(2)	C(10)-P(3)-C(51)	103.7(3)
C(7)-Rh(2)-Rh(1)	177.9(2)	C(10)-P(3)-C(61)	104.4(3)
C(5)-Rh(2)-C(7)	95.6(3)	C(51)-P(3)-C(61)	104.2(3)
P(2)-Rh(2)-C(5)	95.3(2)	C(10)-P(4)-C(71)	105.6(3)
P(4)-Rh(2)-C(5)	95.3(2)	C(10)-P(4)-C(81)	103.8(3)
P(2)-Rh(2)-C(7)	88.2(2)	C(71)-P(4)-C(81)	100.1(3)
P(4)-Rh(2)-C(7)	85.9(2)	P(1)-C(9)-P(2)	109.1(4)
Rh(1)-C(2)-C(3)	118.8(5)	P(3)-C(10)-P(4)	109.5(4)
Rh(2)-C(3)-C(2)	101.2(5)	P(1)-C(11)-C(12)	120.2(3)

Table XVIII continued

Rh(1)-C(2)-C(1)	116.3(5)	P(1)-C(11)-C(16)	119.5(3)
Rh(2)-C(3)-C(4)	129.4(5)	P(1)-C(21)-C(22)	117.4(3)
C(1)-C(2)-C(3)	124.9(7)	P(1)-C(21)-C(26)	122.6(3)
C(2)-C(3)-C(4)	129.3(7)	P(2)-C(31)-C(32)	119.2(3)
F(1)-C(1)-C(2)	111.1(7)	P(2)-C(31)-C(36)	119.9(3)
F(2)-C(1)-C(2)	114.2(7)	P(2)-C(41)-C(42)	121.7(3)
F(3)-C(1)-C(2)	112.5(7)	P(2)-C(41)-C(46)	117.7(3)
F(4)-C(4)-C(3)	114.4(7)	P(3)-C(51)-C(52)	120.0(3)
F(5)-C(4)-C(3)	112.8(7)	P(3)-C(51)-C(56)	119.8(3)
F(6)-C(4)-C(3)	113.6(7)	P(3)-C(61)-C(62)	116.5(3)
F(1)-C(1)-F(2)	104.8(7)	P(3)-C(61)-C(66)	123.5(3)
F(1)-C(1)-F(3)	106.4(7)	P(4)-C(71)-C(72)	121.1(3)
F(2)-C(1)-F(3)	107.1(7)	P(4)-C(71)-C(76)	118.9(3)
F(4)-C(4)-F(5)	104.0(7)	P(4)-C(81)-C(82)	121.5(3)
F(4)-C(4)-F(6)	105.9(7)	P(4)-C(81)-C(86)	118.2(3)
F(5)-C(4)-F(6)	105.3(7)	F(7)-B-F(8)	97(2)
Rh(2)-C(5)-N(1)	178.9(7)	F(7)-B-F(9)	108(2)
Rh(2)-C(7)-N(2)	174.2(8)	F(7)-B-F(10)	96(2)
C(5)-N(1)-C(6)	176.2(9)	F(8)-B-F(9)	125(2)
C(7)-N(2)-C(8)	177.6(10)	F(8)-B-F(10)	114(2)
		F(9)-B-F(10)	111(1)

Table XVIII (continued)

Torsion Angles			
P(1)-Rh(1)-Rh(2)-P(2)	3.94(7)	C(41)-P(2)-Rh(2)-C(5)	-133.0(3)
P(3)-Rh(1)-Rh(2)-P(4)	-3.65(7)	C(71)-P(4)-Rh(2)-C(5)	15.4(3)
P(1)-Rh(1)-Rh(2)-P(4)	173.77(7)	C(81)-P(4)-Rh(2)-C(5)	133.8(3)
P(3)-Rh(1)-Rh(2)-P(2)	-173.47(7)	C(31)-P(2)-Rh(2)-C(7)	78.8(3)
C(9)-P(1)-P(3)-C(10)	-1.7(4)	C(41)-P(2)-Rh(2)-C(7)	-37.6(3)
C(9)-P(2)-P(4)-C(10)	0.3(4)	C(71)-P(4)-Rh(2)-C(7)	-79.8(3)
C(11)-P(1)-P(3)-C(51)	-2.8(3)	C(81)-P(4)-Rh(2)-C(7)	38.5(3)
C(21)-P(1)-P(3)-C(61)	-2.7(3)	C(11)-P(1)-Rh(1)-C(2)	156.9
C(31)-P(2)-P(4)-C(71)	-1.3(3)	C(21)-P(1)-Rh(1)-C(2)	-81.0
C(41)-P(2)-P(4)-C(81)	0.6(3)	C(51)-P(3)-Rh(1)-C(2)	-159.8(3)
C(1)-C(2)-C(3)-C(4)	5.1(1.3)	C(61)-P(3)-Rh(1)-C(2)	78.2(3)
Rh(1)-C(2)-C(3)-Rh(2)	-0.9(6)	C(31)-P(2)-Rh(2)-C(3)	-175.7(3)
C1-Rh(1)-Rh(2)-C(5)	-0.8(2)	C(41)-P(2)-Rh(2)-C(3)	67.9(3)
C(11)-P(1)-P(2)-C(31)	0.4(3)	C(71)-P(4)-Rh(2)-C(3)	174.5(3)
C(21)-P(1)-P(2)-C(41)	-2.4(4)	C(81)-P(4)-Rh(2)-C(3)	-67.2(3)
C(51)-P(3)-P(4)-C(71)	-0.4(3)	C(9)-P(1)-Rh(1)-C(2)	36.1(3)
C(61)-P(3)-P(4)-C(81)	2.9(5)	C(10)-P(3)-Rh(1)-C(2)	-37.7(3)
C(11)-P(1)-Rh(1)-C1	-39.9(2)	C(9)-P(2)-Rh(2)-C(3)	-51.1(3)
C(21)-P(1)-Rh(1)-C1	82.1(2)	C(10)-P(4)-Rh(2)-C(3)	51.6(3)
C(51)-P(3)-Rh(1)-C1	37.1(2)	C1-Rh(1)-C(2)-C(1)	2.6(12)
C(61)-P(3)-Rh(1)-C1	-84.9(2)	C(5)-Rh(2)-C(3)-C(4)	-174.7(8)
C(31)-P(2)-Rh(2)-C(5)	-16.6(3)	C(7)-Rh(2)-C(3)-C(4)	6.4(8)

Table XIX. Least Squares Planes Calculations^a for $[\text{Rh}_2\text{Cl}(\text{CNMe})_2(\mu\text{-HFB})(\text{DPM})_2][\text{BF}_4]$.

Plane	equation	Distances from Planes (Å)																	
		Rh(1)	Rh(2)	Cl	C(1)	C(2)	C(3)	C(4)	C(5)	M(1)	C(6)	C(7)	M(2)	C(8)	P(1)	P(2)	P(3)	P(4)	
1	$0.5285x - 0.6279y - 0.3772z + 0.1991 = 0$																		
2	$0.5238x - 0.6216y - 0.3622z + 0.1604 = 0$																		
3 ^c	$0.5213x - 0.6207y - 0.3632z + 0.1991 = 0$																		
4	$0.5204x - 0.6191y - 0.3432z + 0.4316 = 0$																		
5	$-0.3243x + 0.2007y - 0.6002z - 0.9614 = 0$																		
1	$-0.0271(5)$	$0.0036(6)$	$0.014(2)$	$-0.027(9)$	$-0.001(7)$	$0.016(7)$	$0.116(9)$	$-0.003(6)$	$0.134(7)$	$-0.007(12)$	$-0.053(8)$	$-0.194(8)$	$-0.263(14)$						
2	$-0.0004(9)$	$0.0004(8)$	$0.004(2)$	$-0.003(6)$	$0.012(7)$	$0.029(7)$	$0.138(9)$	$-0.019(8)$	$-0.020(7)$	$-0.041(12)$	$-0.058(8)$	$-0.166(8)$	$-0.274(14)$						
3 ^b	-----	-----	-----	$0.016(9)$	$0.020(7)$	$0.034(7)$	$0.150(9)$	$-0.027(8)$	$-0.034(7)$	$-0.060(12)$	$-0.060(8)$	$-0.166(8)$	$-0.277(14)$						
4	$0.110(1)$	$0.011(6)$	$0.248(2)$	$-0.010(9)$	$0.018(7)$	$-0.018(7)$	$0.011(9)$	$0.002(8)$	$0.132(7)$	$-0.262(8)$	$-0.117(8)$	$0.132(7)$	$-0.415(14)$						
5	$-0.002(3)$	$-0.020(6)$												$0.042(2)$	$0.181(2)$	$0.052(2)$	$0.166(2)$		
Planes																			
Interplane	1,2	1,3	1,4	1,5	2,3	2,4	2,5	3,4	3,5	4,5									
angle	0.41	0.64	2.91	89.77	0.24	3.15	89.37	3.29	89.15	91.70									

a. X, Y and Z are orthogonal coordinates in Å with X along the a axis, Y in the ab plane and Z along the C* axis.

b. Not included in least-squares plane calculation.

c. This plane defined by Rh(1), Rh(2) and Cl.

Description of Structure of Compound 15b

The unit cell of $[\text{Rh}_2\text{Cl}(\text{CNMe})_2(\mu\text{-HFB})(\text{DPM})_2][\text{BF}_4]$, shown in Figure 5, consists of discrete, well-separated anions and cations. A perspective view of the cation, together with the numbering scheme (phenyl hydrogens have the same number as their attached carbons) is shown in Figure 6 and a representation of the inner coordination sphere in the plane of the acetylene and the rhodium atoms, together with some relevant bond distances and angles is given in Figure 7. More complete listings of interatomic distances and angles may be found in Tables XVII and XVIII, respectively, and the results of some least-squares plane calculations are collected in Table XIX.

The tetrafluoroborate anion has a near-tetrahedral geometry, but is significantly distorted from the idealized case; the B-F distances range from 1.25(2) Å to 1.35(2) Å and the F-B-F angles range from 96(2)° to 125(2)°. As noted earlier, this group is probably disordered, so the geometry, although not completely satisfactory, is not unexpected and compares adequately with geometries observed for other disordered BF_4^- anions.¹⁹⁻²²

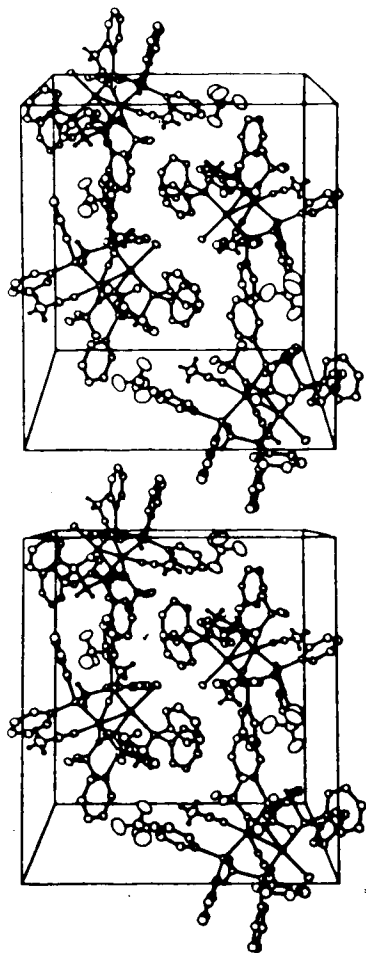


Figure 5. Stereoview of the Unit Cell of $[\text{Rh}_2\text{Cl}(\text{CNMe})_2(\mu\text{-HFB})(\text{DPM})_2][\text{BF}_4]$. As viewed with the title at the bottom, the x-axis comes out of the page, the y-axis goes from top to bottom and the z-axis goes from left to right. 20% thermal ellipsoids are shown.

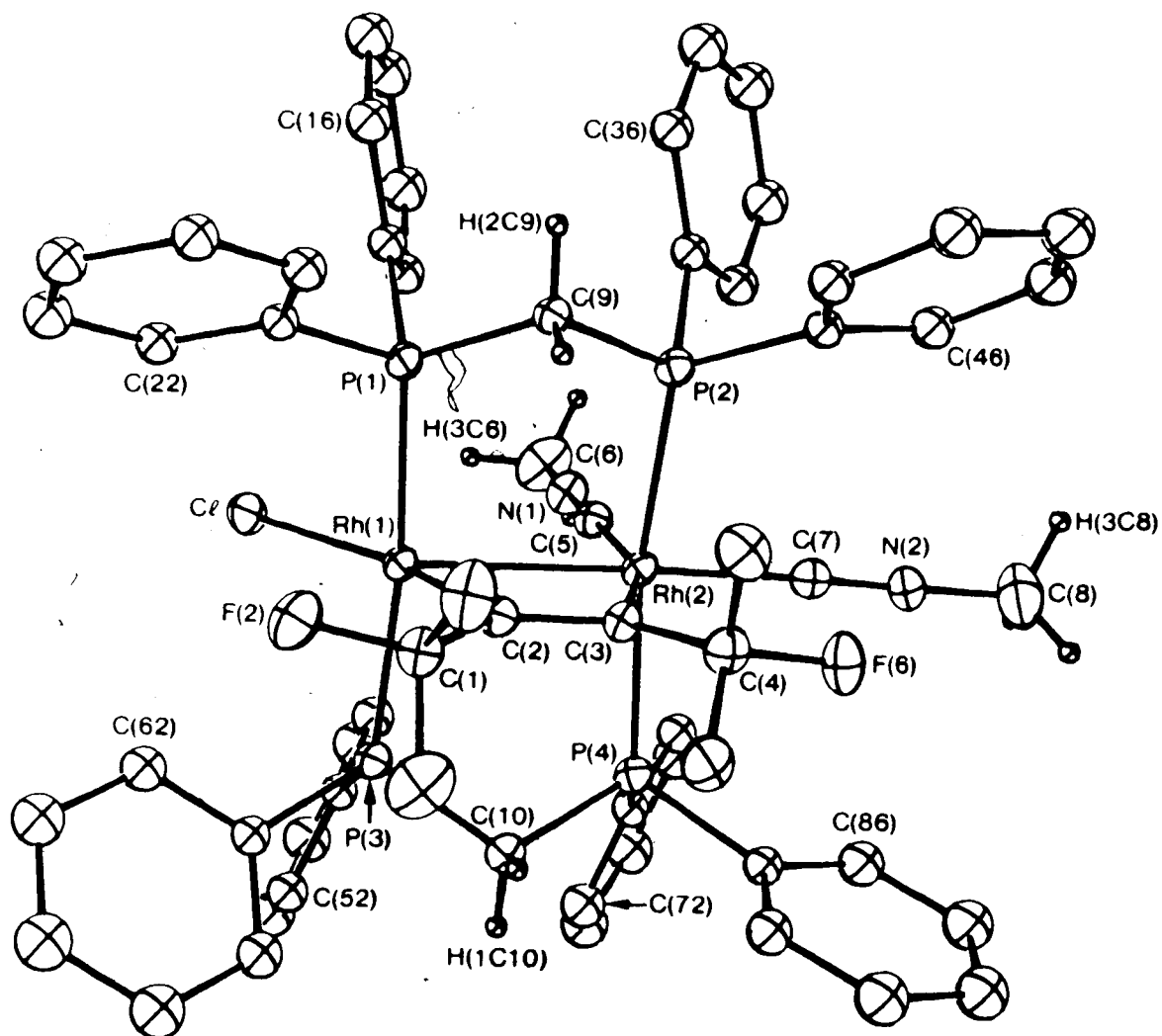


Figure 6. Perspective View of $[\text{Rh}_2\text{Cl}(\text{CNMe})_2(\mu\text{-HFB})(\text{DPM})_2]^+$. The numbering scheme is as shown; the numbering on the phenyl carbon atoms starts at the carbon bonded to phosphorus and increases sequentially around the ring. 20% thermal ellipsoids are shown.

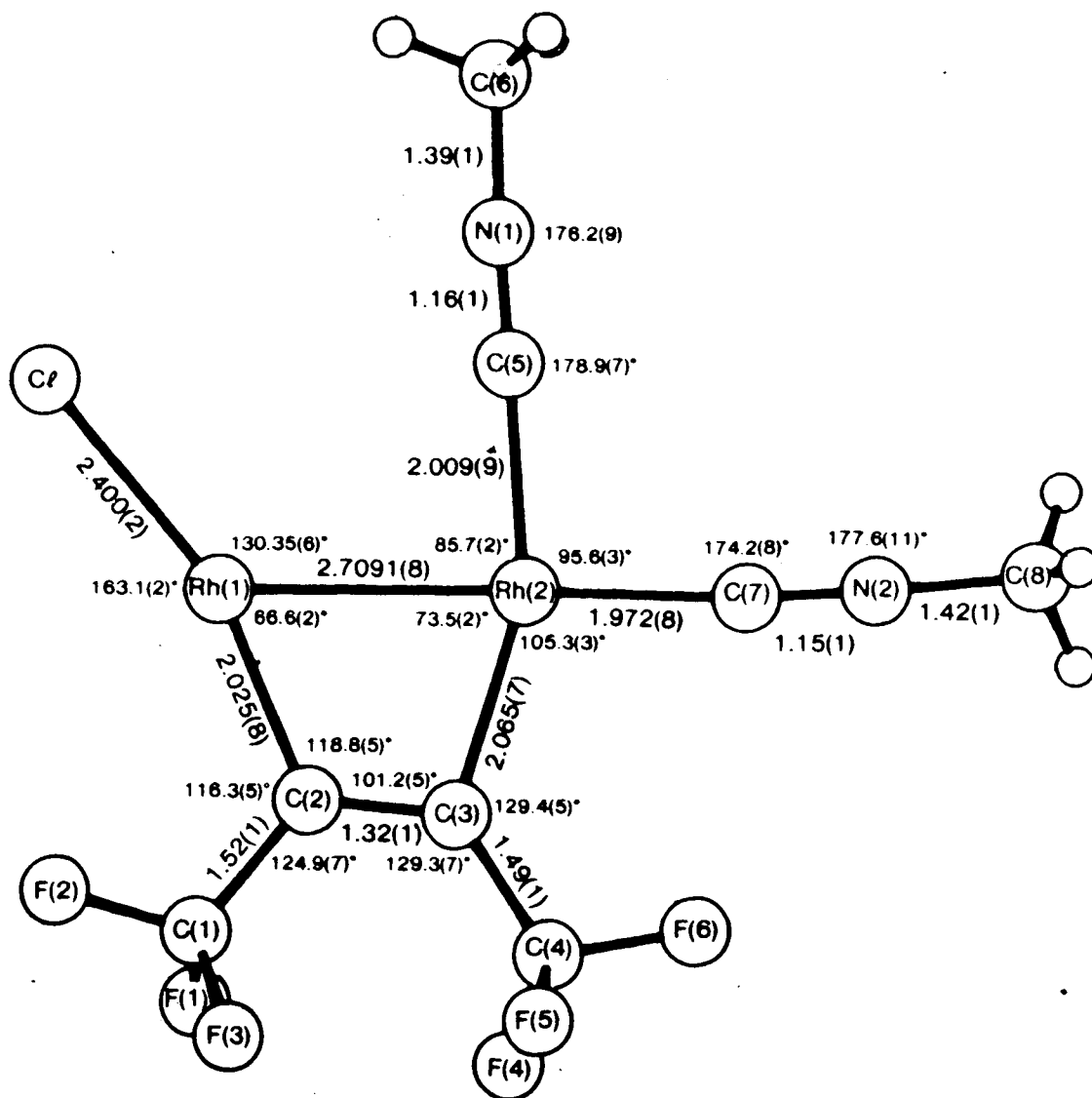


Figure 7. Representation of the Equatorial Plane of $[\text{Rh}_2\text{Cl}(\text{CNMe})_2(\mu\text{-HFB})(\text{DPM})_2]^+$. Some relevant bond lengths and angles are shown.

The cation has an inner-core geometry similar to that observed for many other DPM-bridged binuclear complexes, having two rhodium atoms bridged by two mutually trans DPM ligands. In the equatorial plane (perpendicular to the Rh-P vectors) the metals are bridged by a hexafluoro-2-butyne molecule coordinated as a cis-dimetallated olefin, while Rh(1) has a terminal chloro ligand and Rh(2) has two terminal, linear methyl isocyanide ligands. The metals are also connected by a metal-metal bond.

Each end of the $[\text{Rh}_2\text{Cl}(\text{CNMe})_2(\mu\text{-HFB})(\text{DPM})_2]^+$ cation rather closely resembles one of two known and structurally characterized complexes; on the Rh(1) side, the geometry is reminiscent of that of the precursor, **1**,¹ whereas the geometry about Rh(2) closely approximates that observed for $[\text{Rh}_2(\text{CN}^t\text{Bu})_4(\mu\text{-HFB})(\text{DPM})_2]^{2+}$, which has recently been characterized by Mague *et al.*^{23,24} Considering first the geometry about Rh(1), we can describe it as a very distorted trigonal bipyramid with axial phosphine groups and the equatorial sites occupied by the terminal Cl ligand, the bridging acetylene ligand and Rh(2) or, if we do not consider the Rh-Rh bond, as a distorted square plane. The major difference of this part of the molecule from the conformations about the metals in **1** lies in the position of the chloro ligand,

which is much closer to being trans to the acetylene group than in 1. This may be responsible for the longer Rh-Cl bond in the present compound (2.400(2) Å vs. 2.377(2), and 2.384(2) Å for 1) since a σ -alkenyl group (a metallated olefin in our terminology) has a large trans influence.^{2,5} In $[\text{Rh}_2\text{Cl}_2(\mu\text{-CO})(\mu\text{-DMA})(\text{DPM})_2]$, the CO adduct of compound 3, the chloro ligands are similarly situated with respect to the acetylene moiety and the Rh-Cl distances are again long.⁴ The disposition of the chloro ligand (almost trans to C(2)) results in a relatively large Cl-Rh(1)-C(2) angle of 163.1(2)°; in $[\text{Rh}_2\text{Cl}_2(\mu\text{-HFB})(\text{DPM})_2]$ (1) and the analogous carbonyl-³ and sulfur dioxide-bridged⁵ species the corresponding angles are all close to 145°, even though there are significant differences in the geometries of the bridging groups. The reason for the difference in the present compound may be steric, because the Cl atom has weak van der Waals contacts with the phenyl hydrogens on rings 1 and 2 (Cl-H(22) = 2.81; Cl-H(12) = 2.8). Moving this atom towards the position it formerly occupied in 1 would bring about greater steric interaction with H(22) and the carbons of phenyl group 2.

The geometry about Rh(2), as in $[\text{Rh}_2(\text{CN}^t\text{Bu})_4(\mu\text{-HFB})(\text{DPM})_2]^{2+}$, can be viewed as either distorted octahedral, considering the Rh-Rh bond, or as distorted

trigonal bipyramidal ignoring this bond. The relative positions of the isocyanide ligands in complex 15b and Mague's species are different; in 15b one CNMe group is essentially trans to the Rh-Rh bond while the other is almost at right angles to it but bent towards Rh(1) slightly, away from the position which is trans to the acetylene group (see Figure 7). In Mague's species,²⁴ on the other hand, the two tert-butylisocyanides which are mutually cis on adjacent metals are bent away from each other and are trans to the two Rh-acetylene linkages, while the other two are bent significantly off the Rh-Rh axis. These differences in isocyanide positions are probably a consequence of the significant differences in the bulk of the isocyanide groups and of the much less crowded environment around Rh(1) in the present compound (having one Cl ligand instead of two CN^tRu groups). The isocyanides tend to assume positions which minimize contacts with each other and with the DPM phenyl groups. So in Figure 6 we see that these phenyl groups tend to be staggered with respect to the equatorial ligands.

The geometries of the isocyanide ligands in 15b are normal for terminally bonded, linear isocyanide groups and agree well with each other and with other reported parameters.²⁶⁻²⁸ Although the two metal-isocyanide

distances differ slightly (1.972(8), 2.009(9) Å), the difference is in the direction expected, with the longer distance being the one trans to a group of high trans influence (the metallated olefin). These distances are significantly shorter than those observed for the tert-butylisocyanide groups in Mague's compound.²⁴ However, it is likely that the rather long distances in the latter species result from the severe crowding in this molecule.

Although the overall geometry of the bridging acetylene ligand is not atypical for such a group when bonding as a cis-dim metallated olefin, this moiety does have some curious structural features. The angles about the metallated carbons are reminiscent of sp^2 hybridization and the acetylenic C-C bond has lengthened to 1.32(1) Å, close to that of a normal olefin,^{2,9} as have been previously observed. However, the acetylene group is coordinated in an unsymmetrical manner, appearing to be more tightly bound to Rh(1), as evidenced by the shorter rhodium-carbon distance (2.024(8) Å vs. 2.066(7) Å). In addition, the acetylene ligand is displaced in the equatorial plane such that C(2) is only 2.660(7) Å from Rh(2), whereas the corresponding Rh(1)-C(3) distance is 2.902(7) Å. Although this contact with Rh(2) is well beyond that of a normal covalent bond, it may suggest some interaction of Rh(2) with the

C(2)-C(3) π -bond. In the acetylide-bridged A-frame, $[\text{Rh}_2(\text{CO})_2(\mu\text{-CC}^t\text{Bu})(\text{DPM})_2][\text{ClO}_4]$, the acetylide moiety is coordinated to one metal in a side-on manner and the two Rh-C distances involved are 2.209(6) and 2.616(6) Å,³⁰ suggesting that the above contact in the present complex is not unreasonable for some π interaction. Such an interaction is also consistent with the drop in the infrared stretch associated with the acetylene moiety from 1638 cm^{-1} in **1** to 1590 cm^{-1} in **15b**. This asymmetry could, however, be steric in origin since it is consistent with the end of the acetylene ligand, which is adjacent to the crowded isocyanide end of the complex, being forced away from Rh(2) (see Figure 2). The non-bonded contact between C(7) and F(6) of 2.98(1) Å is consistent with these steric arguments although it seems as though any unfavourable steric interactions could have been relieved by twisting the acetylene moiety out of the plane containing the rhodium atoms, the chloro and the isocyanide ligands as was observed in the tetrakis(tert-butyl isocyanide) compound.²⁴ As it is, the acetylene moiety is twisted from the above plane by only 0.9(6)°. Whatever the reason for the observed asymmetry in acetylene bonding, we would expect to observe less activation at the acetylenic carbon which is less tightly bound (C(3)) and therefore less bending back of the CF_3

group and a shorter C-CF₃ bond (the covalent radius for an sp carbon is less than that of an sp² carbon). Both of these effects are observed, although the difference in the C-CF₃ bonds is not statistically significant and may therefore be fortuitous. However, the difference in the C(2)-C(3)-C(4) and the C(3)-C(2)-C(1) angles is significant, especially since it is opposite to what would be expected based on steric interaction between this CF₃ group and the neighbouring isocyanide ligand. In another complex recently characterized by Mague, [Rh₂(O₂CMe)(P(OMe)₃)(μ-CO)(μ-DMA)(DPM)₂]PF₆·Me₂CO,³¹ the difference in Rh-C_{acetylene} distances is even more pronounced (1.985(12) and 2.053(12) Å) than in our compound, but there is no significant difference in the angles about the acetylenic carbons. It may also be that in the present determination the difference in the bend-back angles of the CF₃ groups is also steric in origin since F(2) is involved in a rather close contact with Rh(1) (3.033(5) Å) which could force this CF₃ group away from Rh(1), resulting in a more acute C(1)-C(2)-C(3) angle.

The Rh(1)-Rh(2) distance (2.7091(8) Å), although typical for a Rh-Rh single bond, is one of the shortest yet observed in DPM-bridged-dirhodium systems. Since each end in the present compound resemble either

$[\text{Rh}_2\text{Cl}_2(\mu\text{-CF}_3\text{C}_2\text{CF}_3)(\text{DPM})_2]$ or $[\text{Rh}_2(\text{C}(\text{Nt-Bu})_4(\mu\text{-CF}_3\text{C}_2\text{CF}_3)-(\text{DPM})_2)]^{+2}$, it might be expected that its Rh-Rh distance would be intermediate between those in the above complexes. In fact, it is less than either of these. However, it should be noted that the Rh-Rh distance in the tetrakis(tert-butylisocyanide) dication²⁴ (2.9653(6) Å) is anomalously long, most probably due to severe crowding about both metal centers. The $\text{Rh}_2(\text{DPM})_2$ framework in 15b is essentially as expected, with some minor distortions. Both diphosphine ligands are bent towards the bridging acetylene group, reflecting the non-bonded interactions of the phenyl groups with the chloro ligand and the isocyanide groups; since the bridging methylene groups of the DPM ligands are bent towards the acetylene ligand, phenyl groups 1, 3, 5 and 7 are thrust towards the isocyanide (C(5)N(1)C(6)H₃) and Cl ligands so interactions of these groups seem to dictate the phosphine geometries. All Rh-P distances (2.301(2)-2.384(2) Å) are within the range normally observed for such DPM-bridged, dirhodium compounds,³² although those on Rh(1) are significantly shorter than those on Rh(2). It seems that the longer distances reflect the more crowded environment about Rh(2). In two other A-frame-like compounds, $[\text{Rh}_2\text{Cl}_3(\mu\text{-H})(\mu\text{-CO})(\text{DPM})_2]$ ⁶ and $[\text{Rh}_2\text{Cl}_2(\text{CO})(\text{SCNMe}_2)(\text{DPM})_2][\text{BF}_4]$,³³ similar variations in

the Rh-P distances were also observed, with the longer distances being associated with the more crowded rhodium centers. All other parameters within the phosphine groups in the present compound are normal.

Discussion of Results

(a) Protonation Reactions

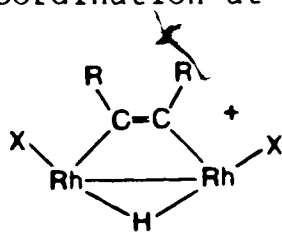
The reactions of $[\text{Rh}_2\text{X}_2(\mu\text{-RC}_2\text{R})(\text{DPM})_2]$ ($\text{R} = \text{CF}_3$, $\text{X} = \text{Cl}$ (1), I (2); $\text{R} = \text{CO}_2\text{Me}$, $\text{X} = \text{Cl}$ (3)) with very strong acids such as $\text{CF}_3\text{SO}_3\text{H}$ and $\text{HBF}_4 \cdot \text{OEt}_2$ yield the cationic species $[\text{Rh}_2\text{X}_2(\mu\text{-H})(\mu\text{-RC}_2\text{R})(\text{DPM})_2][\text{Y}]$ ($\text{R} = \text{CF}_3$, $\text{X} = \text{Cl}$, $\text{Y} = \text{CF}_3\text{SO}_3$ (4a); BF_4 (4b); $\text{R} = \text{CF}_3$, $\text{X} = \text{I}$, $\text{Y} = \text{CF}_3\text{SO}_3$ (5a), BF_4 (5b); $\text{R} = \text{CO}_2\text{Me}$, $\text{X} = \text{Cl}$, $\text{Y} = \text{CF}_3\text{SO}_3$ (6a), BF_4 (5b)). These species are only stable for brief periods at low temperatures in the presence of excess acid, and cannot be isolated. Nevertheless, their NMR spectra establish that protonation at the metal-metal bond has occurred in each case. The 200 MHz ^1H NMR spectrum of compound 4a, for example, displays an 11-peak multiplet at high field ($\delta = -20.44$ ppm, $^1J_{\text{Rh-H}} = 23.4$ Hz, $^2J_{\text{P-H}} = 8.4$ Hz) which integrates as a single proton, and which can be analysed as an overlapping triplet of quintets; the larger splitting arises from coupling to the two

chemically equivalent Rh nuclei to give a triplet, with each of these peaks being further split into a quintet, owing to coupling of the hydrogen to four chemically equivalent P nuclei. In addition, the $^{31}\text{P}\{^1\text{H}\}$ NMR spectrum reveals a symmetric pattern at 11.0 ppm with a separation of 92.0 Hz between the two major peaks, again consistent with a complex in which all four phosphorus nuclei are chemically equivalent. Unfortunately, solvent and ligand absorptions prevent observation of the Rh-H stretch in the infrared spectra of compound **4a** and the other protonation products.

The $^{31}\text{P}\{^1\text{H}\}$ NMR spectra of complexes **4b**, **5a** and **5b** very closely resemble that of **4a**, suggesting that similar protonation of the Rh-Rh bond has occurred. For compounds **4b** and **5b** this conclusion is supported by their ^1H NMR spectra; for **4b**, the spectrum is nearly identical to that of **4a**, while for **5b**, an unresolved resonance is observed in the same region of the spectrum with a ~~peak~~ envelope essentially superimposable on those of **4a** and **4b**. Surprisingly, no hydride resonance was observed for **5a** over the temperature range -80°C to $+20^\circ\text{C}$, yet the $^{31}\text{P}\{^1\text{H}\}$ NMR spectrum of **5a** and the colour change clearly show that a reaction has occurred and suggest a product analogous to the others.

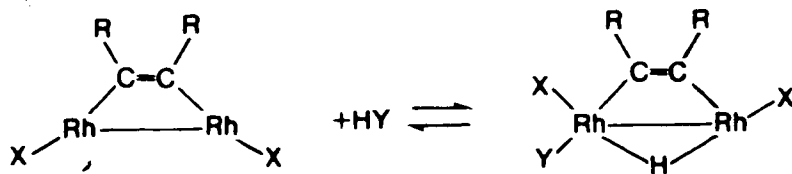
The $^{31}\text{P}\{^1\text{H}\}$ NMR spectra of the DMA-bridged compounds, **6a** and **6b**, again appear typical for a symmetric product and are qualitatively similar to the patterns observed above, but they do differ significantly from the patterns for **4** and **5**, having a wider spacing between the two major peaks. Again no resonance corresponding to the hydride ligand was observed in either of these species. We suspect that for these species a fluctuational process, such as reversible deprotonation, is responsible for our failure to detect the hydride resonances, although no direct evidence of this was observed.

The above spectral information shows that the products are symmetrical (at least on the NMR time scale) and suggests that simple protonation of the Rh-Rh bond has occurred to give the cationic species diagrammed below. However, based on related protonation studies involving the analogous carbonyl-bridged complex $[\text{Rh}_2\text{Cl}_2(\mu\text{-CO})(\text{DPM})_2]$,⁶ we are unable to rule out the possibility that Rh-Rh bond protonation may also be accompanied by anion coordination at one metal centre.



Although the NMR spectra for protonation of the carbonyl-bridged species were very similar to those reported here, and as such were indicative of a symmetric product, careful studies on this carbonyl-bridged system showed that anion coordination was occurring to give the fluxional species $[\text{Rh}_2\text{Cl}_2(\text{Y})(\mu\text{-H})(\mu\text{-CO})(\text{DPM})_2]$, which were symmetrical on the NMR time scale. Based on the very close similarities in the spectral parameters between compounds 4 and 5 and their CO-bridged analogues, we suggest that a similar process may be occurring in the acetylene-bridged species, yielding the oxidative addition products diagrammed below.

As with the CO-bridged analogues, these products would have to be fluxional in order to give the symmetric-species pattern observed in the NMR spectra. Such fluxionality, accompanied by reversible deprotonation, may also explain our inability to locate



the hydride resonances for three of the protonation products, due to exchange broadening of the spectral

lines. The additional studies required to further elucidate any fluxional processes that might be occurring could not be carried out because of the instability of the products and the necessity of utilizing large excesses of acid. No broadening of the $^{31}\text{P}\{^1\text{H}\}$ NMR signals is observed upon cooling sample **4-6**, but this is not surprising since broadening could only be observed for the carbonyl-bridged analogues in the absence of excess acid;⁶ the reactions reported herein require excess acid. Similarly, the excess acid prevented meaningful conductivity measurements from being carried out.

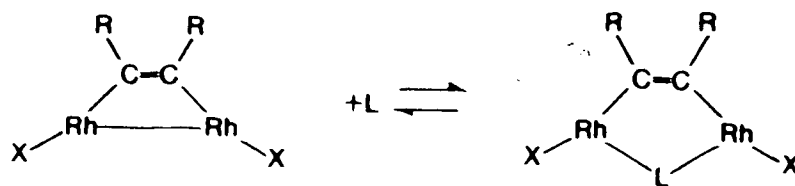
As noted above, the $^{31}\text{P}\{^1\text{H}\}$ NMR spectra for complexes **6a** and **6b** are significantly different from those of compounds **4** and **5**. Although the reasons for the difference are not clear, anion coordination in these species might be inhibited by the bulkier CO_2Me substituents on the acetylene group, possibly giving a different type of species without such anion coordination. Nevertheless, though direct evidence (^1H NMR) is lacking for **6a** and **6b**, we see no reason to suggest that protonation of **3** at the metal-metal bond did not occur for these cases, as did clearly occur for complexes **1** and **2**.

(b) Reactions with CO and SO₂

At the time that this work was undertaken, the only confirmed examples of CO insertion into metal-metal single bonds had been reported for $[M_2X_2(Ph_2YCH_2YPh_2)]$ ($M = Pd, Pt; Y = P, As$),^{34,35} and even now examples of such reactions are rare.³⁴⁻³⁶ Although we had not previously observed such insertions in related dirhodium, DPM-bridged complexes, the reaction of $[Rh_2X_2(\mu-CO)(DPM)_2]$ with acetylenes to give $[Rh_2X_2(\mu-CO)(\mu-acetylene)(DPM)_2]$ suggested to us that CO insertion into the Rh-Rh bond of the acetylene-bridged species 1 might be possible, yielding the above carbonyl- and acetylene-bridged complexes.

Examples of SO₂ insertions into metal-metal bonds, on the other hand, have been known for some time,^{37,38} although such insertions into the Rh-Rh bonds of DPM-bridged A-frames had not been observed by us⁵ or reported by other workers. Again, it seemed that compound 1 and the related species 2 and 3 should be capable of undergoing insertion of SO₂ into the Rh-Rh bonds.

The initial reactions of compounds 1, 2 and 3 with CO and SO₂ do in fact yield species which seem to have resulted from the insertion of these small molecules into the metal-metal bonds as diagrammed below. For the products of CO-insertion (7, 8 and 9), the ³¹P{¹H} NMR



spectra and IR spectra are identical with those observed in the reactions of $[\text{Rh}_2\text{X}_2(\mu\text{-CO})(\text{DPM})_2]$ with the appropriate acetylene molecule⁴ and confirm that identical products are obtained by either route. The $^{31}\text{P}\{^1\text{H}\}$ NMR spectra are all rather similar, and are typical of AA'A'A'XX' spin systems, as expected for symmetrical products resulting from CO-insertion into the Rh-Rh bonds. Furthermore, the infrared spectra show the stretch of the bridging carbonyl ligand at ca. 1700 cm^{-1} for each product. Although this frequency is rather low, it is typical for carbonyl groups which bridge two metals and not accompanied by metal-metal bonds.^{4,34,35} The X-ray structure determination of one product, $[\text{Rh}_2\text{Cl}_2(\mu\text{-CO})(\mu\text{-DMA})(\text{DPM})_2]$ (obtained from $[\text{Rh}_2\text{Cl}_2(\mu\text{-CO})(\text{DPM})_2] + \text{DMA}$), has unambiguously confirmed the above formulations, and shows a carbonyl geometry which corresponds to sp^2 hybridization, in agreement with the low carbonyl stretching frequency.⁴

The products obtained in the reactions of compounds **1**, **2** and **3** with SO_2 are analogous to the above carbonyl adducts and are therefore formulated as $[\text{Rh}_2\text{X}_2(\mu\text{-SO})_2(\mu\text{-RC}_2\text{R})(\text{DPM})_2]$ ($\text{R} = \text{CF}_3$, $\text{X} = \text{Cl}$ (**10**), **I** (**11**); $\text{R} = \text{CO}_2\text{Me}$, $\text{X} = \text{Cl}$ (**12**)) in which the bridging SO_2 and acetylene groups are not accompanied by a Rh-Rh bond. Although elemental analyses of pure samples cannot be obtained, owing to the reversibility of the reactions (vide infra), the spectral parameters clearly support the above formulation. The S-O stretches in the infrared spectrum occur at ca. 1143 cm^{-1} and 1057 cm^{-1} (see Table X). The drop in the higher frequency stretch from that usually observed when the bridging SO_2 is accompanied by a metal-metal bond³⁹ parallels the drop in carbonyl stretching frequencies observed for the carbon-bridged analogues **7**, **8** and **9** from the values observed for bridging carbonyls accompanied by metal-metal bonds. In addition, the $^{31}\text{P}\{^1\text{H}\}$ NMR spectra of the SO_2 adducts are very similar to those of the CO adducts, again showing an increase (to ca. 130 Hz) in the splitting between the two major peaks (as compared to the starting materials (see Table X). Although these spectral results do not rule out the possibility that these symmetrical products might contain two SO_2 ligands (especially since compounds **10** and **11** are prepared under excess SO_2), the reaction of **3** with one

equivalent of SO_2 to yield only **12** excludes the possibility of major species containing more than one SO_2 group.

It is of interest to note that, while complexes **7 - 9** can be obtained either by reaction of compounds **1 - 3** with CO or by reaction of the corresponding carbonyl complex, $[\text{Rh}_2\text{X}_2(\mu\text{-CO})(\text{DPM})_2]$, with the appropriate acetylene, the SO_2 adducts **10 - 12** can only be prepared by reaction of **1 - 3** with SO_2 . Attempts to prepare the SO_2 -bridged products **10 - 12** by reaction of $[\text{Rh}_2\text{X}_2(\mu\text{-SO}_2)(\text{DPM})_2]$ with acetylenes failed.

The reactions of CO and SO_2 with compounds **1 - 3** are all reversible, although a significant range in ligand labilities is observed. In all cases the carbonyl groups are more tightly bound than the SO_2 groups in the analogous compounds. Carbonyl removal from compounds **7** and **8** requires overnight refluxing in CHCl_3 utilizing a N_2 flush to completely regenerate compounds **1** and **2**, respectively, and compound **9** must be refluxed in benzene for ca. 2 days before it is totally consumed. However, under the conditions of the latter reaction, about 10% of the product is found to be $[\text{Rh}_2\text{Cl}_2(\mu\text{-CO})(\text{DPM})_2]$, arising from the loss of the acetylene group. By contrast, the SO_2 ligands in complexes **10 - 12** are very labile, particularly in the hexafluoro-2-butyne complexes **10** and

11. Even after saturating CH_2Cl_2 solutions of **10** and **11** with SO_2 and leaving at least 20-fold excesses of the gas above the solutions, some starting material remains in each case (ca. 15% of **1** in **10** and ca. 7% of **2** in **11**). Flushing these solutions with N_2 under ambient conditions causes complete reversal of these reactions within minutes. Attempts to obtain solid samples of **10** and **11** resulted in large amounts of the starting materials **1** and **2**, particularly for **10**, where mostly starting material was obtained. The small concentration of **10** obtained, and the presence of strong C-F stretches as well as bands due to DPM made location of the S-O stretches in this compound difficult. However, comparisons of its spectrum with those of the pure starting material, of **11** and of **12** do serve to identify the weak bands. The SO_2 group in compound **12** is much less labile than those of the other SO_2 adducts, although it too is lost to some degree upon recrystallization.

In all cases, the acetylene groups are more tightly bound than either the carbonyl or sulfur dioxide ligands; only in the experiment in which compound **9** undergoes prolonged reflux in benzene is any acetylene loss observed.

It seems, from this study, that the iodo complexes bind CO and SO_2 more strongly than do their chloro

analogues and that the DMA complexes bind these molecules more strongly than do the HFB species. The first generalization is consistent with the better π -donor capability of the iodo ligand compared to the chloro ligand; the iodo complexes will therefore have additional electron density at the metals, which would strengthen the π -backbonding to the CO or SO₂ ligands, causing them to be bound more strongly. The second observation suggests that HFB is a more effective electron-withdrawing group than DMA, leaving less electron density on the metals for π -backdonation to CO or SO₂, thereby labilizing these groups. This is consistent with the substituent σ -parameters for CF₃ and CO₂Me moieties,⁴⁰ which indicate that the trifluoromethyl groups on HFB have a higher group electronegativity than the methylcarboxylate groups on DMA.

Although the reactions of CO and SO₂ with compounds 1 - 3 can be most readily visualized as occurring directly at the metal-metal bond, molecular orbital calculations by Hoffmann and coworkers⁴¹ suggest that such attack is actually symmetry-forbidden and that some unsymmetrical intermediate is initially involved. Although no such intermediate was ever observed in our reactions, it cannot be ruled out. Certainly one possible intermediate, diagrammed below, would be



expected to yield the observed products ($L = \text{CO}, \text{SO}_2$) with great facility. Similar unsymmetrical species have been obtained in the reactions of 1 - 3 with methyl isocyanide (vide infra).

(c) Reactions with CNMe

Isocyanides, CNR , are quasi-isoelectronic with CO and might therefore be expected to behave similarly. Consequently they can function as simple π -acid ligands or undergo insertion reactions with metal-metal and metal-carbon bonds,^{42,43} much as is observed for CO and SO_2 . However, isocyanides are much stronger σ -donors and poorer π -acceptors than CO , as exemplified by the changes in IR stretching frequencies associated with these groups upon coordination to metals;⁴³ whereas $\nu(\text{CO})$ invariably decreases on coordination to metals which are capable of π -backdonation, $\nu(\text{CN})$ for coordinated isocyanides are often higher than those of the free molecules. More

effective σ -donation from an orbital which is C-N antibonding and less effective π -backdonation from the metal into the C-N π^* orbitals account for the observed increase in $\nu(\text{CN})$.

This greater σ -basicity of isocyanides can lead to reactions which differ from those normally found for CO. For example, the reaction of methyl isocyanide with $[\text{Pd}_2\text{Cl}_2(\text{DPM})_2]^{26}$ initially gives the product of insertion into the Pd-Pd bond, as is observed for CO and SO_2 . However, this product then reacts further with CNMe via stepwise exchange of CNMe for Cl^- , ultimately giving $[\text{Pd}_2(\text{CNMe})_2(\mu\text{-CNMe})(\text{DPM})_2]^{2+}$, the carbonyl analogue of which has apparently not been observed.

Since the $[\text{Rh}_2\text{X}_2(\mu\text{-RC}_2\text{R})(\text{DPM})_2]$ complexes display Rh-Rh bond reactivity with CO and SO_2 similar to that observed for the above Pd dimer, we chose also to examine the reaction of the acetylene-bridged dirhodium species with CNMe. Our anticipation was that reaction at the Rh-Rh bond would be the first step; this was found not to be the case.

As described in the experimental section, the reactions of CNMe with compounds 1, 2 and 3 were carried out by sequentially adding aliquots of the isocyanide to solutions of the complex, followed by monitoring using IR and NMR spectroscopy. In general, approximately 10

additions and observations were made over the range from 0 to 6 equivalents. A brief word regarding the $^{31}\text{P}\{^1\text{H}\}$ NMR spectra of these species is in order before discussing the results of the isocyanide additions. Two types of peak patterns are generally obtained for these species, examples of which are shown in Figure 8. For the purposes of this study we concluded that detailed analysis of these spectra would offer no additional information of relevance, so no analysis was carried out, although we note that similar spectra have, on other occasions, been successfully analysed by ourselves³³ and others.^{11,23} In Table XI we report the separations between the peaks; these are not true coupling constants but are given as aids in identifying the compounds. The first type of peak pattern is that of a species having chemically equivalent Rh nuclei (and four chemically equivalent P nuclei), and appears as two major peaks with additional minor peaks (see, for example, complex **20** in Figure 8). As usual, we have reported the splitting between the two major peaks and the chemical shift of the centre of the pattern. The second peak pattern appears as two resonances, each of which appears as two sets of three lines (which appear sometimes as pseudo-doublets of triplets), and is indicative of an AA'BB'XY spin system resulting from two chemically inequivalent Rh nuclei

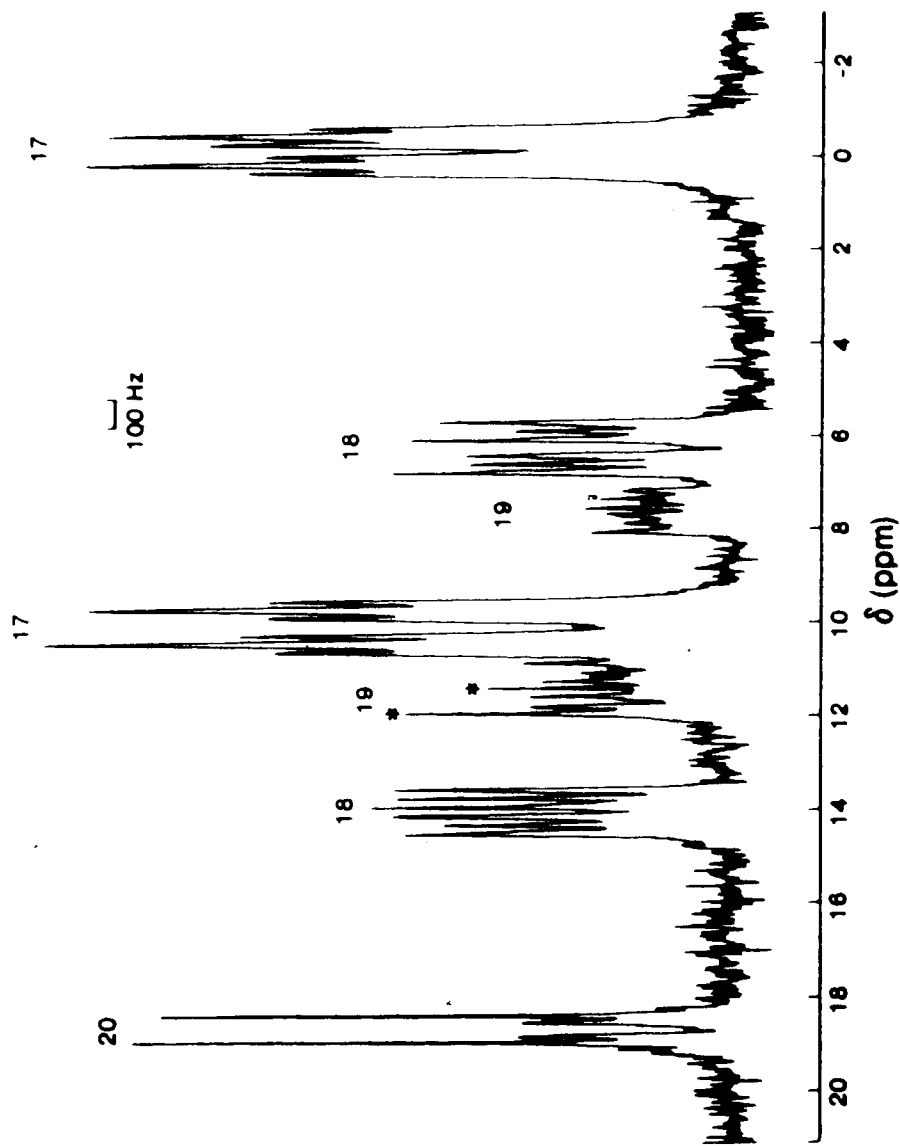


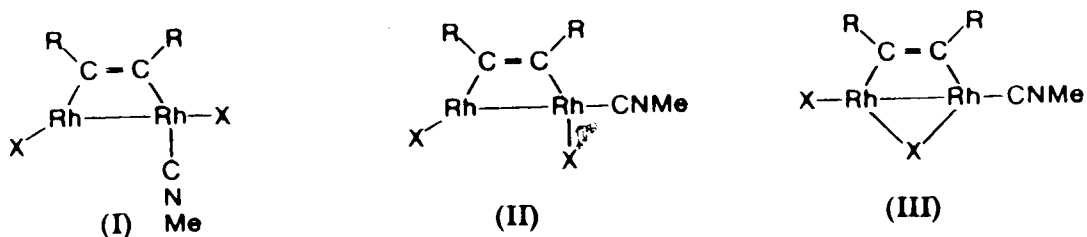
Figure 8. 161.92 MHz $^{31}\text{P}\{^1\text{H}\}$ NMR Spectrum of $[\text{Rh}_2\text{I}_2(\mu\text{-HFB})(\text{DPM})_2] + \sim 1.3 \text{ CNMe}$. The two peaks marked with asterisks are due to resonances from compound 16c superimposed on those from compound 19.

(species 17 and 18 in Figure 8). For this spectral type, the chemical shift of the centre of each pair of three-line patterns is given, as well as the separation between the pairs of "triplets" and the splitting within these "triplets".

After the addition of 1 equivalent of CNMe to compound 1, the $^{31}\text{P}\{^1\text{H}\}$ NMR spectrum (at 161.92 MHz) reveals four approximate doublets of triplets. Homonuclear ^{31}P decoupling reveals that they are linked in pairs; irradiation of one "doublet of triplets" results in the collapse of another to leave a doublet. Thus two asymmetric species 13 and 14, in the approximate molar ratio 4:3, respectively, are present. The ^{19}F NMR spectrum (at 376.41 MHz) at this stoichiometry shows a coupled pair of quartets (confirmed by ^{19}F decoupling) and a broad singlet, which can be assigned to compounds 13 and 14, respectively, on the basis of their relative intensities. Similarly, the corresponding ^1H NMR spectrum (at 400.14 MHz) reveals two new singlets at 3.32 and 2.98 ppm, in a region appropriate for coordinated CNMe groups. These methyl resonances, which again integrate in the ratio 4:3, together integrate as one CNMe group. Two sets of resonances appear for the DPM methylene protons, each of which is an AB quartet which is further split into quintets, as expected for such

groups. The solution infrared spectrum reveals two terminal isocyanide stretches at 2192 and 2212 cm^{-1} , again assigned to compounds 13 and 14 on the basis of their intensities.

Based on the above spectral information, three structures (shown below) seem plausible for these two



isomers. In view of the very low conductivity of the reaction mixture (see Table XII), significant dissociation of Cl^- does not seem likely. Furthermore, attempts to prepare the species likely to be the result of Cl^- loss, $[\text{Rh}_2\text{Cl}(\text{CNMe})(\mu\text{-CF}_3\text{C}_2\text{CF}_3)(\text{DPM})_2]^+$, were unsuccessful; addition of 0.5 equivalents of AgBF_4 in THF solution to the reaction mixture as above led to the formation of roughly equimolar amounts of $[\text{Rh}_2\text{Cl}(\text{CNMe})_2(\mu\text{-HFB})(\text{DPM})_2]^-$ (vide infra) and 1, and further AgBF_4 addition resulted in the decomposition of 1 to unidentified products.

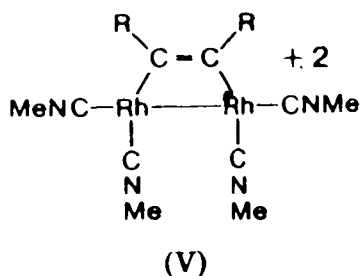
Although we are unable to establish unambiguously the structures of complexes 13 and 14, one thing is clear

- these products are very different from those obtained upon addition of CO (7) or SO₂ (8). In no case do we observe evidence of a bridging isocyanide group. Both structures I and II have precedent in the structure reported herein of compound 15b. Structure I is an interesting possibility since such a structure was suggested by us as the first product of CO addition to compounds 1 - 3; in the CO adduct the carbonyl group readily assumes the bridging position, severing the Rh-Rh bond, whereas here, if I is indeed one of the products, the CNMe group does not move into the bridging site.

After the addition of two equivalents of CNMe to a solution of 1, one species, 15a, predominates, whose ³¹P{¹H} NMR spectrum is typical of an AA'BB'XY spin system arising from an unsymmetrical compound. This is confirmed by a ¹⁹F NMR spectrum which shows a pair of quartets and by the ¹H NMR spectrum which shows two methyl resonances. Solution infrared measurements reveal two terminal isocyanide stretches at 2192 and 2229 cm⁻¹ and conductivity measurements show that the species is a weak electrolyte (see Table XII). Reaction of 15a with a methanolic solution of NaBF₄ leads to the precipitation of the very insoluble species [Rh₂Cl(CNMe)₂(μ-HFB)-(DPM)₂][BF₄] (15b), whose structure was unambiguously established by X-ray techniques (vide supra) to be that

diagrammed as structure IV (see Figure 9). Compound 15b has isocyanide stretches at 2216 and 2244 cm^{-1} . Owing to the very low solubility of 15b a satisfactory $^{31}\text{P}\{^1\text{H}\}$ NMR spectrum could not be obtained, but its ^1H NMR spectrum shows the CNMe resonances, which are shifted somewhat from those of 15a (see Table XI). These differences, we suggest, are due to Cl^- association with the cation in 15a, which is also implied by the conductivity of 15a, which is lower than those of similar 1:1 electrolytes in CH_2Cl_2 .⁴⁴

The addition of CNMe to a solution of 15a results in the formation of a new species, 16a, and after the addition of two equivalents of CNMe conversion to this product is complete. Complex 16a can also be prepared by the addition of 4 equivalents of CNMe to compound 1. No other species is detected between 15a and 16a. The $^{31}\text{P}\{^1\text{H}\}$ NMR spectrum displays two major peaks, characteristic of a symmetrical species, and the ^{19}F NMR spectrum shows one singlet. The ^1H NMR spectrum reveals two resonances, each integrating as 6 protons, indicating that it contains four CNMe ligands grouped into two chemically equivalent pairs. Although its conductivity is low for a 2:1 electrolyte, it is approximately double that found for solutions of 15a, again suggesting association of the Cl^- anions with the cation. We therefore formulate the compound as shown below (with DPM



groups omitted for clarity). This structure is similar to that reported²⁴ by Mague for the CN^tBu analogue, which he prepared²³ by addition of HFB to $[\text{Rh}_2(\text{CN}^t\text{Bu})_4^-(\text{DPM})_2]^{2+}$. In addition, we have prepared Mague's species by a method similar to that reported above for CNMe, by the addition of four equivalents of CN^tBu to compound 1.⁴⁵

Clearly, the addition of two equivalents of CNMe to 15a brings about replacement of the remaining Cl⁻ ligand by two CNMe groups, as was observed for Cl⁻ replacement at the first metal centre. However, in this case no intermediate involving 3CNMe groups, analogous to the 1:1 adducts 13 and 14, is observed. Further addition of CNMe to solutions of 16a causes no further reaction.

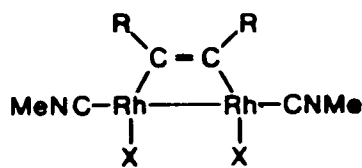
The stepwise addition of CNMe to $[\text{Rh}_2\text{I}_2(\mu\text{-HFB})(\text{DPM})_2]$ (2) has also been monitored as described above for complex 1; on the whole, the results are comparable, although there are some notable differences. Reaction of

2 with one equivalent of CNMe again yields two unsymmetrical species (17 and 18), in approximately a 5:2 ratio for this case. Again, which of the possible isomers (I - III) these products correspond to is not clear, although it seems, based on the ^1H NMR, that it is the same isomer which is the more abundant species in the reaction with compound 1 and that substitution of I^- for Cl^- favours the production of this isomer. The lower abundance of the one isomer on substituting Cl by I is consistent with the involvement of halide-bridged species such as III. Because of the lower tendency of iodine to bridge metal-metal bonds compared with chlorine, we would expect a lower abundance of the halide-bridged isomer in the iodo complex. It may also be that the less abundant isomer actually consists not only of compound III but of a rapidly equilibrating mix of compounds II and III, since these structures are related merely by swinging the halide ligand into or out of the bridging site. We suggest, therefore, that the more abundant 1:1 adduct observed corresponds to isomer I, and the less abundant species corresponds to either isomer III or a rapidly equilibrating mixture of isomers II and III.

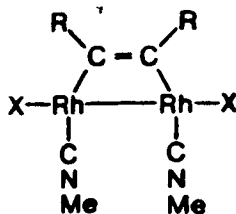
Further CNMe addition results in the appearance of the unsymmetrical 2:1 adduct 19, which is analogous to the chloro species 15a, but also produces a symmetrical

species 20. Unfortunately, infrared spectra and conductivity measurements do not assist greatly in identifying the species other than to establish that only terminal isocyanides are present and that the reaction mixture (which contains five species over a wide range of stoichiometries) is weakly conducting. After the addition of one equivalent of CNMe the major species present is the starting material with the additional compounds 17, 18, 19 and 20 present in the respective ratios 1:0.40:0.25:0.20. Upon further CNMe addition the starting material 2 is consumed while the ratio of products remains the same until the consumption of 2 is complete, after which point the mixture begins to be converted to the tetrakis(methylisocyanide) species 16c. The $^{31}\text{P}\{^1\text{H}\}$ NMR spectrum after the addition of approximately 1.3 equivalents of CNMe to compound 2 is shown in Figure 8, where the 1:1 adducts, 17 and 18, the 2:1 adducts, 19 and 20, and the 4:1 adduct 16c are visible.

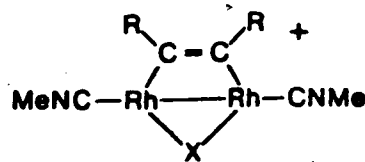
Three possible structures seem reasonable for the symmetrical species 20, as shown below. We consider the



(VI)



(VII)



(VIII)

fourth possibility (that of the dicationic species, $[\text{Rh}_2(\text{CNMe})_2(\mu\text{-HFIB})(\text{DPM})_2]^{2+}$) unlikely, owing to the electron deficiency of the metals in such a complex, and again, attempts to isolate such a species by addition of Ag^+ to solutions of the 2:1 adducts failed. Based on steric grounds, we would expect structure **VIII** to be the most likely; however, based on the lower tendency of the iodo group to bridge two metals relative to Cl, one is then at a loss to explain why no similar species was observed in the reaction of **1** with CNMe. We suggest, therefore, that the symmetrical species **20** has the structure **VI** or **VII**. This is consistent with the lower tendency of these low-oxidation-state Rh complexes to dissociate I^- compared to Cl^- . Possibly the most obvious route to structure **IV** from any of the structures corresponding to the 1:1 adducts (**I** - **III**) involves halide loss from the metal having the first CNMe group attached, followed by CNMe coordination at this metal. Such a dissociative first step seems necessary since the metal involved is coordinatively saturated. Although we tried and failed to isolate such a cationic mono(isocyanide) species (vide supra), this does not rule it out as a reactive intermediate. If, as we suggest, the iodo ligand on the Rh atom having the coordinated CNMe group is less likely to dissociate than Cl^- , attack

by a second CNMe group at this metal centre is inhibited and attack at the other metal centre becomes competitive, yielding both the unsymmetrical and the symmetrical 2:1 adducts (**19** and **20**, respectively). We are unable to assign the symmetric species as either structure **VI** or **VII**, although if, as we suggested, isomer **I** is the more abundant 1:1 product, then the symmetrical 2:1 product could reasonably be expected to be isomer **VII**. Another possible route to the 2:1 adducts involves CNMe attack at the coordinatively unsaturated metal of structure **I** to yield structure **VII**. Chloride loss from one metal, accompanied by migration of the CNMe group from the adjacent metal would yield structure **IV**, or if halide loss were inhibited ($X = I$) then the symmetrical product would remain.

Clearly iodide dissociation is not totally inhibited since both **19** and **20** are produced and both are consumed on further addition of CNMe to give the 4:1 adduct, $[\text{Rh}_2(\text{CNMe})_4(\mu\text{-HFB})(\text{DPM})_2][\text{I}]_2$; if iodide dissociation were completely inhibited, the 18-electron-18-electron complex **20** would be expected to be the only 2:1 adduct, and probably the final product of reaction. It is significant that the tetrakis(isocyanide) product, **16c**, from this reaction has somewhat different spectral parameters than the chloro analogue **16a**, even though the

cations are the same. This is consistent with our notion that significant ion pairing occurs, as implied by the conductivity data.

In order to determine the extent to which the nature of the bridging acetylene might influence the equilibria observed in the reactions of 1 and 2, and also to attempt to obtain further information about the structural details of the products in these reactions, we decided to look at the reaction of $[\text{Rh}_2\text{Cl}_2(\mu\text{-DMA})(\text{DPM})_2]$ (3) with CNMe.

Only one 1:1 adduct (21) is observed in the reaction of compound 3 with CNMe. Based on the position of the ^1H NMR peak for the CNMe group, it seems that this compound corresponds to the less abundant isomer obtained in the equivalent reactions with 1 and 2; we therefore assign it either structure II or structure III. These isomers might seem at first glance to be less sterically favoured than structure I, since attack on Rh at the required site would be hindered by the carboxymethyl group on the adjacent acetylene moiety; however, it should be noted that steric interactions in the product would be minimized if the chloro group were to occupy the bridging site (as in isomer III).

Only one, unsymmetrical 2:1 adduct (22) is obtained with compound 3; this species is similar in its spectral

parameters to the analogous products 15 and 19. It is significant that no symmetrical product analogous to 20 is observed. This is consistent with the large conductivity observed for the DMA-bridged species; a symmetrical 2:1 product was only observed for the complex containing the iodo ligand, which associates more strongly with these complexes than does the chloro ligand.

As in all the previous reactions, addition of further CNMe leads to the formation of the 4:1 adduct, $[\text{Rh}_2(\text{CNMe})_4(\mu\text{-DMA})(\text{DPM})_2]^{2+}$. Again the conductivity of this species is low, but this is not unexpected for such a species having Cl^- anions in a medium of low dielectric constant. However, at all points observed, the conductivity of these DMA-bridged species is higher than those of the HFB-bridged species, corresponding to a smaller extent of ion-pairing. This may be due to the fact that DMA is a less electron-withdrawing acetylene than HFB (vide supra), which would decrease the amount of positive charge localized on the metals in the DMA complexes and thus decrease the extent of ion-pairing.

Based on the data and inferences given above for the reactions of CNMe with compounds 1, 2 and 3, we have proposed a scheme for these reactions (Figure 9). Although all three reaction sequences are closely

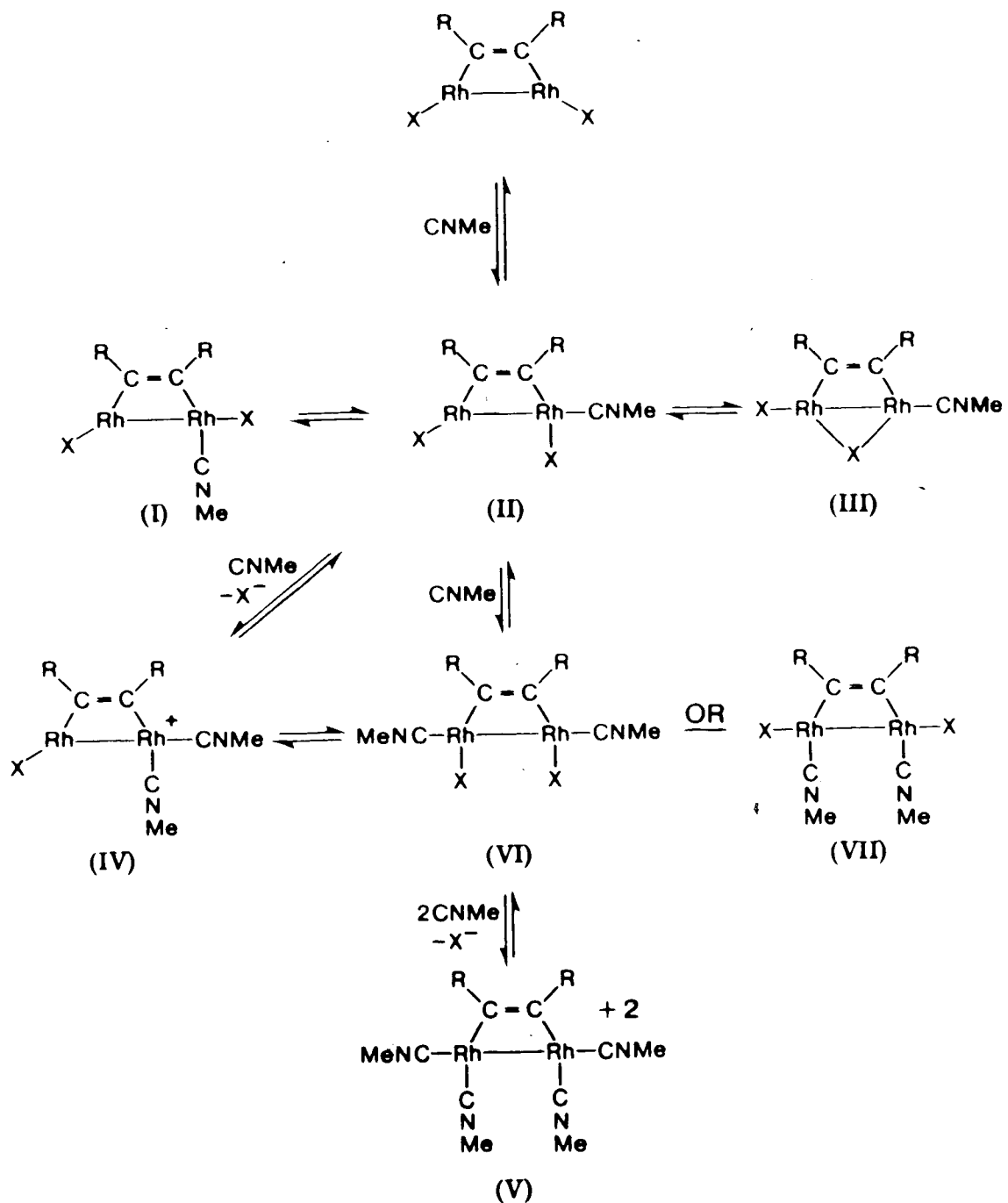


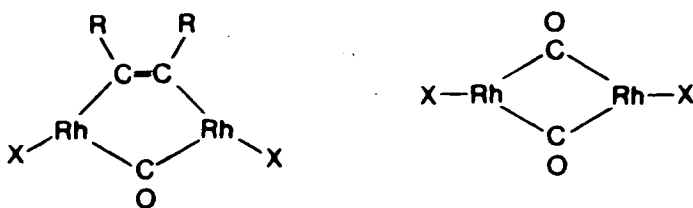
Figure 9. Scheme for Reactions of $[\text{Rh}_2\text{X}_2(\mu\text{-RC}_2\text{R})(\text{DPM})_2]$ with CNMe.

related, there are subtle differences which arise as consequences of the different halide and acetylene groups. For the HFB-bridged complexes two 1:1 adducts are observed, of which the more abundant is proposed to correspond to structure I and the less abundant to either III or to a rapidly equilibrating mixture of isomers II and III. The higher abundance of isomer I for the iodo species is believed to be related to its lower tendency to bridge the metals, which would reduce the abundance of isomer III. The fact that only one isomer of the 1:1 DMA-bridged adduct is observed is believed to be due to structure III being favoured due to steric interactions between the CNMe group and the carboxymethyl groups on the acetylene. Reaction with a second equivalent of CNMe can occur either with halide dissociation to give structure IV or without halide dissociation to give an isomer with structure VI or VII. Only for the iodo complex is any of the symmetrical species obtained, and this can be related to the lower tendency of I^- to dissociate compared to Cl^- . The 2:1 adducts react with two equivalents of CNMe to yield the dicationic tetrakis(isocyanide) species shown in structure V. No 3:1 adduct is observed.

(d) Conclusions

The chemistry of complexes **1**, **2** and **3** with CO, SO₂ and CNMe highlights the differences between CO and SO₂ on one hand and CNMe on the other. The former two small molecules react primarily as strong π -acids, while in this chemistry the σ -basicity of the latter seems to be its predominant characteristic. In rhodium and iridium DPM-bridged complexes, the final products of most small-molecule reactions tend to be A-frame complexes in which the strongest π -acid ligands occupy bridging sites. Methyl isocyanide does not exhibit this tendency; all its complexes characterized by us to date have terminal CNMe groups. It seems that CNMe is not a strong enough π -acceptor to favour the bridging site, but instead it coordinates terminally and is a sufficiently strong σ -base to displace halide ligands from compounds **1** - **3**. The effects of the σ -basicity and π -acidity on sites of ligand attack and residence in these systems could be investigated by reaction of the complexes with various isocyanides of different σ -basicity and π -acidity and also by reaction of other classes of ligand which have both bridging and terminal coordination capabilities, enabling testing over a wider range of ligand electronic characteristics.

Comparing the chemistry of compounds 1 - 3 with that of $[\text{Rh}_2\text{X}_2(\mu\text{-CO})(\text{DPM})_2]$ and $[\text{Rh}_2\text{X}_2(\mu\text{-SO}_2)(\text{DPM})_2]$, it may be noted that both CO and SO_2 insert into the metal-metal bond of complexes 1 - 3, but neither appears to insert into the similar metal-metal bonds of the carbonyl- and sulfur dioxide-bridged species. Instead, these small molecules appear to attack at the terminal sites, with rearrangements occurring at a later stage. One explanation for this avoidance of the bridging site in $[\text{Rh}_2\text{X}_2(\mu\text{-CO})(\text{DPM})_2]$ and $[\text{Rh}_2\text{X}_2(\mu\text{-SO}_2)(\text{DPM})_2]$ may lie in the nature of the products of such reactions. Insertion of CO or SO_2 into the metal-metal bonds of these species would generate species with non-bonded metals and two one-atom bridges as shown below for the hypothetical dicarbonyl-bridged species. Using this as an example, we see that it would have two sp^2 hybridized carbonyl



groups. In this geometry (having Rh-C(O)-Rh angles of ca. 120° and Rh-C distances of ca. 2.00 Å) the non-bonded contact between the two carbonyl groups would be only ca.

2.00 Å - a distance which we feel is much too short for a non-bonded interaction of this sort. In contrast, there is much less contact between the bridging CO and the acetylenic carbons in the acetylene-bridged analogues; this separation is greater than 2.8 Å.⁴ Analogously short contacts would also be present in the products either of CO insertion into the Rh-Rh bond⁴ of the SO₂-bridged complex or of SO₂ insertion into the CO-bridged complex and would presumably contribute to a destabilization of these products. It should be pointed out however that arguments based solely on repulsive van der Waals contacts cannot be the whole answer since a structure involving a bridging SO₂ group, two bridging methylthio groups and no accompanying metal-metal bond ($[\text{Fe}_2(\text{CO})_4(\text{PCH}_3)_2(\mu\text{-SCH}_3)_2(\mu\text{-SO}_2)] \cdot \frac{1}{2} (\text{C}_2\text{H}_5)_2\text{O}$) is known.⁴⁶ In this compound the Fe-S-Fe angles are only ca. 83-89°, increasing the S-S contact distances to near 3.0 Å.

It seems therefore that whether or not reactivity at the metal-metal bond occurs in these binuclear group 8 metal complexes depends both on the relative Lewis acidities of the metal-metal bond and the ligand (with the weaker Lewis acid CNMe failing to react at the Rh-Rh bond in the present series), and on the nature of the bridging groups. It seems to us that complexes

containing two carbonyls (or analogous groups such as SO_2 , CH_2 , CNR , etc.) which bridge two metals not bonded to each other should be severely destabilized owing to the resulting non-bonded contacts.

References

1. Cowie, M.; Dickson, R.S. Inorg. Chem. 1981, 20, 2682.
2. Cowie, M.; Dwight, S.K. Inorg. Chem. 1980, 19, 2500.
3. Cowie, M.; Dwight, S.K. Inorg. Chem. 1980, 19, 2508.
4. (a) Cowie, M.; Southern, T.G. J. Organomet. Chem. 1980, 193, C46.
(b) Cowie, M.; Southern, T.G. Inorg. Chem. 1982, 21, 246.
5. (a) Cowie, M.; Dwight, S.K.; Sanger, A.R. Inorg. Chim. Acta 1978, 31, L407.
(b) Cowie, M.; Dwight, S.K. Inorg. Chem. 1980, 19, 209.
6. Sutherland, B.R.; Cowie, M. Inorg. Chem. in press.
7. Cowie, M.; Gibson, J.A.E.; Dickson, R.S. unpublished results.
8. See Chapter II, Table I.
9. Casanova, J.; Schuster, R.E.; Werner, N.D. J. Chem. Soc. 1963, 4280.
10. The cell was used in an inverted position, with the normal air exit vent sealed and a serum cap covering the open end. Typically, 20 mL of solution was used. The cell was calibrated using 0.1 M KCl in H₂O.

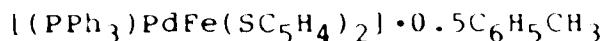
11. Mague, J.T.; DeVries, S.H. Inorg. Chem. 1980, **19**, 3743.
12. Doedens, R.J.; Ibers, J.A. Inorg. Chem. 1967, **6**, 204.
13. See Chapter II, reference 35 for the programs used.
14. Cromer, D.T.; Waber, J.T. "International Tables for X-ray Crystallography", Vol. IV, Kynoch Press, Birmingham, England, 1974, Table 2.2.A.
15. Stewart, R.F.; Davidson, E.R.; Simpson, W.T. J. Chem. Phys. 1965, **42**, 3175.
16. Cromer, D.T.; Liberman, O. J. Chem. Phys. 1970, **53**, 1891.
17. $R = \sum ||F_o| - |F_c|| / \sum |F_o|$; $R_w = [\sum w(|F_o| - |F_c|)^2 / \sum w F_o^2]^{1/2}$
18. Supplementary material is available from Dr. M. Cowie, Department of Chemistry, University of Alberta, Edmonton, Alberta, Canada, T6G 2G2.
19. Krogsrud, S.; Toniolo, L.; Croatto, U.; Ibers, J.A. J. Am. Chem. Soc. 1977, **99**, 5277.
20. Loghry, R.A.; Simonsen, S.H. Inorg. Chem. 1978, **17**, 1986.
21. Cowie, M.; Dwight, S.K. Inorg. Chem. 1979, **18**, 2700.
22. Cowie, M.; Gauthier, M.D. Inorg. Chem. 1980, **19**, 3142.
23. Mague, J.T.; DeVries, S.H. Inorg. Chem. 1982, **21**, 1632.

24. Mague, J.T. Inorg. Chem. 1983, 22, 1158.
25. Cowie, M.; Ibers, J.A. Inorg. Chem. 1976, 15, 552,
and references therein.
26. Olmstead, M.M.; Hope, H.; Benner, L.S.; Balch, A.L.
J. Am. Chem. Soc. 1977, 99, 5502.
27. Goldberg, S.Z.; Eisenberg, R. Inorg. Chem. 1976, 15,
58.
28. Goldberg, S.Z.; Eisenberg, R. Inorg. Chem. 1976, 15,
535.
29. MacGillivray, C.H.; Rieck, G.D. "International Tables
for X-ray Crystallography", Volume III, Kynoch
Press, Birmingham, England, 1968, Table 4.2.2.
30. Cowie, M.; Loeb, S.J. manuscript in preparation.
31. Mague, J.T. Inorg. Chem. 1983, 22, 45.
32. Puddephatt, R.J. Chem. Soc. Rev. 1983, 12, 99.
33. Gibson, J.A.E.; Cowie, M. Organometallics in press.
34. (a) Colton, R.; McCormick, M.J.; Pannan, C.D. J.
Chem. Soc., Chem. Commun. 1977, 823.
(b) Colton, R.; McCormick, M.J.; Pannan, C.D. Aust.
J. Chem. 1978, 31, 1425.
35. Brown, M.P.; Keith, A.N.; Manojlovic-Muir, Lj.;
Muir, K.W.; Puddephatt, R.J.; Seddon, K.R. Inorg.
Chim. Acta 1979, 34, L223.
36. Pringle, P.G.; Shaw, B.L. J. Chem. Soc., Dalton
Trans. 1983, 889.

37. Ruff, J.K. Inorg. Chem. 1967, **6**, 2080.
38. (a) Benner, L.S.; Olmstead, M.M.; Hope, H.; Balch, A.L. J. Organomet. Chem. 1978, **153**, C31.
(b) Balch, A.L.; Benner, L.S.; Olmstead, M.M. Inorg. Chem. 1979, **18**, 2996.
39. Kubas, G.J. Inorg. Chem. 1979, **18**, 182.
40. Kosower, E.M. "An Introduction to Physical Organic Chemistry", Wiley, New York, 1968, p. 49.
41. Hoffman, D.M.; Hoffmann, R.; Fisel, C.R. J. Am. Chem. Soc. 1982, **104**, 3858.
42. Treichel, P.M., Adv. Organomet. Chem. 1973, **11**, 21.
43. Malatesta, L.; Bonati, F. "Isocyanide Complexes of Metals", Wiley, New York, 1969.
44. For $[\text{Rh}_2(\text{CO})_2(\mu\text{-Cl})(\mu\text{-CO})(\text{DPM})_2][\text{BPh}_4]$, which is a normal 1:1 electrolyte, $\Lambda_{\text{M}} (10^{-3} \text{ M}) = 45.8 \Omega^{-1} \text{ cm}^2 \text{ equiv}^{-1}$ in CH_2Cl_2 .
45. Hames, B.W.; Cowie, M. unpublished results.
46. Taylor, N.J.; Arabi, M.S.; Mathieu, R. Inorg. Chem. 1980, **19**, 1740.

Chapter IV

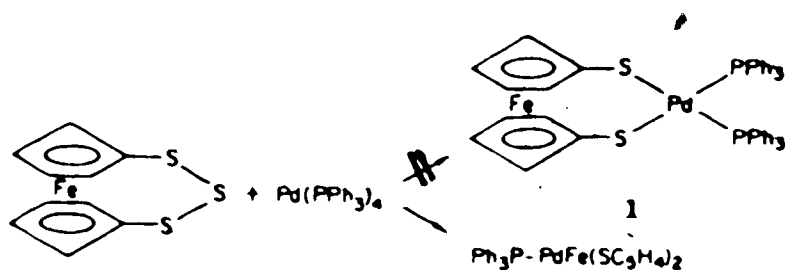
The Structure of a Novel Heterobinuclear Compound



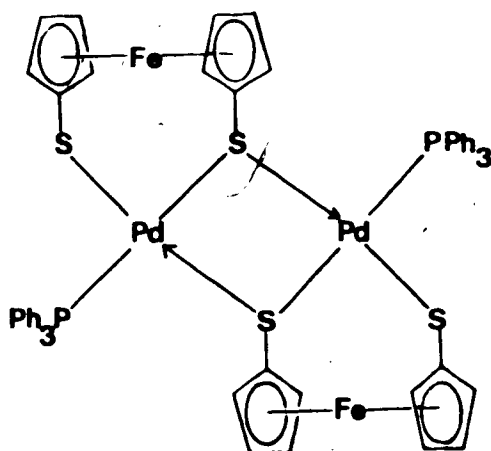
Introduction

More recently, as an extension of our studies on binuclear metal complexes, this group has been investigating such complexes in which the two metal centres are different. In addition to the possibility of cooperative ligand binding and activation by both metals, these heterobinuclear complexes should also display unique reactivity features by virtue of the different chemical properties of the adjacent metals.

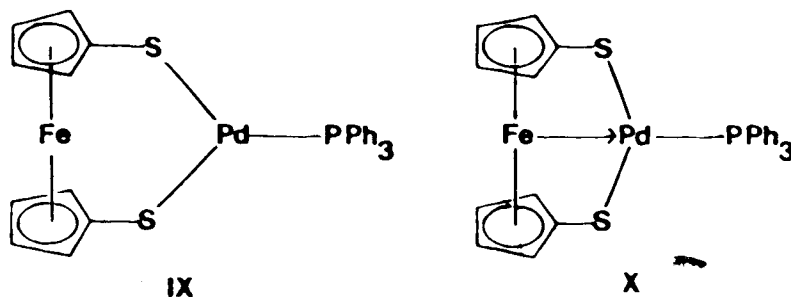
One such heterobinuclear complex was prepared at M.I.T. by the reaction of 1,2,3-trithia-[3]-ferrocenophane with the Pd⁰ complex, [Pd(PPh₃)₄].¹ The insertion of low-valent, coordinatively unsaturated moieties of the type L₂M (M = Ni, Pd, Pt; L = tertiary phosphine) into the S-S bond of [(μ-S₂)Fe₂(CO)₆] had already been reported,² so the above reaction seemed like a reasonable route to prepare the mixed-metal complex [(PPh₃)₂PdFe(C₅H₄S)₂], as shown below. However, the species actually obtained was the apparently



ligand-deficient compound $[(\text{PPh}_3)_2\text{PdFe}(\text{C}_5\text{H}_4\text{S})_2]$, as established by elemental analysis. This unsaturated species was originally formulated as the dimer shown below, in which S \rightarrow Pd dative bonding provides electrons



for the otherwise highly unsaturated Pd atom. However, the field desorption mass spectrum showed the compound to be monomeric, and the ^1H NMR spectrum indicated that the two cyclopentadienyl rings of the ferrocenophane moiety were equivalent at room temperature, ruling out this dimeric formulation. Two alternative structures for the monomeric formulation are shown below; the first, IX, has



a highly unsaturated trigonal Pd centre and the second, closely related structure, X, has additional Fe \rightarrow Pd dative bonding to help satisfy this unsaturation. The product seemed too unreactive for a coordinatively unsaturated Pd complex (for example, it showed no reaction at room temperature with PPh_3 , CO or NO), suggesting the unusual structure X. An X-ray structural determination was therefore undertaken to unambiguously establish the structure of this complex.

X-ray Data Collection. Red-brown, plate-like crystals of $[(PPh_3)PdFe(SC_5H_4)_2] \cdot C_6H_5CH_3$, obtained by slow recrystallization from a cooled solution of the product in a CH_2Cl_2 /toluene/hexanes mixture were kindly supplied by Mr. T.G. Rucker, Dr. B.W. Hames and Professor D. Seyferth. A suitable crystal was mounted in air on a glass fibre. Unit cell parameters were obtained from a least-squares refinement of the setting angles of 23 reflections, in the range $13.0^\circ < 2\theta < 29.0^\circ$, which were accurately centred on an Enraf-Nonius CAD4 diffractometer using $MoK\alpha$ radiation. The 2/m diffraction symmetry and the systematic absences ($hkl: h + k$ odd; $h0l:l$ odd) are consistent with the space groups Cc and $C2/c$. The centrosymmetric space group was chosen and later verified as the more probable one based on the successful refinement of the structure with acceptable thermal and positional parameters, reasonable agreement indices and by the location of all hydrogen atoms except those on the toluene methyl group.

Intensity data were collected with the CAD4 diffractometer in the bisecting mode by employing the ω - 2θ scan technique up to $2\theta = 52.0^\circ$ with graphite monochromated $MoK\alpha$ radiation. Backgrounds were scanned for 25% of the peak width on either end of the peak

scan. The intensities of three standard reflections were measured every 1 h of exposure time to assess possible crystal decomposition or movement. No significant variation in these standards was noted so no correction was applied to the data. 5713 unique reflections were measured and processed in the usual way using a value of 0.04 for μ^4 and, of these, 3255 were considered to be observed and were used in all subsequent calculations. Absorption corrections were applied to the data using Gaussian integration.⁵ See Table XX for pertinent crystal data and the details of data collection.

Structure Solution and Refinement. The structure was solved in space group C2/c using standard Patterson, Fourier and least-squares techniques. All atoms, excluding the toluene methyl hydrogens, were ultimately located. Atomic scattering factors for non-hydrogen atoms⁶ and hydrogen⁷ were taken from the usual sources. Anomalous dispersion terms⁸ for Pd, Fe, S and P were included in F_c . The carbon atoms of the PPh₃ phenyl groups were refined as rigid groups having idealized D_{6h} symmetry, C-C distances of 1.392 Å and independent isotropic thermal parameters. All hydrogen atoms except the toluene methyl hydrogens, which are disordered, (vide infra) were input as fixed contributions. Their

idealized positions were calculated after each cycle of refinement from the geometries of their attached carbon atom using a C-H distance of 0.95 Å. These hydrogen atoms were assigned isotropic thermal parameters of 1 \AA^2 greater than the B (or equivalent isotropic B) of their attached carbon atom. All other non-group atoms were refined anisotropically.

The toluene molecules sit on the 4(e) crystallographic diad axes and as a result the methyl hydrogens are at least two-fold disordered. In fact, the expected six half-weighted hydrogens were not unambiguously located suggesting further rotational disorder about the $C_{Me}-C_{Ph}$ bond.

On the final difference Fourier map the highest 20 peaks ($1.60-0.58 \text{ e \AA}^{-3}$) were in the vicinities of the rigid phenyl groups, the disordered methyl hydrogens and the heavier atoms (Pd, Fe, S and P). A typical carbon atom on earlier syntheses had a peak intensity of about 8.7 e \AA^{-3} .

The final positional and thermal parameters of the individual non-hydrogen atoms appear in Table XXI, the parameters for the carbon atoms of the rigid phenyl groups are given in Table XXII, the idealized hydrogen parameters are in Table XXIII and some least-squares planes are given in Table XXIV. A listing of observed

and calculated structure amplitudes is available.⁹ The independent toluene carbon atoms are numbered C(40) for the methyl carbon through C(44) for the para carbon atom and the phenyl hydrogen atoms are given the same number as their attached carbon atom.

Results

Table XX. Summary of Crystal Data and Intensity Collection
Details

compound	(PPh ₃)PdFe(SC ₅ H ₄) ₂ ·0.5C ₆ H ₅ CH ₃
formula weight	664.9
formula	PdFeS ₂ PC _{31.5} H ₂₆
space group	C _{2h} ⁶ - C2/c
cell parameters	
a, Å	39.258(5)
b, Å	10.548(2)
c, Å	13.612(4)
β, °	101.69(2)
V, Å ³	5519.7
Z	8
density, g cm ⁻³	1.595(calculated), 1.594(observed)
crystal dimension, mm	0.052 x 0.293 x 0.262
crystal shape	monoclinic plate with short distance along a* and faces of the forms {100}, {101}, {011}, {111}
crystal volume, mm ³	0.0475
temperature, °C	23
radiation	MoKα (λ = 0.71069 Å) graphite monochromated

(continued...)

Table XX. (continued)

μ , cm^{-1}	13.905
range in absorption correction factors	0.646 - 0.924
receiving aperture	2.00+0.5 $\tan\theta$ mm wide by 4.0 mm high, 173 mm from crystal
scan speed, degrees min^{-1}	10.058 to 0.891
scan width, degrees	0.50 + 0.350 $\tan \theta$ in omega
2 θ limits, degrees	1.0 - 52.0
unique data measured	5713
unique data used	3255
$(F_o^2 > 3\sigma(F_o^2))$	
final number of parameters varied	205
error in observation of unit weight (GOF)	1.136
R	0.040
R_w	0.046

Table XXI. Atomic Positional Parameters ($\times 10^4$) and Thermal Parameters^a ($\times 10^2$) for the Non-group Atoms of $[(\text{PPh}_3)_3\text{PdFe}(\text{SC}_5\text{H}_4)_2] \cdot 0.5\text{CH}_3\text{C}_6\text{H}_5$.

Atom	x	y	z	U11	U22	U33	U12	U13	U23
Pd	3488.5 (1)	4329.8 (5)	2064.5 (3)	2.99 (2)	3.21 (3)	3.33 (2)	0.15 (2)	0.98 (2)	0.08 (2)
Fe	3028.2 (2)	6310.0 (9)	2447.5 (6)	3.34 (5)	3.32 (5)	3.14 (5)	0.30 (4)	0.92 (4)	0.00 (4)
S(1)	3229.6 (5)	3164 (2)	3148 (1)	5.2 (1)	3.52 (9)	5.1 (1)	0.31 (8)	2.29 (8)	0.95 (8)
S(2)	3709.9 (4)	5830 (2)	1146 (1)	4.4 (1)	4.8 (1)	5.4 (1)	0.22 (9)	2.48 (8)	0.64 (9)
P	3788.2 (4)	2661 (2)	1673 (1)	2.98 (8)	3.46 (9)	3.57 (9)	0.15 (7)	0.90 (7)	0.24 (8)
C(1)	2986 (1)	4542 (6)	3152 (4)	3.2 (3)	3.6 (4)	3.7 (3)	0.5 (3)	1.4 (3)	0.0 (3)
C(2)	2677 (1)	4864 (7)	2460 (4)	2.4 (3)	5.4 (4)	4.0 (4)	0.9 (3)	0.8 (3)	0.1 (3)
C(3)	2547 (2)	6009 (7)	2765 (5)	3.4 (4)	6.8 (6)	5.4 (5)	1.1 (4)	1.7 (3)	1.2 (4)
C(4)	2553 (2)	6434 (7)	3630 (5)	5.2 (4)	5.2 (5)	4.3 (4)	0.0 (4)	2.6 (3)	0.6 (4)
C(5)	3056 (2)	5546 (6)	3870 (4)	4.0 (4)	4.5 (4)	3.2 (3)	0.5 (3)	1.0 (3)	0.5 (3)
C(6)	3394 (2)	6741 (6)	1510 (5)	5.2 (4)	2.9 (4)	4.2 (4)	0.1 (3)	2.0 (3)	0.8 (3)
C(7)	3039 (2)	6868 (7)	999 (4)	5.3 (4)	4.7 (4)	3.4 (3)	1.0 (4)	1.3 (3)	1.6 (3)
C(8)	2874 (2)	7783 (7)	1490 (6)	6.3 (5)	5.1 (5)	6.0 (5)	2.2 (4)	2.1 (4)	1.7 (4)
C(9)	3117 (2)	8220 (6)	2332 (6)	7.6 (6)	2.8 (4)	6.6 (5)	0.4 (4)	3.4 (4)	0.7 (4)
C(10)	3431 (2)	7565 (7)	2376 (5)	6.6 (5)	4.6 (4)	4.7 (4)	0.9 (4)	2.2 (4)	0.3 (4)
C(40)	5000	9632 (15)	2500	17 (2)	8 (1)	13 (1)	0	8 (1)	0
C(41)	5000	8232 (14)	2500	9 (1)	10 (1)	4.7 (7)	0	2.7 (7)	0
C(42)	4698 (2)	7509 (11)	2169 (6)	5.7 (5)	10.6 (8)	4.6 (5)	1.0 (6)	1.4 (4)	0.4 (5)
C(43)	4702 (2)	6225 (12)	2155 (6)	5.2 (5)	13.3 (9)	5.1 (5)	0.6 (6)	0.1 (4)	0.3 (6)
C(44)	5000	5564 (14)	2500	10 (1)	10 (1)	6.2 (8)	0	2.3 (8)	0

^a Estimated standard deviations in this and other tables are given in parentheses and correspond to the least significant digits. The positional parameters are $\times 10^4$ and the thermal parameters are $\times 10^2$. $U_{ij} = B_{ij} / (2 \times 10^3 \text{ \AA}^2)$. The thermal ellipsoid is given by $\exp[-(B_{11}h^2 + B_{22}k^2 + B_{33}l^2 + 2B_{12}hk + 2B_{13}hl + 2B_{23}kl)]$.

Table XXII. Parameters for the Rigid-Group Atoms of $[(PPh_3)_2PdFe(SC_5H_4)_2] \cdot 0.5 CH_3C_6H_5$

Derived Parameters									
Atom	x	y	z	B	Atom	x	y	z	B
C(11)	0.4009(1)	0.1816(4)	0.2796(3)	3.0(1)	C(24)	0.3110(1)	-0.0358(4)	-0.0269(3)	3.9(1)
C(12)	0.4054(1)	0.0507(4)	0.2839(3)	4.3(2)	C(25)	0.3469(1)	-0.0360(4)	-0.0193(3)	4.8(2)
C(13)	0.4252(1)	-0.0051(3)	0.3693(4)	5.7(2)	C(26)	0.3673(1)	0.0555(4)	0.0385(3)	4.1(1)
C(14)	0.4406(1)	0.0700(5)	0.4504(3)	5.5(2)	C(31)	0.4134(1)	0.2948(4)	0.0969(3)	2.9(1)
C(15)	0.4360(1)	0.2009(5)	0.4460(3)	5.3(2)	C(32)	0.4479(1)	0.2645(4)	0.1364(3)	4.0(1)
C(16)	0.4162(1)	0.2567(3)	0.3606(4)	4.3(2)	C(33)	0.47330(8)	0.2860(5)	0.0803(3)	5.3(2)
C(21)	0.3519(1)	0.1472(4)	0.0886(3)	2.9(1)	C(34)	0.4641(1)	0.3380(5)	-0.0154(3)	4.8(2)
C(22)	0.3160(1)	0.1473(4)	0.0811(3)	3.2(1)	C(35)	0.4296(1)	0.3683(4)	-0.0550(3)	4.6(2)
C(23)	0.29554(7)	0.0558(4)	0.0233(3)	3.7(1)	C(36)	0.40420(9)	0.3468(4)	0.0012(3)	3.8(1)

Rigid Group Parameters					
	x_c^a	y_c	z_c	Delta ^b	Eta
Ring 1	0.42072(7)	0.1258(3)	0.3650(2)	-0.188(3)	0.906(3)
Ring 2	0.33143(7)	0.0557(3)	0.0309(2)	-2.027(3)	-0.513(3)
Ring 3	0.43875(8)	0.3164(3)	0.0407(2)	1.094(4)	-1.085(4)

^a x_c , y_c and z_c are the fractional coordinates of the centroid of the rigid group.

^b The rigid group orientation angles Delta, Epsilon and Eta (radians) have been defined previously: S.J. La Placa and J.A. Ibers, *Acta Crystallogr.* 1965, 18, 511.

Table XXIII. Idealized Positional and Thermal Parameters for the
Hydrogen Atoms of $[(PPh_3)PdFe(SC_5H_4)_2] \cdot 0.5C_6H_5CP_3$.

Atom	x	y	z	B(\AA^2)	Atom	x	y	z	B(\AA^2)
H(2)	0.2574	0.4385	0.1884	4.07	H(22)	0.3054	0.2100	0.1151	4.16
H(3)	0.2338	0.6421	0.2448	5.02	H(23)	0.2710	0.0560	0.0181	4.64
H(4)	0.2762	0.7192	0.3991	4.70	H(24)	0.2970	-0.0983	-0.0662	4.90
H(5)	0.3251	0.5604	0.4412	4.01	H(25)	0.3574	-0.0986	-0.0535	5.76
H(7)	0.2931	0.6406	0.0419	4.46	H(26)	0.3918	0.0554	0.0435	5.14
H(8)	0.2640	0.8062	0.1289	5.45	H(32)	0.4542	0.2292	0.2019	4.94
H(9)	0.3075	0.8851	0.2790	5.26	H(33)	0.4969	0.2653	0.1074	6.31
H(10)	0.3634	0.7645	0.2888	5.09	H(34)	0.4815	0.3525	-0.0537	5.75
H(12)	0.3950	-0.0006	0.2287	5.31	H(35)	0.4233	0.4036	-0.1203	5.55
H(13)	0.4283	-0.0943	0.3725	6.71	H(36)	0.3807	0.3675	-0.0258	4.80
H(14)	0.4541	0.0322	0.5088	6.60	H(42)	0.4481	0.7937	0.1942	6.49
H(15)	0.4464	0.2524	0.5013	6.23	H(43)	0.4493	0.5777	0.1904	7.31
H(16)	0.4131	0.3461	0.3575	5.31	H(44)	0.5000	0.4663	0.2500	7.01

Table XXIV. Least-Squares Plane Calculations^a for $[(PPh_3)_2PdFe(SC_5H_4)_2] \cdot 0.5C_6H_5CH_3$.

plane number	equation	plane number	equation
1	$0.6536X + 0.4933Y - 0.5740Z - 7.0582 = 0$	5	$-0.3446X - 0.2769Y - 0.7917Z + 10.5762 = 0$
2	$0.4074X + 0.7271Y - 0.5527Z - 9.2934 = 0$	6	$-0.6063X + 0.2048Y - 0.7664Z + 11.0164 = 0$
3	$0.6458X + 0.5047Y - 0.5734Z - 7.0511 = 0$	7	$-0.5520X - 0.2700Y + 0.7689Z + 10.5917 = 0$
4	$0.4248X + 0.7239Y - 0.5568Z - 9.3766 = 0$		

plane number	Pd	Fe	S(1)	S(2)	P	C(1)	C(2)	C(3)	C(4)	C(5)	C(6)	C(7)	C(8)	C(9)	C(10)
1	2.1945(5)	1.6817(9)	-0.101(2)	2.466(2)	-0.013(6)	0.015(6)	-0.001(7)	0.010(6)	0.020(6)	-0.016(7)	0.005(8)	0.013(7)	-0.024(7)		
2	-2.1488(5)	-1.6914(9)	0.136(2)	-2.817(2)											
3	2.1498(5)	1.6752(9)	-0.148(2)	2.391(2)	-0.037(6) ^b	0.003(6)	0.005(7)	-0.002(6)							
4	-2.0756(5)	-1.6607(9)	0.212(1)	-2.496(2)											
5	-0.0150(5)	0.0441(8)	-0.105(2)	-0.095(2)	0.186(2)	0.023(6) ^b									
6	0.0082(5)	0.3478(8) ^b	-0.032(2)	-0.054(2)	-0.009(2)	0.227(6) ^b									
7	-0.0279(5) ^b	0.0312(8)	-0.139(2)	-0.138(5)	0.120(2)	0.007(6) ^b									

Distances from Planes (Å)													
plane number	angle	plane number	angle	plane number	angle								
1	19.59	1	6	93.23	2	5	89.18	3	5	92.14	4	6	86.61
1	0.77	1	7	92.36	2	6	88.35	3	6	93.11	4	7	89.50
1	18.33	2	3	18.82	2	7	89.15	3	7	92.31	5	6	5.60
1	92.19	2	4	1.26	3	4	17.56	4	5	89.32	5	7	0.60
													5.00

Dihedral Angles Between Planes (Deg)					
plane numbers	angle	plane numbers	angle	plane numbers	angle
1, 2, 3	102.1	1, 2, 4	102.1	1, 2, 5	102.1
1, 3, 4	102.1	1, 3, 5	102.1	1, 3, 6	102.1
1, 4, 5	102.1	1, 4, 6	102.1	1, 4, 7	102.1
1, 5, 6	102.1	1, 5, 7	102.1	1, 5, 8	102.1
1, 6, 7	102.1	1, 6, 8	102.1	1, 6, 9	102.1
1, 7, 8	102.1	1, 7, 9	102.1	1, 7, 10	102.1
1, 8, 9	102.1	1, 8, 10	102.1	1, 8, 11	102.1
1, 9, 10	102.1	1, 9, 11	102.1	1, 9, 12	102.1
1, 10, 11	102.1	1, 10, 12	102.1	1, 10, 13	102.1
1, 11, 12	102.1	1, 11, 13	102.1	1, 11, 14	102.1
1, 12, 13	102.1	1, 12, 14	102.1	1, 12, 15	102.1
1, 13, 14	102.1	1, 13, 15	102.1	1, 13, 16	102.1
1, 14, 15	102.1	1, 14, 16	102.1	1, 14, 17	102.1
1, 15, 16	102.1	1, 15, 17	102.1	1, 15, 18	102.1
1, 16, 17	102.1	1, 16, 18	102.1	1, 16, 19	102.1
1, 17, 18	102.1	1, 17, 19	102.1	1, 17, 20	102.1
1, 18, 19	102.1	1, 18, 20	102.1	1, 18, 21	102.1
1, 19, 20	102.1	1, 19, 21	102.1	1, 19, 22	102.1
1, 20, 21	102.1	1, 20, 22	102.1	1, 20, 23	102.1
1, 21, 22	102.1	1, 21, 23	102.1	1, 21, 24	102.1
1, 22, 23	102.1	1, 22, 24	102.1	1, 22, 25	102.1
1, 23, 24	102.1	1, 23, 25	102.1	1, 23, 26	102.1
1, 24, 25	102.1	1, 24, 26	102.1	1, 24, 27	102.1
1, 25, 26	102.1	1, 25, 27	102.1	1, 25, 28	102.1
1, 26, 27	102.1	1, 26, 28	102.1	1, 26, 29	102.1
1, 27, 28	102.1	1, 27, 29	102.1	1, 27, 30	102.1
1, 28, 29	102.1	1, 28, 30	102.1	1, 28, 31	102.1
1, 29, 30	102.1	1, 29, 31	102.1	1, 29, 32	102.1
1, 30, 31	102.1	1, 30, 32	102.1	1, 30, 33	102.1
1, 31, 32	102.1	1, 31, 33	102.1	1, 31, 34	102.1
1, 32, 33	102.1	1, 32, 34	102.1	1, 32, 35	102.1
1, 33, 34	102.1	1, 33, 35	102.1	1, 33, 36	102.1
1, 34, 35	102.1	1, 34, 36	102.1	1, 34, 37	102.1
1, 35, 36	102.1	1, 35, 37	102.1	1, 35, 38	102.1
1, 36, 37	102.1	1, 36, 38	102.1	1, 36, 39	102.1
1, 37, 38	102.1	1, 37, 39	102.1	1, 37, 40	102.1
1, 38, 39	102.1	1, 38, 40	102.1	1, 38, 41	102.1
1, 39, 40	102.1	1, 39, 41	102.1	1, 39, 42	102.1
1, 40, 41	102.1	1, 40, 42	102.1	1, 40, 43	102.1
1, 41, 42	102.1	1, 41, 43	102.1	1, 41, 44	102.1
1, 42, 43	102.1	1, 42, 44	102.1	1, 42, 45	102.1
1, 43, 44	102.1	1, 43, 45	102.1	1, 43, 46	102.1
1, 44, 45	102.1	1, 44, 46	102.1	1, 44, 47	102.1
1, 45, 46	102.1	1, 45, 47	102.1	1, 45, 48	102.1
1, 46, 47	102.1	1, 46, 48	102.1	1, 46, 49	102.1
1, 47, 48	102.1	1, 47, 49	102.1	1, 47, 50	102.1
1, 48, 49	102.1	1, 48, 50	102.1	1, 48, 51	102.1
1, 49, 50	102.1	1, 49, 51	102.1	1, 49, 52	102.1
1, 50, 51	102.1	1, 50, 52	102.1	1, 50, 53	102.1
1, 51, 52	102.1	1, 51, 53	102.1	1, 51, 54	102.1
1, 52, 53	102.1	1, 52, 54	102.1	1, 52, 55	102.1
1, 53, 54	102.1	1, 53, 55	102.1	1, 53, 56	102.1
1, 54, 55	102.1	1, 54, 56	102.1	1, 54, 57	102.1
1, 55, 56	102.1	1, 55, 57	102.1	1, 55, 58	102.1
1, 56, 57	102.1	1, 56, 58	102.1	1, 56, 59	102.1
1, 57, 58	102.1	1, 57, 59	102.1	1, 57, 60	102.1
1, 58, 59	102.1	1, 58, 60	102.1	1, 58, 61	102.1
1, 59, 60	102.1	1, 59, 61	102.1	1, 59, 62	102.1
1, 60, 61	102.1	1, 60, 62	102.1	1, 60, 63	102.1
1, 61, 62	102.1	1, 61, 63	102.1	1, 61, 64	102.1
1, 62, 63	102.1	1, 62, 64	102.1	1, 62, 65	102.1
1, 63, 64	102.1	1, 63, 65	102.1	1, 63, 66	102.1
1, 64, 65	102.1	1, 64, 66	102.1	1, 64, 67	102.1
1, 65, 66	102.1	1, 65, 67	102.1	1, 65, 68	102.1
1, 66, 67	102.1	1, 66, 68	102.1	1, 66, 69	102.1
1, 67, 68	102.1	1, 67, 69	102.1	1, 67, 70	102.1
1, 68, 69	102.1	1, 68, 70	102.1	1, 68, 71	102.1
1, 69, 70	102.1	1, 69, 71	102.1	1, 69, 72	102.1
1, 70, 71	102.1	1, 70, 72	102.1	1, 70, 73	102.1
1, 71, 72	102.1	1, 71, 73	102.1	1, 71, 74	102.1
1, 72, 73	102.1	1, 72, 74	102.1	1, 72, 75	102.1
1, 73, 74	102.1	1, 73, 75	102.1	1, 73, 76	102.1
1, 74, 75	102.1	1, 74, 76	102.1	1, 74, 77	102.1
1, 75, 76	102.1	1, 75, 77	102.1	1, 75, 78	102.1
1, 76, 77	102.1	1, 76, 78	102.1	1, 76, 79	102.1
1, 77, 78	102.1	1, 77, 79	102.1	1, 77, 80	102.1
1, 78, 79	102.1	1, 78, 80	102.1	1, 78, 81	102.1
1, 79, 80	102.1	1, 79, 81	102.1	1, 79, 82	102.1
1, 80, 81	102.1	1, 80, 82	102.1	1, 80, 83	102.1
1, 81, 82	102.1	1, 81, 83	102.1	1, 81, 84	102.1
1, 82, 83	102.1	1, 82, 84	102.1	1, 82, 85	102.1
1, 83, 84	102.1	1, 83, 85	102.1	1, 83, 86	102.1
1, 84, 85	102.1	1, 84, 86	102.1	1, 84, 87	102.1
1, 85, 86	102.1	1, 85, 87	102.1	1, 85, 88	102.1
1, 86, 87	102.1	1, 86, 88	102.1	1, 86, 89	102.1
1, 87, 88	102.1	1, 87, 89	102.1	1, 87, 90	102.1
1, 88, 89	102.1	1, 88, 90	102.1	1, 88, 91	102.1
1, 89, 90	102.1	1, 89, 91	102.1	1, 89, 92	102.1
1, 90, 91	102.1	1, 90, 92	102.1	1, 90, 93	102.1
1, 91, 92	102.1	1, 91, 93	102.1	1, 91, 94	102.1
1, 92, 93	102.1	1, 92, 94	102.1	1, 92, 95	102.1
1, 93, 94	102.1	1, 93, 95	102.1	1, 93, 96	102.1
1, 94, 95	102.1	1, 94, 96	102.1	1, 94, 97	102.1
1, 95, 96	102.1	1, 95, 97	102.1	1, 95, 98	102.1
1, 96, 97	102.1	1, 96, 98	102.1	1, 96, 99	102.1
1, 97, 98	102.1	1, 97, 99	102.1	1, 97, 100	102.1
1, 98, 99	102.1	1, 98, 100	102.1	1, 98, 101	102.1
1, 99, 100	102.1	1, 99, 101	102.1	1, 99, 102	102.1
1, 100, 101	102.1	1, 100, 102	102.1	1, 100, 103	102.1
1, 101, 102	102.1	1, 101, 103	102.1	1, 101, 104	102.1
1, 102, 103	102.1	1, 102, 104	102.1	1, 102, 105	102.1
1, 103, 104	102.1	1, 103, 105	102.1	1, 103, 106	102.1
1, 104, 105	102.1	1, 104, 106	102.1	1, 104, 107	102.1
1, 105, 106	102.1	1, 105, 107	102.1	1, 105, 108	102.1
1, 106, 107	102.1	1, 106, 108	102.1	1, 106, 109	102.1
1, 107, 108	102.1	1, 107, 109	102.1	1, 107, 110	102.1
1, 108, 109	102.1	1, 108, 110	102.1	1, 108, 111	102.1
1, 109, 110	102.1	1, 109, 111	102.1	1, 109, 112	102.1
1, 110, 111	102.1	1, 110, 112	102.1	1, 110, 113	102.1
1, 111, 112	102.1	1, 111, 113	102.1	1, 111, 114	102.1
1, 112, 113	102.1	1, 112, 114	102.1	1, 112, 115	102.1
1, 113, 114	102.1	1, 113, 115	102.1	1, 113, 116	102.1
1, 114, 115	102.1	1, 114, 116	102.1	1, 114, 117	102.1
1, 115, 116	102.1	1, 115, 117	102.1	1, 115, 118	102.1
1, 116, 117	10				

Table XXV. Selected Interatomic Distances (Å) in
 $[(\text{PPh}_3)_2\text{PdFe}(\text{SC}_5\text{H}_4)_2] \cdot 0.5 \text{CH}_3\text{C}_6\text{H}_5$.

Bonding Distances

Pd-Fe	2.878(1)	P-C(11)	1.829(4)
Pd-P	2.241(2)	P-C(21)	1.838(4)
Pd-S(1)	2.309(2)	P-C(31)	1.837(5)
Pd-S(2)	2.294(2)	C(1)-C(2)	1.419(8)
Fe-C(1)	2.119(6)	C(2)-C(3)	1.406(10)
Fe-C(2)	2.060(7)	C(3)-C(4)	1.417(9)
Fe-C(3)	2.048(7)	C(4)-C(5)	1.410(9)
Fe-C(4)	2.041(7)	C(1)-C(5)	1.430(8)
Fe-C(5)	2.080(6)	C(6)-C(7)	1.432(9)
Fe-C(6)	2.154(7)	C(7)-C(8)	1.403(11)
Fe-C(7)	2.067(6)	C(8)-C(9)	1.411(10)
Fe-C(8)	2.039(7)	C(9)-C(10)	1.404(11)
Fe-C(9)	2.056(7)	C(6)-C(10)	1.448(10)
Fe-C(10)	2.080(8)	C(40)-C(41)	1.48(2)
S(1)-C(1)	1.741(6)	C(41)-C(42)	1.40(4)
S(2)-C(6)	1.720(7)	C(42)-C(43)	1.36(3)
		C(43)-C(44)	1.36(2)

Non-Bonding Distances

Fe-Cp1 ^a	1.683	S(1)-H(3) ^c	2.88
Fe-Cp2	1.693	S(1)-H(22)	2.89
H(5)-H(36) ^b	2.27	S(2)-H(43)	3.04
S(1)-C(11)	3.494(5)	S(2)-H(36)	3.04
S(2)-C(36)	3.332(5)		

^a Cp1 and Cp2 are the centroids of cyclopentadienyl groups 1 and 2, respectively.

^b H(36) of the molecule at $x, 1-y, 1/2+z$

^c H(3) of the molecule at $1/2-x, y-1/2, 1/2-z$

Table XXVI. Selected Angles (Deg) in
 $[(\text{PPh}_3)_2\text{PdFe}(\text{SC}_5\text{H}_4)_2] \cdot 0.5\text{CH}_3\text{C}_6\text{H}_5$.

<u>Bond Angles</u>			
Fe-Pd-S(1)	84.09(5)	C(10)-C(6)-C(7)	105.5(4)
Fe-Pd-S(2)	85.38(5)	C(6)-C(7)-C(8)	109.2(4)
Fe-Pd-P	172.97(4)	C(7)-C(8)-C(9)	108.2(4)
S(1)-Pd-S(2)	168.60(7)	C(8)-C(9)-C(10)	108.4(4)
S(1)-Pd-P	93.09(6)	C(9)-C(10)-C(6)	108.5(4)
S(2)-Pd-P	97.86(7)	Pd-P-C(11)	111.5(1)
Cp1-Fe-Cp2 ^a	165.20	Pd-P-C(21)	114.0(1)
Pd-Fe-Cp1	98.20	Pd-P-C(31)	118.2(1)
Pd-Fe-Cp2	96.51	C(11)-P-C(21)	105.9(2)
Pd-Fe-C(1)	63.5(2)	C(11)-P-C(31)	104.0(2)
Pd-Fe-C(6)	61.8(2)	C(21)-P-C(31)	102.0(2)
Pd-S(1)-C(1)	82.6(2)	P-C(11)-C(12)	123.6(2)
Pd-S(2)-C(6)	81.6(2)	P-C(11)-C(16)	116.2(2)
S(1)-C(1)-C(2)	126.5(3)	P-C(21)-C(22)	119.8(2)
S(1)-C(1)-C(5)	126.3(2)	P-C(21)-C(26)	120.2(1)
S(2)-C(6)-C(7)	126.8(3)	P-C(31)-C(32)	121.7(2)
S(2)-C(6)-C(10)	127.6(3)	P-C(31)-C(36)	118.4(2)
C(5)-C(1)-C(2)	107.3(4)	C(40)-C(41)-C(42)	122.9(10)
C(1)-C(2)-C(3)	108.8(3)	C(41)-C(42)-C(43)	122.5(5)
C(2)-C(3)-C(4)	107.6(4)	C(42)-C(43)-C(44)	121.3(18)
C(3)-C(4)-C(5)	108.7(4)	C(43)-C(44)-C(43) ^b	118.3(25)
C(4)-C(5)-C(1)	107.6(3)		

(continued...)

Table XXVI. (continued)

<u>Torsion Angles</u>			
C(1)-Cp1-Cp2-C(6)	1.18	S(1)-Pd-Fe-Cp2	177.76
C(2)-Cp1-Cp2-C(7)	1.24	S(1)-Pd-Fe-C(6)	176.56
C(3)-Cp1-Cp2-C(8)	1.19	S(2)-Pd-Fe-Cp1	-179.50
C(4)-Cp1-Cp2-C(9)	0.88 _b	S(2)-Pd-Fe-C(1)	-177.56
C(5)-Cp1-Cp2-C(10)	0.67	S(1)-Pd-P-C(11)	-48.31
S(1)-Cp1-Cp2-S(2)	1.37	S(1)-Pd-P-C(21)	71.50
S(1)-C(1)-C(6)-S(2)	1.33	S(1)-Pd-P-C(31)	-168.71
S(1)-Pd-Fe-Cp1	-3.88	S(2)-Pd-P-C(11)	128.50
S(1)-Pd-Fe-C(1)	-1.94	S(2)-Pd-P-C(21)	-111.69
S(2)-Pd-Fe-Cp2	2.14	S(2)-Pd-P-C(31)	8.10
S(2)-Pd-Fe-C(6)	0.94	C(41)-C(42)-C(43)-C(44)	2.47

^a Cp1 and Cp2 are the centroids of cyclopentadienyl groups 1 and 2, respectively.

^b The second C(43) is related to the first by the symmetry operation $1-x, y, 1/2-z$.

Description of Structure

This structure determination of $[(C_5H_4S)_2FePd(PPh_3)] \cdot 0.5C_6H_5CH_3$ confirms the monomeric formulation suggested by the mass spectral and 1H NMR data. The unit cell of this compound contains eight of these monomeric units with four toluene molecules of crystallization as shown in Figure 10. There are no unusual intermolecular contacts involving either the complex molecules or the solvent molecules. Apart from the methyl group disorder, the toluene molecule is well behaved and quite unexceptional. A perspective view of the complex, with some relevant bond lengths and angles, is shown in Figure 11. More complete bond length and angle tabulations are given in Tables XXV and XXVI, respectively.

The complex molecule is a rather unusual hetero-binuclear Fe-Pd complex in which the metal centres are held together by the cyclopentadienethiolato groups (SC_5H_4) and what appears to be a dative Fe-Pd bond (vide infra). The SC_5H_4 ligands are η^5 -bound in a pseudo-trans configuration to iron (much as in ferrocene and its derivatives) and are σ -bound to Pd through the sulfur atoms.

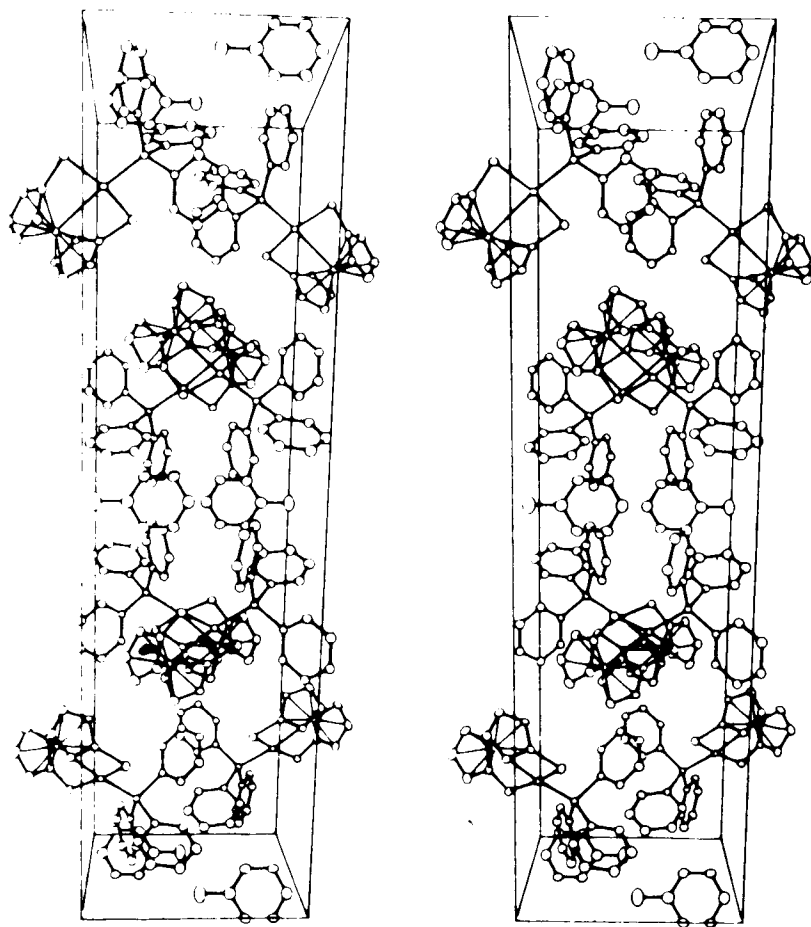


Figure 10. Stereoview of the Unit Cell of
 $[(PPh_3)PdFe(SC_5H_4)_2] \cdot 0.5C_6H_5CH_3$. As viewed with
the title at the bottom, the x-axis runs from top
to bottom, the y-axis runs from left to right and
the z-axis comes out of the page. 20% thermal
ellipsoids are shown.

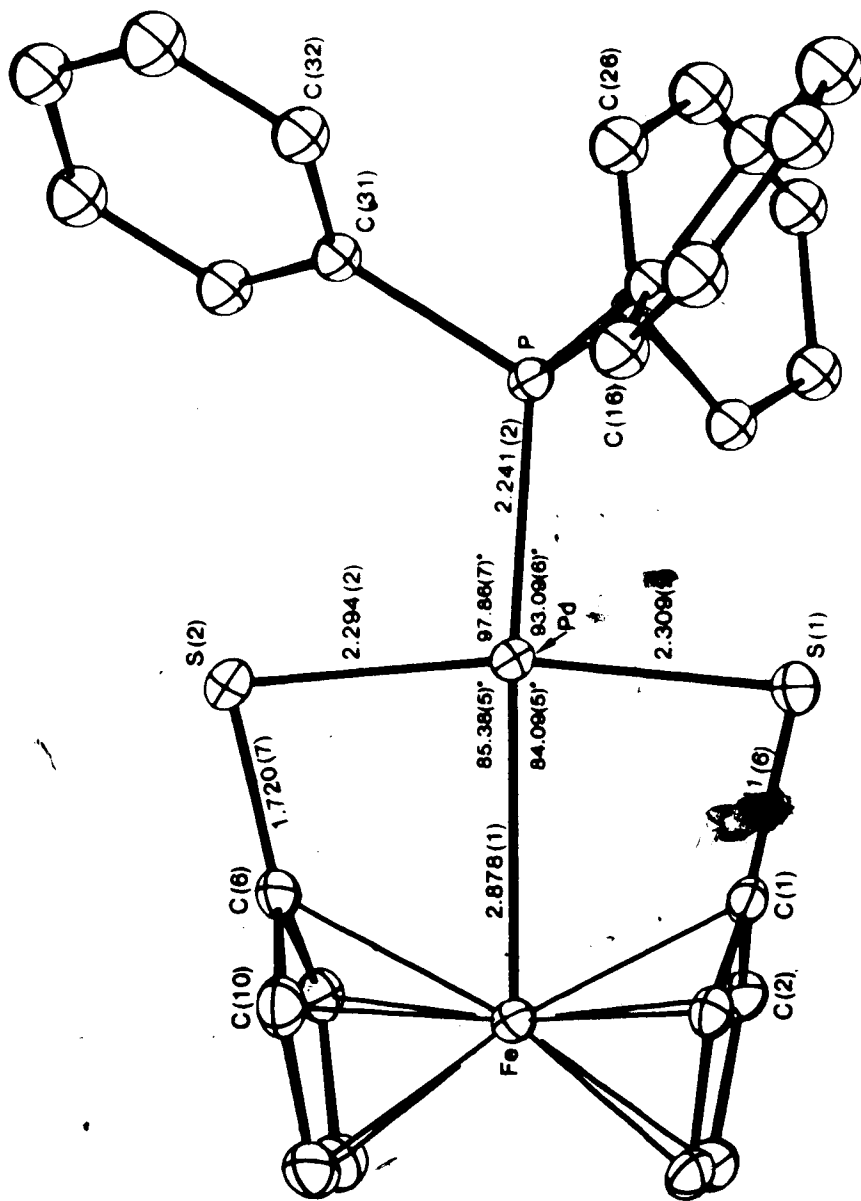


Figure 11. Perspective View of $[(PPh_3)PdFe(SC_5H_4)]$. The numbering scheme and some relevant bond lengths and angles are shown.

The coordination about Pd is a slightly distorted square plane in which the sulfur atoms are mutually trans, as are the PPh₃ group and the Fe atom of the ferrocenyl moiety. The major distortion from square planar geometry results because Pd lies towards the PPh₃ group, away from Fe such that the S-Pd-Fe angles are acute (see Figure 11). In addition, the PPh₃ group is bent away from S(2) toward S(1) in order to relieve the interactions between phenyl ring 3 and S(2), which are eclipsed (S(2)-Pd-P-C(31) torsion angle = 8.10°). The most significant such non-bonded contact (3.332(5) Å), between S(2) and C(36), is much smaller than the van der Waals distance of ca. 3.70 Å and in the absence of the observed distortion would be even less favourable. S(1), on the other hand, is staggered with regard to the other phenyl groups (Table XXVI) resulting in less severe interactions involving these groups; the shortest S(1)-phenyl carbon contact (S(1)-C(11) = 3.494(5) Å) is significantly longer than that observed for S(2). The Pd-S distances (av. 2.302 Å) appear normal although they are at the short end of the range observed (2.288(3) - 2.431(3) Å) in a variety of mono- and dithiolato Pd(II) complexes.¹⁰⁻¹⁴ Similarly the Pd-P distance (2.241(2) Å) is one of the shortest observed in typical Pd-PPh₃ complexes (2.230(4) - 2.344(2) Å)^{12,15-20} and is also

shorter than such distances obtained in several compounds in which the phosphine ligand is coordinated trans to another metal (2.271 - 2.296 Å).²¹⁻²³ These short Pd-S and Pd-P distances may be a consequence of the coordinative unsaturation at Pd which would result in these electron donating ligands being tightly bound to the electron deficient metal centre.

The geometry about Fe is surprisingly close to that of ferrocene even though Pd seems to be coordinated to the iron centre; the two eclipsed SC_5H_4 groups are only 19.6° from parallel. This small tilt of the SC_5H_4 groups away from the Pd atom results in a rather large Cp1-Fe-Cp2 ²⁴ angle of 165.2° . By comparison, in other bis(cyclopentadienyl) metal complexes, Cp_2ML_n , in which one or more groups, L_n , are bound to the metal, the Cp-M-Cp angles are within the range 126° - 143° .²⁵⁻³¹ The relatively small tilt of the SC_5H_4 groups in the present species may suggest that the Fe-Pd interaction is weak. It is also possible that this small tilt represents a compromise between the electronic requirements of the Fe, Pd and S atoms. A significantly greater tilt of the SC_5H_4 groups would result in longer (and presumably less favourable) Pd-S contacts, and C-S-Pd angles which are even more acute than those presently observed; these values ($81.6(2)^\circ$ and $82.6(2)^\circ$) are already much smaller

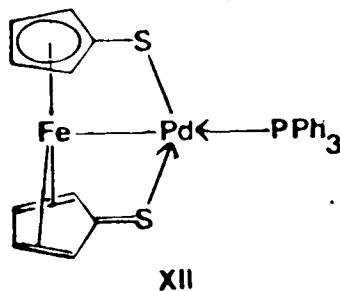
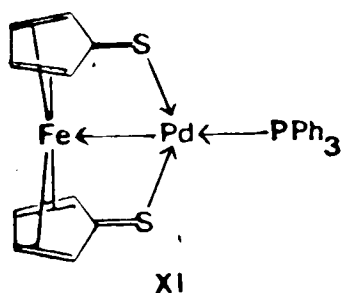
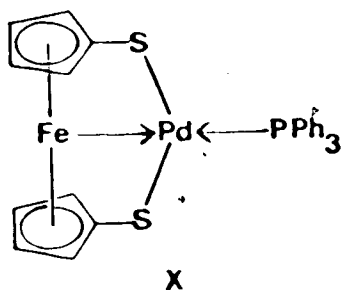
than the idealized value which would be near to the tetrahedral limit.

The parameters within the cyclopentadienethiolato groups are essentially as expected; for example, the average C-C distance of 1.42 Å compares well with the predicted value of 1.43 Å³² and the C-C-C angles (av. 108.0°) are quite typical. Both S-C distances (1.741(6) and 1.720(7) Å) appear normal for such distances in thiolato groups¹⁰⁻¹⁴ but show some shortening suggesting a slight degree of multiple bond character. A normal S-C single bond involving an sp² carbon might be expected at about 1.77 Å.³³ In both SC₅H₄ ligands the rings are tilted such that the carbons bound to sulfur are furthest from Fe whereas those at the opposite side of the Cp rings (C(3), C(4), C(8) and C(9)) are closest to Fe. Nevertheless, the range in Fe-C distances (2.154(7) Å - 2.039(7) Å) again appears to be normal. Although the Cp rings are close to being planar (see Table XXIV), calculations excluding the carbon atoms bound to S indicate that these carbon atoms are outwardly displaced from the planes of the other Cp carbon atoms by 0.037(6) Å for Cp ring 1 and 0.059(6) Å for Cp ring 2. Similarly S(1) and S(2) are displaced 0.148(2) and 0.212(2) Å from these same planes. The greater distortion of Cp ring 2 is probably due to its steric interactions with phenyl ring 3 (vide supra).

The Fe-Pd distance (2.878(1) Å) is rather long for a single bond but corresponds, we suggest, to a weak dative Fe→Pd bond. This bond is necessary to give Pd a favourable 16e configuration; without it a very unsaturated and reactive 14e configuration would result. Although the Fe-Pd distance is long (it is significantly greater than those observed in clusters containing Fe-Pd single bonds (2.599(1) - 2.698(1) Å),³⁴ it is not unreasonably long for such a bond; Pd-Pd bonding distances up to 2.790(2) Å³⁵ and Fe-Fe bonding distances up to 2.890(6) Å³⁶ have been reported. Somewhat similar weak iron-metal interactions have also been noted in silver and copper dimethylaminomethylferrocene complexes^{37,38} (3.091(3) and 2.945(5) Å, respectively) and in [(C₅H₅)Fe(C₅H₄Au₂(PPh₃)₂)]⁺ (2.818(9) Å).³⁹ It is also significant that rather small tilts of the Cp rings (6.5° to 16°) were again observed in these latter compounds and that the largest tilt, in the gold complex, seems to correspond to the strongest metal-iron interaction and corresponds closely to the value which we observe in the Fe-Pd complex.

Though we have suggested that the bonding in the present complex involves a dative Fe→Pd bond, this is based only on the consideration of the Fe(C₅H₄S)₂ moiety as a ferrocene-like system with an 18-electron iron.

Other canonical forms which should be considered are sketched below. Structure X is the electronic form we have considered in our previous discussions; however, structure XI may also be a significant contributor to the actual electronic structure, having an electron-deficient



16-electron iron, until the 2-electron donor bond from the 16-electron palladium is considered. Such a structure would certainly explain the somewhat shortened C-S bonds (vide supra), which suggest some multiple-bond character, and also the tilting of the Cp-S planes, which suggest a weaker bonding of the sulfur-bound carbons to the iron. The C-C bond lengths within the Cp rings also show tendencies toward lengths consistent with this

canonical structure, but not at a statistically significant level; such small differences could well be masked by thermal vibration of the ring atoms. Structure XI is therefore a plausible alternative. Structure XII and its obvious "twin" (with the localized double bonds on the other ring) show more conventional metal-metal bonds, with one electron contributed from each metal, and would be consistent with the same bonding distance trends as structure XI. Most probably, the actual structure has significant contributions from all three resonance forms.

The crystal structures of several [1]-, [2]- and [3]-ferrocenophanes provide useful comparisons with the parameters of the present compound. Of these, the [3]-ferrocenophanes generally display significantly smaller tilts of the Cp rings from the parallel configuration (8.8° - 12.5° for C₃ bridges,⁴⁰⁻⁴⁴ 2.4° - 5.6° for bridges involving large heteroatoms)⁴⁵⁻⁴⁸ than those for [2]-ferrocenophanes (about 23°)⁴⁹⁻⁵² or [1]-ferrocenophanes (16.6° - 26.7° ; heteroatom bridges only).⁵³ The tilts for the [1]- and [2]-ferrocenophanes clearly result from the short bridge lengths, which pinch the cyclopentadienyl groups together at the bridge location. For the carbon-bridged [3]-ferrocenophanes, the smaller tilts are due to the increased bridge length and flexibility. For the heteroatom-bridged

[3]-ferrocenophanes, the rings are actually forced apart very slightly at the bridges, but the angles remain small due to the flexibility of the bridges. In the present compound the bridge is also three atoms in length, but has a rigid structure by virtue of the trans-alignment of the thiolate sulfurs about Pd and the Pd-Fe bond. This rigidity forces the Cp groups apart, causing them to tilt significantly away from the bridge. The three ferrocenophane structures which probably offer the best comparisons with the present compound are $[\text{Fe}(\text{C}_5\text{H}_4\text{S})_2\text{S}]$ ⁴⁵ and $[\text{Fe}(\text{C}_5\text{H}_4\text{S})_2\text{Se}]$,⁴⁶ in which the Pd(PPh₃) unit of the present molecule is replaced by S and Se, respectively, and $[\text{Fe}(\text{C}_5\text{H}_4\text{AsMe}_2)_2\text{NiI}_2(\text{CO})]$.⁴⁷ The major difference between these compounds and $[(\text{C}_5\text{H}_4\text{S})_2\text{FePd}(\text{PPh}_3)]$ is the angle at the central bridging atom (S, Se, Ni or Pd). In the two trichalogen species, the angles at these bridgehead atoms are 103.9(2)° and 100.5(1)°, for S and Se respectively, while the angle at the Ni bridgehead of the arsine complex is 93.49(8)°; the As atoms are mutually cis on the Ni atom. These parameters contrast markedly with the almost-trans arrangement about Pd in the present complex (S(1)-Pd-S(2) = 168.60(7)°), which induces the previously mentioned Cp-Cp tilt. The Cp-Cp tilt angles for the above ferrocenophanes in which the bridgehead atom is not directly bound to Fe are in the

2°-3° range; the Pd complex has a Cp-Cp tilt angle of 19.6°.

Other angles and distances in the present compound indicate that it has other associated steric strains. The C-S-Pd angles in this Pd complex are very acute, averaging 82.1°, while the comparable angles average 102.8° and 102.3° for the S- and Se species, and 118.0° for the nickel arsine complex; these angles corroborate the existence of Fe-Pd bonding in this complex. Furthermore, the sulfur atoms in the present compound are displaced 0.15 Å and 0.21 Å out of the Cp ring planes, away from the iron, while the sulfur atoms are coplanar with the Cp rings in the S-bridged species and only 0.04 Å out of the plane with the Se-bridged species. In the nickel arsine complex the arsenic atoms are 0.00 Å and 0.06 Å out-of-plane towards the iron. The only situation in which a similar direction and magnitude of displacement is seen is for $\text{Sn}[(\text{SeC}_5\text{H}_4)_2\text{Fe}]_2$,⁴⁸ in which the selenium atoms are displaced outward from the Cp planes by 0.25 Å; the displacement was attributed to the large sizes of the Sn and Se atoms, which also prevented the ferrocene moieties from pivoting to relieve the strain. In the present Pd complex, this outward displacement of the S atoms from their Cp planes indicates that the palladium atom does not restrict the

Cp-Fe-Cp angle from bending more; on the contrary, it seems that more bending would relieve the outward strain at C(1) and C(6). Since steric reasons cannot account for the angle at iron, some more subtle electronic influences must favour a more nearly linear Cp-Fe-Cp angle. The observed geometry strongly supports the existence of an Fe-Pd bond, since without it the Pd atom could adopt a trigonal arrangement in which the strain at the sulfur atoms would be relieved. Such a mode is certainly plausible, as illustrated by the nickel complex,⁴⁷ in which the arsenic atoms adopt a near 90° angle at nickel. In view of this, it is rather surprising that one more triphenylphosphine was not retained, to give an unremarkable cis-phosphine-cis-thiolato complex. In either this geometry or the trigonal geometry previously mentioned, the palladium atom could pucker away from the FeS₂ plane, affording further relief of steric strain.

References

1. Seyferth, D.; Hames, B.W.; Rucker, T.G.; Cowie, M.; Dickson, R.S. Organometallics 1983, 2, 472.
2. Seyferth, D.; Henderson, R.S.; Gallagher, M.K. J. Organomet. Chem. 1980, 193, C75.
3. Day, V.W.; Lesch, D.A.; Rauchfuss, T.B. J. Am. Chem. Soc. 1982, 193, C75.
4. Doedens, R.J.; Ibers, J.A. Inorg. Chem. 1967, 6, 204.
5. In addition to local programs and modifications, a package of programs from the University of British Columbia was used, including: FASTFO, a modified version of FORDAP, the Fourier summation program by A. Zalkin; BUCILS, a structure factor and least-squares refinement program descended from ORFLS; BICABS, an absorption correction program which uses the Coppens-Leiserowitz-Rabinovitch logic for Gaussian integration; ORTEP, the plotting program by C.K. Johnson; ORFFE, the program for calculating bond lengths, angles and associated standard deviations by W. Busing and H.A. Levy.
6. "International Tables for X-ray Crystallography"; Kynoch Press: Birmingham, England, 1974; Vol. IV,

Table 2.2A.

7. Stewart, R.F.; Davidson, E.R.; Simpson, W.T. J. Chem. Phys. 1965, **42**, 3175.
8. Cromer, D.T. and Liberman, D. J. Chem. Phys. 1970, **53**, 1891.
9. Supplementary material is available from Dr. Martin Cowie, Department of Chemistry, University of Alberta, Edmonton, Alberta, Canada T6G 2G2.
10. Bailey, P.M.; Taylor, S.H.; Maitlis, P.M. J. Am. Chem. Soc. 1978, **100**, 4711.
11. Piovesana, O.; Sestili, L.; Bellitto, C.; Flamini, A.; Tomassini, M.; Zanazzi, P.F.; Zanzari, A.R. J. Am. Chem. Soc. 1977, **99**, 5190.
12. Ahmed, J.; Itoh, K.; Matsuda, I.; Ueda, F.; Ishii, Y.; Ibers, J.A. Inorg. Chem. 1977, **16**, 620.
13. Chen, H.W.; Fackler, J.P. Inorg. Chem. 1978, **17**, 22.
14. Roundhill, D.M.; Roundhill, S.G.N.; Beaulieu, W.B.; Bagchi, U. Inorg. Chem. 1980, **19**, 3365.
15. Kai, Y.; Yasuoka, N.; Kasai, N. Bull. Chem. Soc. Jap. 1979, **52**, 737.
16. Zenitani, Y.; Inoue, K.; Kai, Y.; Yasuoka, N.; Kasai, N. Bull. Chem. Soc. Jap. 1976, **49**, 1531.
17. Zenitani, Y.; Tokunan, H.; Kai, Y.; Yasuoka, N.; Kasai, N. Bull. Chem. Soc. Jap. 1978, **51**, 1730.

18. Horike, M.; Kai, Y.; Yasuoka, N.; Kasai, N. J. Organomet. Chem. 1974, 72, 441.
19. Del Piero, G.; Cesari, M. Acta Crystallogr., Sect. B., 1979, B35, 2411.
20. Miki, K.; Kai, Y.; Yasuoka, N.; Kasai, N. J. Organomet. Chem. 1979, 165, 79.
21. Jolly, P.W.; Kruger, C.; Schick, K.-P.; Wilke, G. Z. Naturforsch. 1980, 35B, 926.
22. Kobayashi, Y.; Iitaka, Y.; Yamazaki, H. Acta Crystallogr. Sect. B. 1972, B28, 899.
23. Ducruix, A.; Felkin, H.; Pascard, C.; Turner, G.K. J. Chem. Soc., Chem. Commun. 1975, 615.
24. Cp1 and Cp2 refer to the centroids of the cyclopentadiene groups.
25. Cowie, M.; Gauthier, M.D. Inorg. Chem. 1980, 19, 3142.
26. Jones, T.; Hanlan, A.J.L.; Einstein, F.W.B.; Sutton, D. J. Chem. Soc., Chem. Commun. 1980, 1078.
27. Schultz, A.J.; Stearley, K.L.; Williams, J.M.; Mink, R.; Stucky, G.D. Inorg. Chem. 1977, 16, 3303.
28. Kirillova, N.I.; Gusev, A.I.; Struchkov, Yu. T. Zh. Strukt. Khimii 1972, 13, 473.
29. Van Bolhuis, F.; de Boer, E.J.M.; Teuben, J.H. J. Organomet. Chem. 1979, 170, 299.

30. Prout, K.; Cameron, T.S.; Forder, R.A.; Critchley, S.R.; Denton, B.; Rees, G.V. Acta Crystallogr., Sect. B. 1974, **B30**, 2290; and references therein.
31. Prout, K.; Critchley, S.R.; Rees, G.V. Acta Crystallogr., Sect. B. 1974, **B30**, 2305.
34. Fachinetti, G.; Floriani, C.; Marchetti, F.; Mellini, M. J. Chem. Soc., Dalton Trans. 1978, 1398.
33. A typical S-CH₃ single bond is given as 1.81 Å in "International Tables for X-ray Crystallography"; Kynoch Press: Birmingham, England, 1974; Vol. III, Table 4.2.6. The difference in covalent radii between sp² and sp³ carbon is 0.04 Å.
34. Longoni, G.; Manassero, M.; Sansoni, M. J. Am. Chem. Soc. 1980, **102**, 3242.
35. Holloway, R.G.; Penfold, B.R.; Colton, R.; McCormick, M.J. J. Chem. Soc., Chem. Commun. 1976, 485.
36. Einstein, F.W.B. and Trotter, J. J. Chem. Soc. (A) 1967, 824.
37. Nesmeyanov, A.N.; Sedova, N.N.; Struchkov, Yu. T.; Andrianov, V.G.; Stakheeva, E.N.; Sazonova, V.A. J. Organomet. Chem. 1978, **153**, 115.
38. Nesmeyanov, A.N.; Struchkov, Yu. T.; Sedova, N.N.; Andrianov, V.G.; Volgin, Yu. V.; Sazonova, V.A. J. Organomet. Chem. 1977, **137**, 217.

39. Andrianov, V.G.; Struchkov, Yu. T.; Rossinskaya, E.R. Zh. Strukt. Khim. 1974, 15, 74.
40. Jones, N.D.; Marsh, R.E.; Richards, J.H. Acta Crystallogr. 1965, 19, 330.
41. Lecomte, C.; Dusasoy, Y.; Protas, J.; Moise, C.; Tirouflet, J. Acta Crystallogr., Sect. B 1973, B29, 488.
42. Batail, P.; Grandjean, D.; Astruc, D.; Dabard, R. J. Organomet. Chem. 1975, 102, 79.
43. Lecomte, C.; Dusasoy, Y.; Protas, J.; Moise, C. Acta Crystallogr., Sect. B 1973, B29, 1127.
44. Spaulding, L.D.; Hillman, M.; Williams, G.J.B. J. Organomet. Chem. 1978, 155, 109.
45. Davis, B.R.; Bernal, I., J. Cryst. Mol. Struct. 1972, 2, 107.
46. Osborne, A.G.; Hollands, R.E.; Howard, J.A.K.; Bryan, R.F. J. Organomet. Chem. 1981, 205, 395.
47. Pierpont, C.G.; Eisenberg, R. Inorg. Chem. 1972, 11, 828.
48. Osborne, A.G.; Hollands, R.E.; Bryan, R.F.; Lockhart, S. J. Organomet. Chem. 1982, 226, 129.
49. Yasufuku, K.; Aoki, K.; Yamazaki, H. Inorg. Chem. 1977, 16, 624.
50. Abramovitch, R.A.; Atwood, J.L.; Good, M.L.; Lampert, B.A. Inorg. Chem. 1975, 14, 3085.